SSEC PUB #82.02.P1

National Science Foundation Atmospheric Science Programs
Grant ATM 7913097

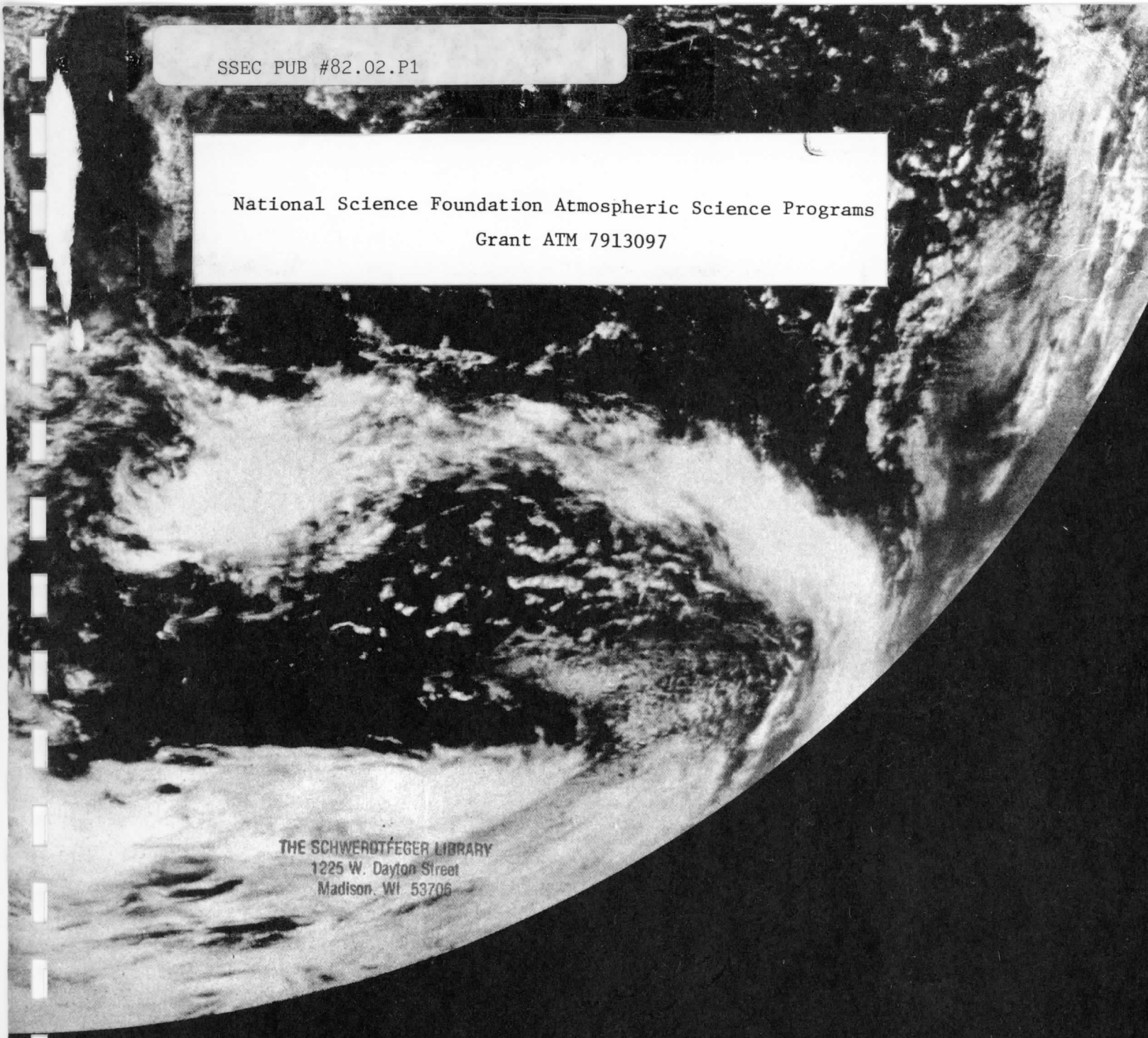

A REPORT

from the space science and engineering center
the university of wisconsin-madison
madison, wisconsin

National Science Foundation Atmospheric Science Programs

Grant ATM 7913097

FINAL PROJECT REPORT

National Science Foundation Atmospheric Science Programs
Grant ATM 7913097

15 October 1979 through 30 November 1981

Preparation of a Composite Surface Stress Data Set For the Summer Phase of MONEX

The Space Science and Engineering Center
at the University of Wisconsin-Madison
1225 West Dayton Street
Madison, Wisconsin 53706

Verner E. Suomi
Principal Investigator

Donald P. Wylie
Co-Investigator

Barry B. Hinton
Co-Investigator

20 February 1982

NATIONAL SCIENCE FOUNDATION
Washington, D.C. 20550

FINAL PROJECT REPORT

NSF FORM 98A

PLEASE READ INSTRUCTIONS ON REVERSE BEFORE COMPLETING

PART I–PROJECT IDENTIFICATION INFORMATION

1. Institution and Address	2. NSF Program	3. NSF Award Number
University of Wisconsin, Space Science and Engineering Center, 1225 West Dayton St., Madison, WI 53706	Atmospheric Sciences	ATM-7913097
	4. Award Period: From 15 Oct 79 To 30 Nov 81	5. Cumulative Award Amount: $78100

6. Project Title

Preparation of a Composite Surface Stress Data Set for the Summer Phase of MONEX

PART II–SUMMARY OF COMPLETED PROJECT *(FOR PUBLIC USE)*

The purpose of this work was to provide improved data on the force exerted by winds on the Indian Ocean. The marked seasonal change in the winds associated with the onset and cessation of the summer monsoon is of interest to oceanographers. The winds set up changing ocean currents, and in certain regions bring up cold nutrient-laden water from deeper levels in the ocean. This initiates a complex food chain with ultimate implications for fisheries. Moreover, the cold water directly affects local climates, and probably indirectly the monsoon rains in India. These effects are of interest to meteorologists.

The novel feature of this investigation was the use of cloud motions seen in satellite images to obtain the winds and hence the stress, or force, on the ocean. By combining these with observations from ships it was possible to obtain data in remote regions and determine forcing with coverage and detail never possible before.

The results are now being used by oceanographers to calculate the effects on the ocean.

PART III–TECHNICAL INFORMATION *(FOR PROGRAM MANAGEMENT USES)*

1. ITEM *(Check appropriate blocks)*	NONE	ATTACHED	PREVIOUSLY FURNISHED	TO BE FURNISHED SEPARATELY TO PROGRAM	
				Check (✓)	Approx. Date
a. Abstracts of Theses	X				
b. Publication Citations		X			
c. Data on Scientific Collaborators		X			
d. Information on Inventions	X				
e. Technical Description of Project and Results		X			
f. Other *(specify)*					

2. Principal Investigator/Project Director Name *(Typed)*	3. Principal Investigator/Project Director Signature	4. Date
Verner E. Suomi, Principal Investigator	Verner E. Suomi	2/20/82

CONTENTS

Summary of Activities

Attachments

1. Background

The work proposed for this grant was to map surface stress in the Indian Ocean for the summer MONEX special observing period of the Global Weather Experiment. Data from the Indian Ocean geostationary satellite (cloud drift observations and sunglint reflections) were to be used along with all available ship and island reports. In the course of the work it was found unnecessary to use sunglint. Extensive cloud free areas where the technique could be used were adequately covered by ship reports. Moreover, island reports were not considered because of their small numbers. Largely because of the cost savings associated with not processing sunglint data, we were able to extend the period under study to include the entire year of the Global Weather Experiment.

2. Work Done

The work done for this grant falls into two categories. First it was necessary to develop and verify the data handling and processing techniques. In essence these consisted of adapting conventional objective analysis methods for converting randomly located data to a grid point representation. This was preceded by a step in which the wind observations at various altitudes, ranging from ~10m to ~10^3m, were converted to stress vectors. The methods developed have been documented in two papers (Attachment 1, Wylie, Hinton and Millett, 1981) and (Attachment 2, Wylie and Hinton, 1981a). A third paper presented certain results of interest to others developing objective analysis methods (Attachment 3, Wylie and Hinton 1981b).

The second category of work was production of the gridded stress fields, along with associated products such as the vertical component of

$\nabla \times \tau$, and $\nabla \cdot \tau$. This work was presented in preliminary form at an international conference in January 1981 (Hinton and Wylie, 1981c) for the summer MONEX period. The summer MONEX data are also being published in the February 1982 issue of the Journal of Physical Oceanography (Attachment 4, Wylie and Hinton, 1982a). The work for the remainder of the year of the Global Weather Experiment has been completed. A publication on the relation of cloud motions to surface wind has been accepted for publication in Boundary Layer Meteorology (Attachment 5) and a series of stress charts has been prepared (Attachment 6).

3. Evaluation and Prospects

The investigator's original intent was to use the SEASAT microwave scatterometer as the primary data source with cloud motions and ship observations as adjuncts--primarily to determine the direction of the stress. The work discussed here was conceived when microwave data became unavailable due to the failure of SEASAT A. The techniques we developed succeeded well in providing data with space and time resolutions and coverage never before available. Our stress fields should help advance the art of numerical simulation of oceanic response if their limitations are properly respected. They are presently being used by one researcher for modelling studies, Dr. D. L. Anderson of Clarendon Laboratory, Oxford, England.

We plan to finish the Indian Ocean analysis in the near future and publish two papers based on techniques and results for the GWE year, Attachment 5, (Wylie and Hinton 1982b) and the stress analyses which will be developed from the material in Attachment 6. We have also proposed to extend our techniques to other ocean basins.

4. Publication Citations

All the publications listed below are contained in the attachments except the WMO report (item 4). This material was published in a more complete form in item 5.

(1) Wylie, Donald P., Barry B. Hinton and Kellie M. Millett, 1981: A comparison of three satellite-based methods for estimating surface winds over the oceans. J. Appl. Meteor., 20, 439-449.

(2) Wylie, Donald P., and Barry B. Hinton, 1981a: The feasibility of estimating large-scale surface wind fields for the summer MONEX using cloud motion and ship data. Boundary-Layer Meteor., 21, 357-367.

(3) Wylie, Donald P., and Barry B. Hinton, 1981b: Some statistical characteristics of cloud motion winds measured over the Indian Ocean during the summer monsoon., Mon. Wea. Rev., 109, 1810-1812.

(4) Hinton, Barry B., and Donald P. Wylie, 1981c: Estimates of sea surface stress for summer MONEX from cloud motions, in International Conference on Early Results of FGGE and Large-Scale Aspects of its Monsoon Experiments, World Meteorological Organization, Geneva 1981.

(5) Wylie, Donald P., and Barry B. Hinton, 1982: The wind stress patterns over the Indian Ocean during the summer monsoon of 1979. J. Phys. Ocean. (in press).

(6) Wylie, Donald P., and Barry B. Hinton, 1982: A comparison of cloud motion and ship wind observations over the Indian Ocean for the year of FGGE., accepted for publication in Boundary-Layer Meteorology.

5. Data on Scientific Colaborators

This work was carried out under the general supervison of Verner E. Suomi, Professor in Department of Meteorology, and Director of the Space Science and Engineering Center. Day-to-day conduct of the research was the responsibility of the Co-Investigators, Dr. Donald P. Wylie and Dr. Barry B. Hinton. Both are Assistant Scientists at the Space Science and Engineering Center.

Reprinted from JOURNAL OF APPLIED METEOROLOGY, Vol. 20, No. 4, April 1981
American Meteorological Society
Printed in U. S. A.

Attachment 1

A Comparison of Three Satellite-Based Methods for Estimating Surface Winds over Oceans

DONALD P. WYLIE, BARRY B. HINTON AND KELLIE M. MILLETT[1]

Space Science and Engineering Center, University of Wisconsin-Madison, Madison, WI 53706

(Manuscript received 11 August 1980, in final form 24 January 1981)

ABSTRACT

The feasibility of using satellites for providing surface winds or wind stress data was explored. Three popular methods were compared using nearly colocated data to assess the accuracies of each and the coverage that each could provide. The three methods tested were 1) the use of the sun glitter reflection seen on visible images of the ocean surface; 2) the use of active microwave sensors (flown on SEASAT) which reflect microwaves off the ocean surface; and 3) the use of cloud motions as indicators of the surface winds.

Close agreement in wind speed estimates was found among the three methods. The biases were <0.6 m s^{-1} for comparisons between comparable methods of estimating surface winds (1 and 2). Cloud motion comparisons to the other methods exhibited biases of <3.0 m s^{-1}. Individual point-by-point comparisons between wind measurements had an average scatter of 2.0 m s^{-1} (rms) or less after the mean biases were removed. Atmospheric variability caused as many of the differences as the instrumental errors indicating that meaningful wind information could be obtained from all three methods.

Very detailed spacial coverage was obtained with the sun-glitter method for wind speeds. However, the coverage was restricted to a narrow band 5° of latitude wide in the tropics. SEASAT also provided good coverage for two swaths (4° longitude wide) on each side of the satellite's orbit. Gaps between the swaths and orbits (polar non-synchronous orbits) were left unsampled. Both methods required external data on the wind directions which were obtained from cloud motions. The cloud motions provided coverage over larger areas than the other two methods because of the abundance of low-level cumuli.

1. Introduction

In this paper three methods of estimating low-level winds are examined to demonstrate the quality of oceanographic information that can be obtained from satellite platforms. Two methods were developed using image data from the Geostationary Operational Environmental Satellite (GOES). SEASAT-A provided a third method using an active microwave scatterometer. All three methods have potential for being operationally used in the future.

The strengths and weaknesses of each method are discussed based on comparisons between methods using colocated data in two geographical areas. Comparisons to ship and buoy observations were made when it was possible. However, very few ship observations of acceptable quality were found (19 total on 4 days) in the areas we focused on which were in the tropics and not in any highly traveled shipping routes. The satellite methods produce 4–10 times more observations in the same areas. Therefore, most of our findings were based on comparisons between the satellite methods because of data availability.

[1] Also Marine Studies, University of Wisconsin-Madison.

2. The satellite methods tested

a. The sun-glitter method

Detailed observations of the sun's reflection from the ocean surface were originally made by Cox and Munk (1954) from aircraft. These studies established how the intensity and shape of the sun-glitter reflection changed with the sea state. They developed empirical relationships for measuring surface winds using photographs of the sun glitter taken from aircraft.

Their method was adapted to satellite imagery by Levanon (1971). In satellite images of the ocean the curvature of the earth modified the shape of the sun glitter pattern. The glitter area was ~4–6° of latitude or longitude wide in the satellite pictures. Over such a large area a homogenous assumption of the wind field could not be made as done by Cox and Munk. To use satellite images, wind estimates had to be made at individual points inside the glitter area.

For estimating surface wind speeds, the Cox and Munk (1954) empirical relationships require either measurements of the brightness of a point, given the sun-satellite viewing geometry, or measurements

0021-8952/81/040439-11$06.75

of the width of the glitter area. Because Levanon (1971) had to work with a satellite sensor that was uncalibrated (ATS-3) he chose to measure the width of the glitter area. The brightness of one point location was measured in time using a sequence of satellite images to approximate the east–west width of the glitter area as the sun passed overhead.

In our application we were able to calibrate the satellite which greatly simplified the method. Observations of the sun and space were used to calibrate the three GOES-East spacecraft that were used in the course of this study. The procedure is described in Norton *et al.* (1980).

The shape of the glitter area is elongated in the direction of the wind as described by Cox and Munk (1954). To accurately account for this distortion, we estimated the direction of the wind at each point independent of the wind speed. The direction of the cloud motions seen on sequences of geostationary images was used to estimate the wind direction at the surface. Given this information the Cox and Munk (1954) relationships were applied to sea surface brightness measurements at any location in the glitter area where wind estimates were needed.

GOES image sequences of three pictures were displayed on the Man computer Interactive Data Access System (McIDAS) of the University of Wisconsin-Madison. Methods for measuring cloud motions on the McIDAS had been previously developed and used on an operational basis (Mosher, 1979).[2] The method for extracting wind information from the sea surface brightness also was installed into operational software on the McIDAS.

The glitter method was applicable only to wind speeds < 16 m s^{-1}. Under light winds the glitter patch was very small and very bright in the center. As the wind roughened the surface the width of the area grew while the center maximum brightness decreased. The Cox and Munk (1954) data indicated that for winds > 16 m s^{-1} the maximum glitter brightness would have been too small to distinguish from the ambient brightness of the sea surface using the GOES sensors. We thus confined our measurements to areas where the speeds were somewhat below this level.

Contamination of the sensor's field of view by small clouds (<4 km) and random sensor noise were sources of error that had to be eliminated. To avoid these problems we manually chose areas of the image displayed on the McIDAS that appeared to be mostly cloud free inside a 40 × 40 km box.

Cumulative brightness distributions were made for the area inside the selected box. The value of the lowest ⅛ of the distribution was automatically chosen by the software as the best representation of the surface brightness inside the box. This value had the highest probability of being free from cloud contamination and sensor noise.

An exception to this rule was found near the center of the glint pattern in areas of very low wind speeds (<4 m s^{-1}). Under these conditions, clouds sometimes appear dark against the bright background of the sun's reflection. These data were manually edited to remove cloud contamination. The results from this procedure were presented as wind speed magnitudes at 10 m altitude using the relationships of Cox and Munk (1954).

To test this method, a comparison of sun-glitter wind-speed estimates with moored buoy observations was made in the eastern Pacific (110°W longitude at the equator). Four research buoys were moored at this location in a diamond-shaped pattern 1° of latitude or longitude apart centered on the equator. Wind measurements were made at 3 m above the surface. Sun glitter wind estimates were made at each buoy site on seven days in March (8th, 9th, 10th, 12th, 14th, 20th and 24th) and on two days in April (28th and 30th) 1979 using one or two satellite images when the sun's reflection was closest to the buoys (2200 or 2230 GMT). The results are shown in Fig. 1.

The glitter estimated winds were 1.0 m s^{-1} higher than buoy observations, ±1.1 m s^{-1} rms, for 32 cases. These differences were partially caused by the anemometer heights of the buoys. The Cox and Munk relationships were made for a 10 m anemometer height while the buoy data used here was taken at 3 m. If a logarithmic wind profile u with height Z for a neutral boundary layer were assumed,

$$u = \frac{u_*}{0.4} \ln(Z/Z_0), \tag{1}$$

then most of these differences could be explained. For a wind speed of 5 m s^{-1}, Amorocho and DeVries (1980) predicted a $u^* = 0.16$ m s^{-1} and $Z_0 = 3.7 \times 10^{-5}$ m. The wind speeds at 3 m would be 0.5 m s^{-1} lower than at 10 m. Thus in reality, the glitter estimates were only 0.5 m s^{-1} greater than the surface (buoy) observations, which is within the accuracies of either the buoy anemometer measurements or the Cox and Munk method.

From this comparison we concluded that the sun-glitter method was as accurate as any other data source for our comparisons if care were taken to eliminate cloud contamination.

b. The SEASAT scatterometer

SEASAT-A (Apel, 1976) flew a microwave sensor specifically designed for monitoring the surface wind or wind stress. The scatterometer (SASS) monitored the ocean surface by transmitting a microwave pulse

[2] Mosher, F. R., 1979: Cloud drift winds from geostationary satellites. *Atmospheric Technology*, NCAR, Boulder, CO, December 1978–February 1979, 53–60.

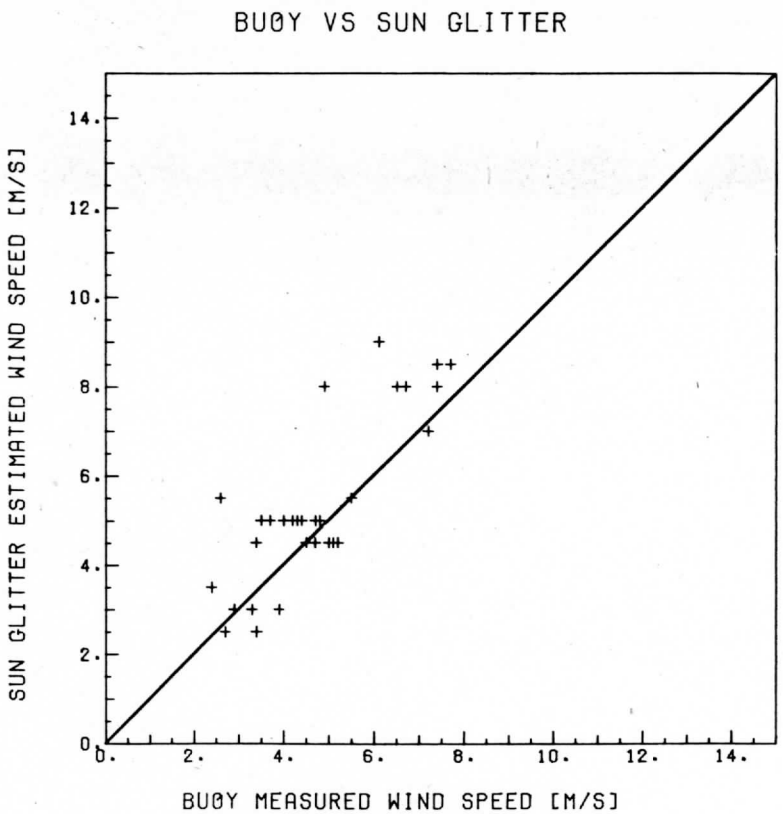

FIG. 1. A comparison of the sun glitter estimates of the surface winds to buoy measurements near 110°W longitude and the equator.

of 14.6 GHz (~2 cm) and measuring the magnitude of the returned reflection. This sensor is described by Grantham *et al.*, (1977) and Jones *et al.*, (1979).

The returned reflection came mainly from Bragg scattering off of oceanic waves of similar length (2 cm or less) with some energy from Fresnel scattering by longer waves. Based on the combined physical processes, Jones *et al.* (1979) formulated an analytical representation of the dependence of the backscatter cross section on friction velocity, (u^*) and the direction of u^* relative to the wave propagation direction. Their model contained 10 parameters whose values were determined by least-squares fit to a carefully selected set of "calibration data" or "surface truth."

The SASS data for the present study were derived using an algorithm similar to the Jones model by the Jet Population Laboratory, Pasadena, California, in August 1979. This algorithm has been modified by the SEASAT experiment team[3] to remove a bias in their wind-speed estimates. To make our results comparable to more recently produced SASS wind estimates, we have removed a mean bias of 1.3 m s^{-1} from all of our data. This correction was based on changes in the SASS algorithm made between August 1979 and December 1980[3].

The SASS results were given as a 19.5 m wind (neutral stability) because u^* data were difficult to obtain by independent methods for calibrating the SASS. This level was chosen because it is the near mean level of most ship observations. For comparisons to the sun-glitter method a height correction [Eq. (1)] of -0.3 m s^{-1} was made. Thus a total correction of -1.6 m s^{-1} was applied to the August 1979 data set. Grantham *et al.* (1977) discussed the sources and expected magnitudes of errors in the SASS wind estimates, which were mainly from system noise. When bias errors were removed, SASS was expected to give winds within ± 2 m s^{-1} or 10%.

Directional information was obtained from the fact that the returned pulse was stronger for waves aligned with crests perpendicular to the transmitting antenna direction than parallel to it, and slightly stronger in the upwind direction than the downwind direction. Theoretically, by looking at a surface patch from two different observation points (forward and aft-viewing antennai) the wind direction could be determined. However the direction of the component measured by one antenna toward or away from the satellite was seldom determined because of the uncertainty introduced by the system

[3] W. L. Jones, NASA Langley Research Center, Hampton Roads, VA, personal communication.

TABLE 1. A summary of the relations between surface wind and winds aloft on 52 soundings from Swan Island (Station 78501, 17.4°N, 83.9°W, 11 m above MSL) from August 1978–March 1979.

	Altitude above mean sea level (m)			
	609	914	1219	1829
Mean veering: direction at altitude less the direction at the surface.	8°	15°	19°	20°
Deviation of estimate of surface direction from actual direction (deg).*	22°	24°	27°	37°
Mean speed shear: speed at altitude less speed at surface (m s^{-1}).	2.1	1.7	1.5	1.4
Deviation of estimate of surface speed from acutal speed (m s^{-1}).*	2.1	2.3	2.4	2.5

* Root-mean-squared differences between observed surface values and that predicted from the observations at the indicated altitudes using linear regressions.

For the 609 m level which is slightly above the normal cloud bases the regressions found were:

Dir(sfc) = 0.96 Dir (609 m) −2.5°

Spd(sfc) = 0.47 Spd (609 m) + 1.9 m s^{-1}.

noise. Very often four possible directions result with the possibilities reduced to two directions (180° apart) on occasions.

To resolve these ambiguities the cloud motions measured from GOES images were used. The SEASAT wind estimates were overlayed on GOES image sequences and the SEASAT winds that were closest to the directions of the clouds were chosen as the correct solutions.

c. *Cloud motions*

Cloud motions were tracked on sequences of three GOES images taken 0.5 h apart (Mosher, 1979).[2] Displacements of the clouds were determined by correlating the digital data in a small area or box containing the clouds on successive images. The locations of the boxes were selected manually by operators viewing the images while the correlations were calculated objectively by the McIDAS. The locations of the correlation maxima were used to determine the cloud motion vectors.

Aircraft studies of the trade winds by LeMone and Pennell (1976) found little speed and direction changes on the average (less than 15° direction and 3 m s^{-1} speed) between the cloud-level winds and the surface in the western Atlantic. Wylie and Ropelewski (1980) also found the same close relationship between the cloud level and the surface winds. This is a result of the turbulent mixing in the atmospheric boundary layer which is generally of neutral thermal stability or slightly unstable.

To test the feasibility of using cloud motions as estimates of the surface wind we inspected 52 radiosonde soundings taken at Swan Island in the Caribbean for the speed and directional shear as a function of altitude (Table 1). The cloud bases in the trades are typically reported from 500 to 600 m. We analyzed the wind shears for four of the levels reported on the soundings from 609 m to 1829 m which roughly corresponded to a range from the cloud base level to near the top of most small cumulus cloud groups.

The mean directional shear (surface to altitude) ranged from 8° at 609 m to 20° at 1829 m while the speed shear ranged from 2.1 m s^{-1} (609) to 1.4 m s^{-1} (1829 m). A wind-speed maximum was found in the average wind profile at the 609 m level.

Using regression equations the surface wind speeds and directions were predicted from the observations at the altitude levels on an individual sounding basis. For the 52 soundings used, the surface directions that were empirically predicted had a scatter around the observed directions (rms) that ranged from 22° using the 609 m data, to 37° using the 1829 m data. Wind-speed predictions also showed the same characteristics with height. The predicted scatter increased from 2.2 m s^{-1} (rms) using the 609 m observations to 3.1 m s^{-1} using the 1829 m observations. These results indicate the magnitudes of the errors that would be expected from using observations above the boundary layer to predict surface winds.

The boundary-layer wind shear has commonly been observed to change in different weather situations and geographical areas. Therefore, we have not applied any corrections to the cloud-motion data based on the Swan Island statistics. Instead, we will use our comparisons of cloud-motions to the surface-wind estimates of SEASAT and the sun-glitter method to show the differences in the boundary-layer wind shears that were observed in two different geographical areas.

Studies of the accuracies of using trade wind cumulus clouds as wind indicators were made by Hasler *et al.*, (1976, 1979). They found that the cloud groups tracked on satellite images moved at the speeds of their bases and that they approximated the base-level winds within 1.9 m s^{-1}. This indicates that the surface winds could be reasonably estimated using cloud motions if the boundary-layer shear is removed.

3. The locations of the comparisons

All three methods were compared in two geographical areas: the eastern Pacific off the coast of Columbia, South America, and the Atlantic northeast of Brazil. Both areas were in the tropics because of the restrictions of the sun glitter method (see Table 2).

TABLE 2. The basic characteristics of the areas used for the comparisons.

	Pacific	Atlantic
Bounds		
Latitude	2°S–6°N	4–19°N
Longitude	80–99°W	39–55°W
Range of cloud-motion speeds	3–10 m s^{-1}	3–15 m s^{-1}
Range of surface wind speeds (glitter method)	2–8 m s^{-1}	3–10 m s^{-1}
Range of air-sea temperature difference (ship reports)	−1 to −5°C	−8 to +7°C

Two days were studied in each area. One SEASAT oribt per day was chosen for the comparisons. All SEASAT orbits used passed through the areas within 3 h of the time of passage of the sun glitter. GOES images also were selected to coincide with the passage of the sun glitter.

In the Pacific comparisons with two ship observations indicated that the atmospheric boundary layer was unstable with reported air temperatures of 1–5°C colder than the water on both days. The exact magnitude of the temperature difference was difficult to assess because a 5°C air-sea temperature difference is not realistic over the ocean. However, consistently unstable conditions for this area were found in the climatological analysis of Hastenrath and Lamb (1977).[4]

Shallow cumulus cells were found in the Pacific area (see figure 2). The cells were organized into patterns roughly similar to the mesoscale cells observed in unstable regions by Agee *et al.* (1973). Cloud tops were below 850 mb on both days as indicated from their temperatures found on the infrared images. North of 5°N latitude deep cumulonimbus clouds developed in the southerly flow. (Cirrus from the southern edges of the Cb's are visible in Fig. 2.) All wind data were taken south of the Cb cells.

In the Atlantic both stable and unstable boundary-layer conditions were reported by the merchant ships. However, ships in close proximity to each other often disagreed on the air-sea temperatures and the stability of the boundary layer. Hastenrath and Lamb (1977)[4] found unstable conditions over most of the area except near the Brazilian coast. The satellite images contained mainly cumulus groups which are commonly found in the tropical regions of the world. Thus, we felt the Atlantic area was typical of most tropical regions and the temperature stratification was probably neutral in the locations of most of our observations.

A line of cumulonimbus cells was present at 10°N latitude (Fig. 3). Both north and south of the Cb cells scattered trade wind cumulus groups were found. The tops of the trade wind cumulus were usually below 800 mb.

4. Comparisons of surface wind-speed estimates

The wind estimates were grouped into pairs for the comparisons. All cloud vectors, SEASAT vectors, or glitter vectors within 1° latitute and longitude were averaged. One sun-glitter estimate was made in the area of each SEASAT vector or cloud. Because small cloud contamination presented a

[4] Hastenrath, S., and P. J. Lamb, 1977: *Climate Atlas of the Tropical Atlantic and Eastern Pacific Oceans*. University of Wisconsin Press, 116 pp.

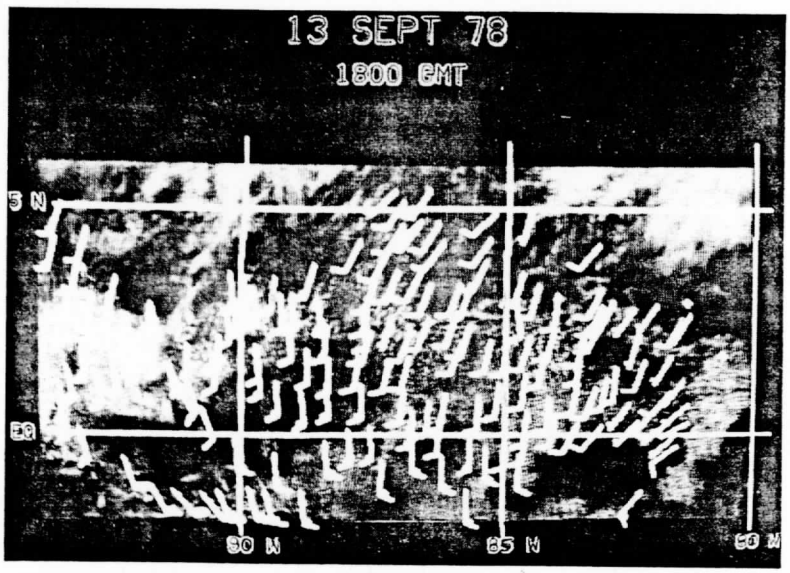

FIG. 2. An example of the cloud motion coverage in the Pacific region of study, 13 September 1978.

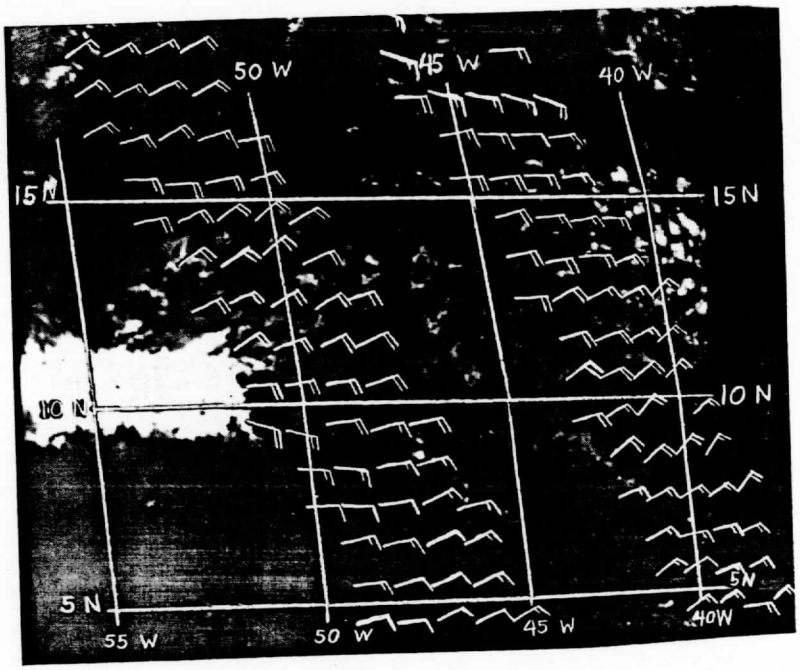

FIG. 3. An example of the SEASAT wind coverage in the Atlantic region of study, 16 July 1978. The vectors shown were selected from four possible directions based on the cloud motions.

problem in obtaining valid glitter data we chose to select mostly clear areas for the glitter measurements. This limited the number of vector pairs obtained. SEASAT data were readily obtained in areas of cloud cover and thus many cloud-SEASAT pairs were compared. No adjustments were made to the cloud motions for boundary-layer wind shear.

TABLE 3. Average differences between colocated wind-vector pairs (m s^{-1}) within 1° of latitude or longitude of each other. The number of paired vectors is given in parentheses.

Date	Location	Clouds* − Sun glitter	SEASAT − Sun glitter	Clouds* − SEASAT
16 Jul 78	Atlantic	3.0 (12)	0.6 (13)	0.8 (148)
17 Jul 78	Atlantic	2.2 (38)	−0.2 (33)	2.2 (116)
13 Sep 78	Pacific	−0.9 (17)	0.3 (24)	−0.8 (43)
16 Sep 78	Pacific	0.8 (12)	−0.2 (11)	0.5 (8)
Both Atlantic				9.7° (264)
Both Pacific				−3.3° (51)

* Corrections for wind shear in the boundary layer have not been applied.

The averages of each type of vector in the pairs indicated the biases between the different methods were small (Table 3). Scatter plots for these comparisons are shown in Figs. 4, 5 and 6. Cloud motions were faster than the glitter estimates (3.0 and 2.2 m s^{-1}) in the Atlantic area on the average. This indicated only slightly larger wind shears than found in the Swan Island radiosonde data. Comparisons of cloud motions to buoy observations by Halpern (1978, 1979) in other areas also have shown very similar results.

In the Pacific the cloud motions were not faster than the glitter wind estimates. The comparisons averaged −0.9 and 0.8 m s^{-1} on the two days studied. This was possibly a result of strong mixing in the atmospheric boundary layer which has commonly been found under cellular convection (Agee *et al.*, 1973).

SEASAT wind estimates averaged very close to the glitter estimates ranging from being 0.6 m s^{-1} higher to −0.2 m s^{-1} lower for the different days studied. This was expected because they are similar methods. The cloud motion measurements were usually faster than the SEASAT wind estimates in the Atlantic comparisons (0.8 and 2.2 m s^{-1}), but were nearly the same in the Pacific comparisons (−0.8 and 0.5 m s^{-1}) which again illustrated the different below cloud wind shears that were found in the two areas.

The scatter of these wind estimates was within

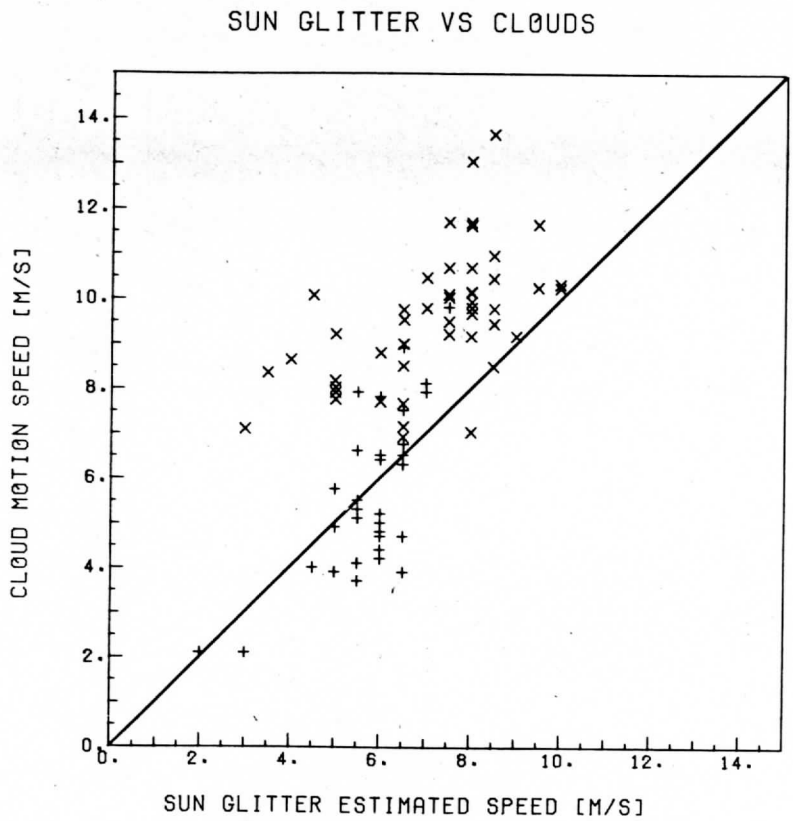

FIG. 4. The comparison of cloud motions to the sun glitter surface wind estimates: (+) Pacific area, (×) Atlantic area.

that found by comparisons of cloud motions to radiosonde observations or radiosondes to neighboring radiosondes. Hubert and Thomasell (1979)[5] and Bauer (1976) compared cloud motions to radiosondes and found disagreements of 4 m s^{-1} (rms). They estimated that the spacial variability of the wind field in the atmosphere caused a 2–3 m s^{-1} difference by itself. Our data averaged 0.6–1.9 m s^{-1} (Table 4, Figs. 4, 5 and 6) which was less than the atmospheric variability estimates. This was probably a result of using only one type of cloud, tropical cumulus, and confining our comparison to only data that were in close proximity (1° of separation).

The correlations found between the different wind estimates were reasonably good as indicated by Figs. 4, 5 and 6. The correlation coefficients found for these comparisons were as follows: cloud-glitter 0.6, clouds-SEASAT 0.7, and glitter-SEASAT 0.6.

Comparisons of cloud motions and SEASAT winds to ship reports also were made in the Atlantic area (Table 5). For the two days studied the ship reports indicated cloud motions were only 1.4 m s^{-1} faster than the ship reports while the SEASAT speeds were 2.6 m s^{-1} faster. This differs slightly from the comparisons of both methods to the sun glitter method shown in Table 3. However, because of the small number of ships available (19) and the large scatter of the ship comparisons we have less faith in the ship related comparisons.

5. Comparisons of wind-direction estimates

To assess the ability of each method to provide wind-direction information we compared cloud motions to the edited SEASAT data (Tables 3 and 4) and also each satellite method to the few ships found in the areas studied (Table 5). Comparisons were not made to the buoys discussed in Section 2a because few cloud tracers were found close to the buoys on the days studied and SEASAT was not operating during this period.

In general, we found close agreement between the cloud directions and the SEASAT vectors on the average (−3.3° and 9.7° of boundary-layer veering) as expected from our editing process which removed the worst cases (three total out of 267 in the Atlantic). The Pacific data indicated little direc-

[5] Hubert, L. F., and A. Thomasell Jr., 1979: Error characteristics of satellite-derived winds. NOAA Tech. Rep. NESS 79, 35 pp.

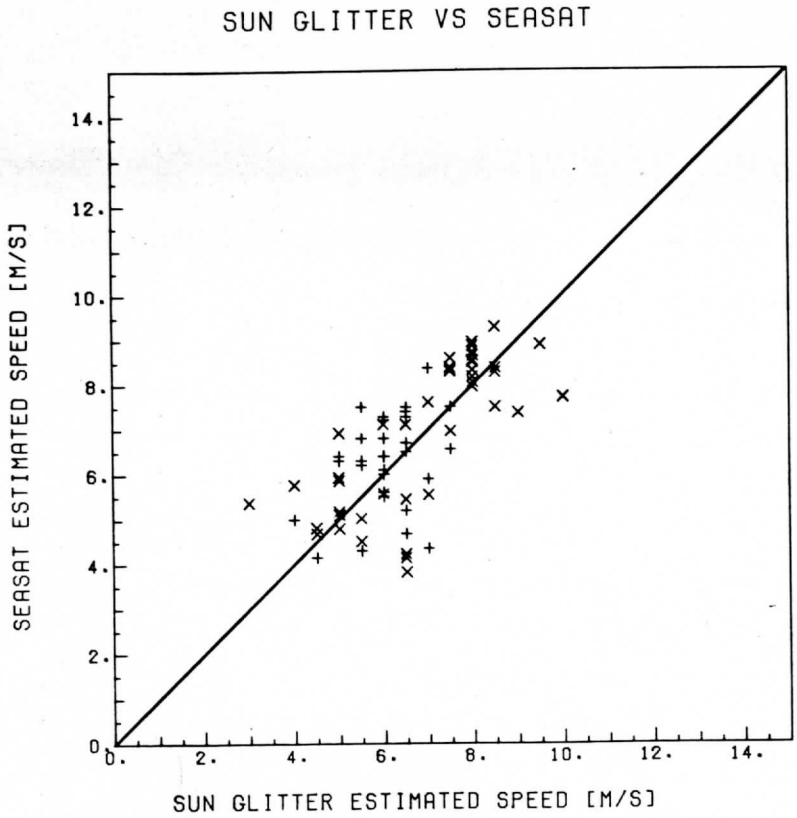

FIG. 5. The comparison of SEASAT wind estimates to the sun glitter wind estimates: (+) Pacific, (×) Atlantic.

tional shear (−3.3° average) which was a result of the unstable boundary layer present and the lower altitudes of the clouds that were found. In the Atlantic directional relationships of wind veering were found for a large majority of comparisons made. Satellite comparisons with ship observations in the Atlantic also found similar veering conditions averaging 16° for the cloud-ship data and 10° for the SEASAT-ship data. The rms scatter per paired comparison was ~16° for cloud-SEASAT, 13° for SEASAT-ships, and 22° for clouds-ships.

The results shown here were better than the cloud-buoy comparison reported by Halpern (1979) because we inspected the satellite-derived wind-field patterns and eliminated one ship report because of obvious error.

6. Areal coverage

An example of the areal coverage that was obtained from all three methods is shown in Figs. 7 and 8 for the Pacific area. Very dense coverage was obtained. Each sensor identified features in the wind field which were unique. They will be discussed individually.

a. Cloud motions

Cloud-motion data produced very smooth flow fields. Southerly winds were found which curved to the northeast near the deep cumulonimbus cells (Cb).

b. SEASAT

When the SEASAT data were added, more details were observed. A shift in the wind direction from southerly to southwesterly was analyzed southwest of the Cb cells. The wind shift analysis was made assuming that a convergent flow into the Cb cells was the most reasonable flow pattern when the SEASAT directional choices deviated from cloud motions. The cloud motions also indicated this directional change but in a more gradual manner. A similar directional shift is evident north of the Cb cells in the Atlantic shown in Fig. 2.

c. Sun glitter

North of the Gallapagos Islands, bright patches were evident on the GOES images (Fig. 8). These patches indicated very low sea states downwind of

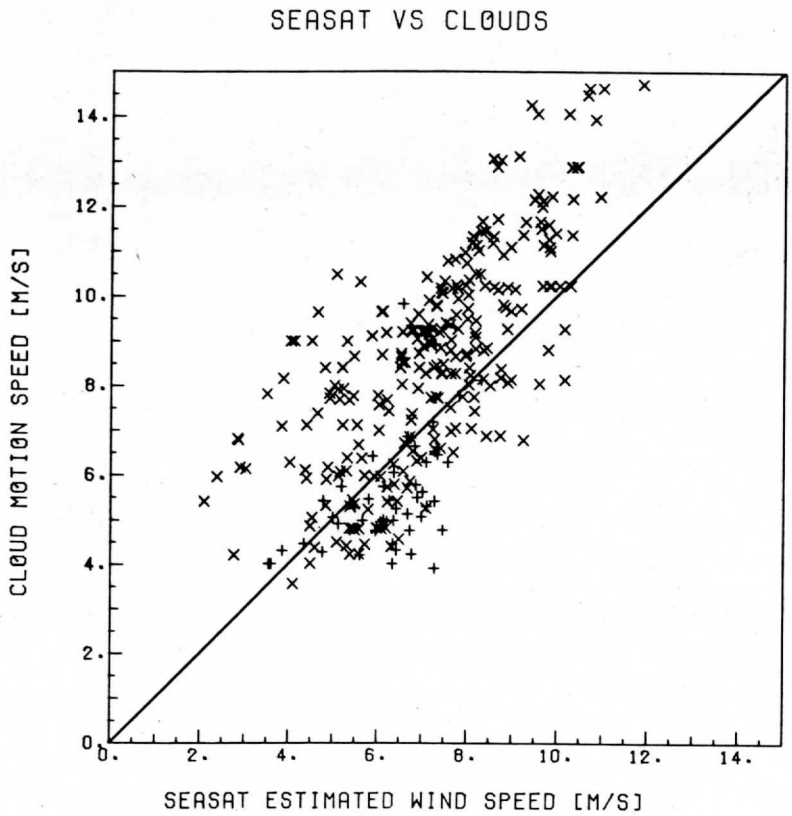

FIG. 6. The comparison of cloud motions to SEASAT wind estimates: (+) Pacific area, (×) Atlantic area.

the major islands. These areas were very dark until the center of the glitter pattern approached. At that time they became very bright. This was expected under low wind conditions because the Cox and Munk relationships predicted a very small and very bright sun-glitter area for low sea states. Under higher wind conditions the surface brightnesses exhibited smaller changes in time because of the wider distribution of the glitter (more reflections from inclined wave surfaces).

In some of the wake regions behind the islands the winds were <5 kt (3 m s^{-1}) because of the blocking of islands. These calm spots have been commonly observed in other island areas. A calm area near one Cb system also was found on an image not used for these comparisons. These GOES data illustrate that very fine detail can be obtained on the stress from the sun glitter.

TABLE 4. The rms deviations (m s^{-1}) of the vector pair differences, i.e., the scatter of one measurement about the other using colocated vector pairs.

Date	Clouds − Sun glitter	SEASAT − Sun glitter	Clouds − SEASAT
16 Jul 78	±1.4	±0.7	±1.9
17 Jul 78	1.5	1.2	1.2
13 Sep 78	0.6	0.9	0.9
16 Sep 78	1.3	1.3	1.3
Atlantic			15.8°
Pacific			14.2°

7. Conclusions

In general, it was found that all three methods could be combined for making detailed data sets because the biases between the methods were small. The preferential sensor would be the SEASAT scatterometer because it was capable of providing data at all latitudes and did not depend on cloud coverage.

TABLE 5. The average differences and scatter between satellite surface wind estimates and merchant ships reports on 16 and 17 July 1978, in the Atlantic area. The scatter (rms deviations) between ship and satellite observations are indicated by ±.

Type	Cloud − ship	SEASAT − ship
Speed (m s^{-1})	1.4 ± 3.3	2.6 ± 2.1
Direction (deg)	16 ± 22	10 ± 13
Number of observations	12	7

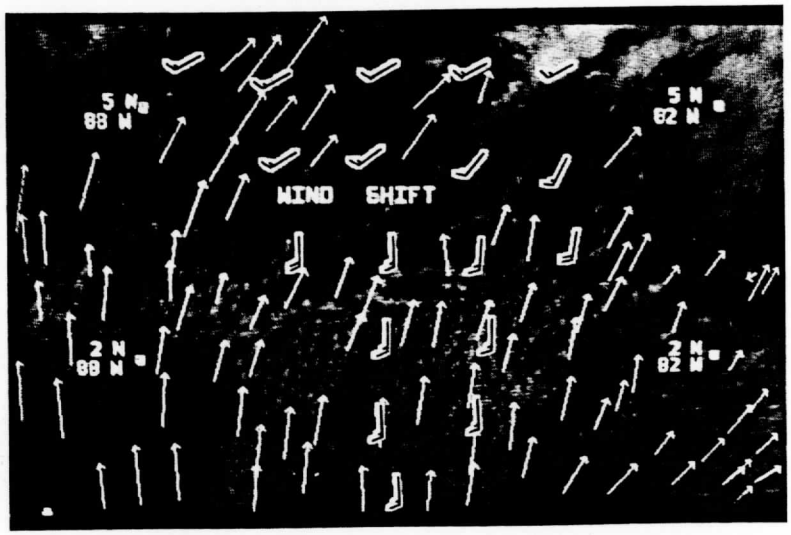

FIG. 7. An example of the wind directional detail contained in the SEASAT data (flags) as compared to cloud motions (arrows). The wind shift area reported by the SEASAT data is labeled.

However, this sensor required data on the general wind direction from an external source. We found that cloud motions could easily provide this information.

In the tropics the polar orbiting SEASAT left gaps between orbits that were equal in size to the swaths covered by the scatterometer. For daily coverage of the tropics other data such as cloud motions or ship reports will be needed to fill in these areas. This could be important for the monitoring of transient storm systems that produce intense wind patterns that deviate from climatological means.

The scatterometer will not be flown again until the next generation of satellites, the NOSS series which will not be launched until 1985 or later. Until that time cloud motions could be used to estimate the surface winds, providing the characteristics of the clouds used as tracers are identified and known.

We have shown that two different cloud fields had two different relationships to the surface wind

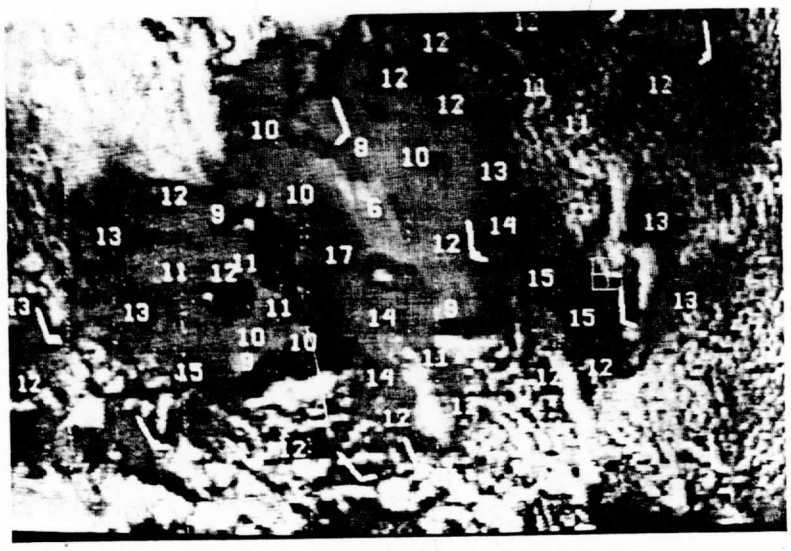

FIG. 8. An example of the detailed wind-speed coverage provided by the sun glitter method in the region of the Gallapagos Islands. Glitter speeds (kt) are indicated numerically. Cloud motions are indicated by the flags. The spot area sampled on the image for the glitter reflection was approximately the same size as the numbers shown and the glitter sample areas were centered on the upper left corner of the numbers.

fields, the Atlantic area versus the Pacific area. Similar differences were found between the tropics and clouds around frontal systems in higher latitudes by Hasler *et al.* (1976, 1979). It is evident that different categories of clouds (trade cumulus, cellular cumulus, etc.) should be studied along with the different characteristics of different geographical areas so that the best possible information can be extracted from the cloud-motion data. Studies of higher wind-speed regimes also are needed for both scatterometer and cloud-motion data.

For more detailed information the sun glitter method can be used. This method is restricted to the tropics but it can provide higher spacial details in coastal areas and around islands where wind fields are very complicated. It also has one advantage over other methods of estimating stress which is shared with the cloud motion measurements—it can be applied to archives of existing operational satellites.

Acknowledgments. The authors are grateful to Professor V. E. Suomi for his encouragement in the course of this work. The computer programming assistance of D. Santek also was greatly appreciated. The advice of Peter Woiceshyn of the Jet Propulsion Laboratory and the SEASAT experiment team provided much helpful insight into sea surface stress measurements that the authors appreciated. This work was funded by NOAA Grant MO-A01-78-00-Y3331 and NSF Grant ATM-79-13097.

REFERENCES

Agee, E. M., T. S. Chen and K. E. Dowell, 1973: A review of mesoscale cellular convection. *Bull. Amer. Meteor. Soc.*, **54,** 1004–1012.

Apel, J. R., 1976: Ocean science from space. *Trans. Amer. Geophys. Union,* **57,** 612–624.

Amorocho, J., and J. J. DeVries, 1980: A new evaluation of the wind stress coefficient over water surfaces. *J. Geophys. Res.*, **85,** 433–442.

Bauer, K. T., 1976: A comparison of cloud motion winds with coinciding radiosonde winds. *Mon. Wea. Rev.*, **104,** 922–931.

Cox, C., and W. Munk, 1954: Measurements of the roughness of the sea surface from photographs of the sun's glitter. *J. Opt. Soc. Amer.*, **44,** 838–850.

Grantham, W. L., E. M. Bracalente, W. L. Jones and J. W. Johnson, 1977: The SEASAT-A satellite scatterometer. *IEEE J. Ocean. Eng.*, **OE-2,** 200–206.

Halpern, D., 1978: Comparison of low-level cloud motion vectors and moored buoy winds. *J. Appl. Meteor.*, **17,** 1866–1871.

——, 1979: Surface wind measurements and low-level cloud motion vectors near the Intertropical Convergence Zone in the central Pacific Ocean from November 1977 to March 1978. *Mon. Wea. Rev.*, **11,** 1525–1534.

Hasler, A. F., W. C. Skillman and W. E. Shenk, 1979: *In situ* aircraft verification of the quality of satellite cloud winds over oceanic regions. *J. Appl. Meteor.*, **18,** 1481–1489.

——, W. E. Shenk and W. C. Skillman, 1976: Wind estimates from cloud motions—Phase I of an *in situ* aircraft verification experiment. *J. Appl. Meteor.*, **16,** 812–815.

Jones, W. L., P. G. Black, D. M. Boggs, E. M. Bracalente, R. A. Brown, G. Dome, J. A. Ernst, I. M. Halberstam, J. E. Overland, S. Peteherych, W. J. Pierson, F. J. Wentz, P. M. Woiceshyn and M. G. Wurtele, 1979: SEASAT scatterometer: Results of the Gulf of Alaska Workshop. *Science*, **204,** 1413–1415.

LeMone, M. A., and W. T. Pennell, 1976: The relationship of trade wind cumulus distribution to subcloud layer fluxes and structure. *Mon. Wea. Rev.*, **104,** 524–539.

Levanon, N., 1971: Determination of the sea surface slope distribution and wind velocity using sun glitter viewed from a synchronous satellite. *J. Phys. Oceanogr.*, **3,** 214–220.

Norton, C. C., F. R. Mosher, B. Hinton, D. W. Martin, D. Santek and W. Kuhlow, 1980: A model for calculating atmospheric turbidity over the oceans from geostationary satellite data. *J. Appl. Meteor.*, **19,** 633–644.

Wylie, D. P., and C. F. Ropelewski, 1980: The GATE boundary layer instrumentation system (BLIS). *Bull. Amer. Meteor. Soc.*, **61,** 1002–1011.

Attachment 2

THE FEASIBILITY OF ESTIMATING LARGE-SCALE SURFACE WIND FIELDS FOR THE SUMMER MONEX USING CLOUD MOTION AND SHIP DATA

DONALD P. WYLIE and BARRY B. HINTON

Space Science and Engineering Center, University of Wisconsin-Madison, Madison, Wis. 53706, U.S.A.

(Received in final form 16 February, 1981)

Abstract. Cloud motion data were compared to ship observations over the Indian Ocean during the summer monsoon, 1 May to 31 July 1979, with the objective of using the cloud data for estimating surface wind and ultimately the wind stress on the ocean. The cloud-ship comparison indicated that the cloud motions could be used to estimate surface winds within reasonable accuracy bounds, 2.6 m s^{-1} r.m.s. speeds and 22° to 44° r.m.s. directions (22° r.m.s. for winds > 10 m s^{-1}). A body of statistics is presented which can be used to construct an empirical boundary layer with the eventual goal of producing a stress analysis for the summer MONEX from cloud motion data.

1. Introduction

A very dense set of cloud motion observations was collected over the Indian Ocean for the summer MONEX program. From these data a highly detailed description of the wind fields during the summer monsoon has been made (Young *et al.*, 1980). Because the atmospheric monsoon has a profound effect on ocean circulations, a logical use of these data is to study the patterns of wind stress on the ocean. In this paper we examine the relationships between cloud motions and low-level winds to develop methods for using the cloud motions for that purpose.

Previous studies of air-sea interactions on synoptic scales (Hastenrath and Lamb, 1979) have been limited to climatological time scales (> 20 yr) because ship data have been too sparse for detailed studies of one season (Ramage *et al.*, 1980). With cloud data, we can focus on the detailed events of one season.

To use the cloud data as estimates of surface winds, we have statistically compared a large volume of cloud observations with ship observations. From these comparisons we have derived relationships that will be used for extrapolating the cloud data to the surface and combining it with ship data. This paper will develop the foundation for future studies of the air-sea interactions during the monsoon of 1979.

2. Data

2.1. Cloud motion data

The cloud motion data set was presented in the atlas compiled by Young *et al.* (1980) for the period 1 May to 31 July 1979. The cloud motions were interpolated to uniform grids at 2° of latitude and longitude spacing using the method described

Boundary-Layer Meteorology **21** (1981) 357–367. 0006–8314/81/0213–0357$01.65.

by Endlich and Mancuso (1968). The observations were weighted according to their distance from each grid point, $w = 4/(4 + R^2)$, where R is the cloud-to-grid distance in degrees. This weighting function roughly approximated a gaussian low-pass filter with a 50% value at 2°, the grid spacing. Only cloud observations within 6° of each grid point were used with a minimum of 2 observations per grid point required. Where these criteria were not met, the grid points were left unfilled. This method avoided problems in interpolating data over large distances. In data rich areas, only the 10 closest observations were used.

All cloud motions below 700 mb were combined into the low-level gridded fields. The cloud motion analyses were made between 830 and 1030 GMT during the period when the entire area was under sunlight. Thus only visible satellite images were used for cloud tracking. A second set of analyses made after dark on infrared images were ignored in this study because the data were incomplete due to several malfunctions in the infrared sensor. The area covered by this analysis was from 30° E to 110° E, 40° N to 40° S (Figure 1). For the comparison to ship data, all land areas, the Red Sea, and the Persian Gulf were ignored.

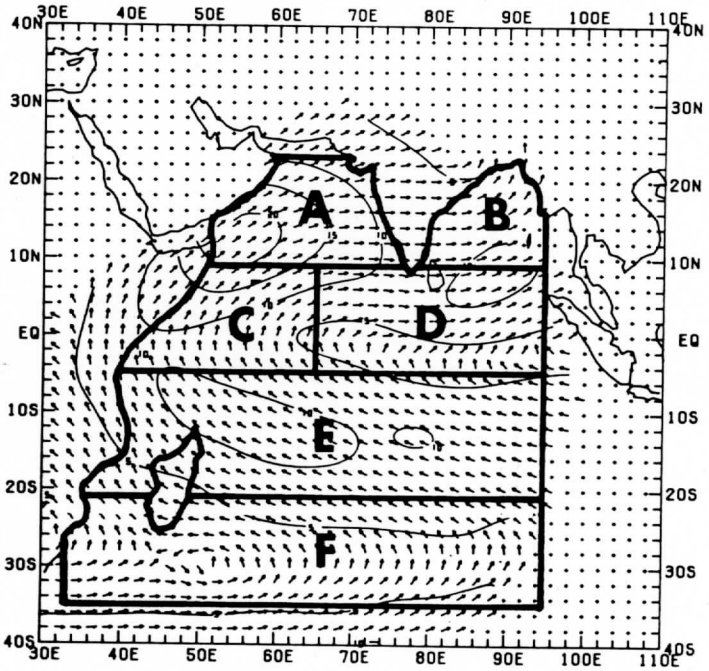

Fig. 1. The area covered by satellite observations of cloud motions for the summer MONEX. Smaller portions indicate local areas studied (see section 4). The portions are: (A) Arabian Sea, (B) Bay of Bengal, (C) Somali Coast, (D) Equatorial Latitudes, (E) Southern Trades, and (F) Southern Mid-Latitudes. The arrows and contours (m s^{-1}) represent the average wind field for the month of July, 1979 from Young *et al.* (1980).

From previous observations, low-level cloud motions have been found to represent the wind fields at their base levels with accuracies ≤ 2 m s^{-1} for tropical

cumulus clouds (Hasler *et al.*, 1976, 1979). Over the Indian Ocean area very similar clouds were found because of similar air-sea temperature relationships. Thus similar accuracies were expected from the MONEX data set.

To evaluate the consistency in the cloud motion measurements, an auto-correlation statistic (C) was evaluated as a function of the distance (d) between the original (ungridded) cloud observations.

$$C(d) = \frac{\frac{1}{M}\sum^{M} U'U'(d)}{\frac{1}{N}\sum^{N} U'^{2}}. \tag{1}$$

The correlation was evaluated for the zonal wind (U) and meridional wind components (V) separately. The means of (U) and (V) in each wind field were removed on a daily basis and the perturbations $U' = U - \overline{U}$ were used in (1). Correlations were calculated at distance intervals of 1° of latitude or longitude. In (1) the sum of the cross-products ($\Sigma U'U'(d)$) for each distance interval were normalized by the total variance of the data set for each day. The average of the daily compiled correlations is presented in Figure 2. Between 700 and 2000 cloud observations made on each day were used.

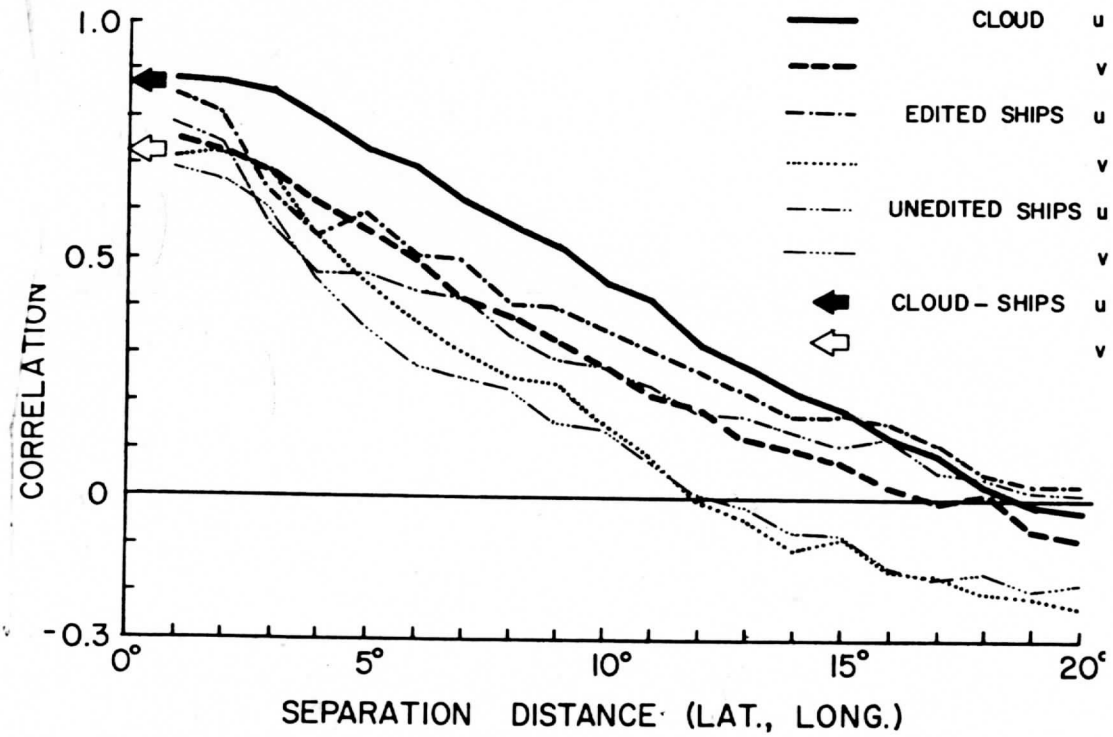

Fig. 2. Spatial correlation functions for cloud motions and ship observations. The editing procedure for ships is described in Section 2. The arrows indicate co-located cloud vs ship correlations.

The correlation functions indicate a high degree of horizontal consistency as shown in Figure 2. Correlations above 0.5 were found up to 6° of distance between observations. The shape of these correlation functions indicates that the cloud motion data depict mainly the large-scale flow features over the ocean; thus the weighting function used in the interpolation scheme should not have changed the spatial patterns of the cloud motion analyses.

2.2. The ship data

The Marine Deck compiled by the FGGE Level II-b Mobile Ship Data Center, Hamburg, FRG, was used as the source of merchant and scientific ship observations for the period studied. All observations reported between 600 and 1200 GMT were used in the area described by Figure 1. Observations at other times of the day were ignored because only cloud motion measurements taken during daylight hours were used. An average of 54 ship reports per day was found in the area studied.

The autocorrelations were calculated for the ship reports in the same manner as done for the cloud motions using (1). The ship autocorrelations were lower than the cloud correlations at all distances. The ship correlations also decreased with separation distance faster than the cloud correlations. This implies that the ship data were more sensitive to small-scale wind variances and that the ship data may have contained some bad reports.

To insure that only valid ship observations were used, these data were edited. Each ship observation was compared to the average of all other reports within 5° of latitude or longitude on the same day. If the reported direction was more than 45° from the vector average wind in the $5 \times 5°$ box or if the reported speed was more than 5 m s^{-1} different than the vector averaged speed, the ship report was discarded. In areas where no other reports could be found for comparision, the reports also were discarded. Unfortunately, about 22% of the data on each day were eliminated by the editing procedure leaving an average of 48 usable ship reports per day. Admittedly some good reports were discarded because of small-scale atmospheric variability or the lack of neighboring reports for verification. We chose the conservative approach, preferring to elimate reports rather than risk using bad ones.

The editing improved the autocorrelations for the ship data (see Figure 2). The ship correlations approached the cloud correlations at close distances ($\leq 1°$) for the (U) component and were slightly better than the cloud correlations for the (V) component. The ship correlations for distances $> 2°$ also improved after editing. These results imply that meaningful comparisons between the ship reports and cloud motions could be made because most of the anomalous data had been removed.

The ship reports were not uniformly distributed over the Indian Ocean (see Figure 3). A large number of reports were found in the Arabian Sea, along the East African Coast and in a line from Shrilanka to Malaysia. A route from Malaysia to

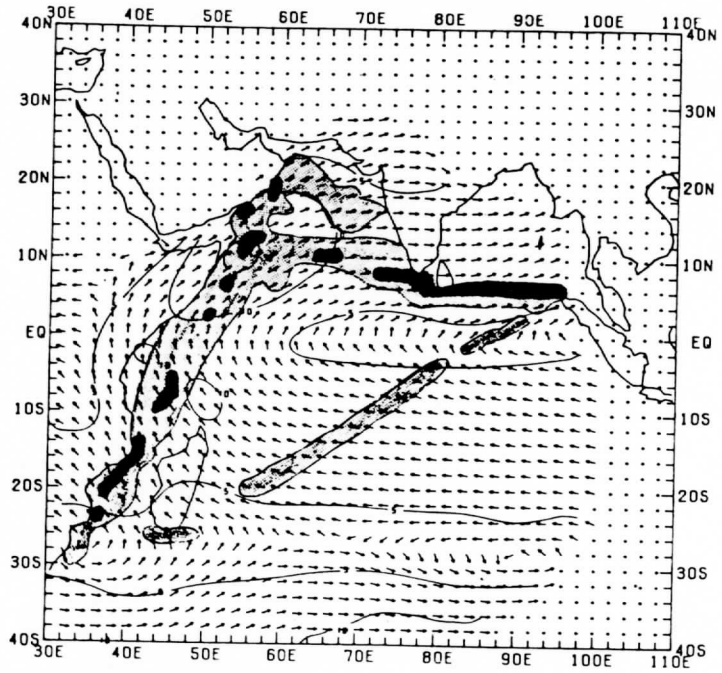

Fig. 3. The number of ship reports used (after editing) for the period 1 May to 31 July 1979. Light shading indicates areas that contain >10 ship reports per 2° square while heavy shading indicates >25 reports. The arrows and contours (m s^{-1}) represent the average wind field for the month of June 1979 from Young *et al.* (1980).

South Africa through the center of the Indian Ocean also had several observations. Very few observations were found outside of these main merchant routes. The uneven distribution of the ship coverage in Figure 3 implies that ship data alone could not provide adequate coverage of the Indian Ocean during this period and affirms the necessity of using cloud motion data.

3. Cross-correlations between Data

3.1. Background

To derive statistical relationships between the cloud motion data and surface winds, a large volume of ship and cloud comparisons were made. The ship reports were compared to the cloud motion values at the nearest grid point to the ship's position. If the grid point did not have any interpolated value because of a lack of cloud motion measurements, then the ship observation was not used. A total of 4293 comparison pairs was found for the 3-month period.

The cross-correlations between the gridded cloud and non-gridded ship data were calculated. For the zonal component (U), a cross-correlation of 0.87 was found, while 0.72 was found for the meridional component (V). These values are indicated

by the arrows on Figure 2. The values were approximately the same as the cloud auto-correlations within 2° of distance, 0.88 for U and 0.75 for V.

Because the speed and direction measurements were made by separate sensors on ships, we shall also discuss scalar comparisons between cloud and ship measured speeds and directions. Ships typically use either an anemometer and vane system, or estimate winds using the Beaufort method. In the data set used, 81% of the observations were made by estimation methods.

3.2. Wind speeds

The relationship between wind speeds measured by ships and clouds (co-located) is shown in Figure 4. It is apparent that the cloud-ship difference, or shear in the

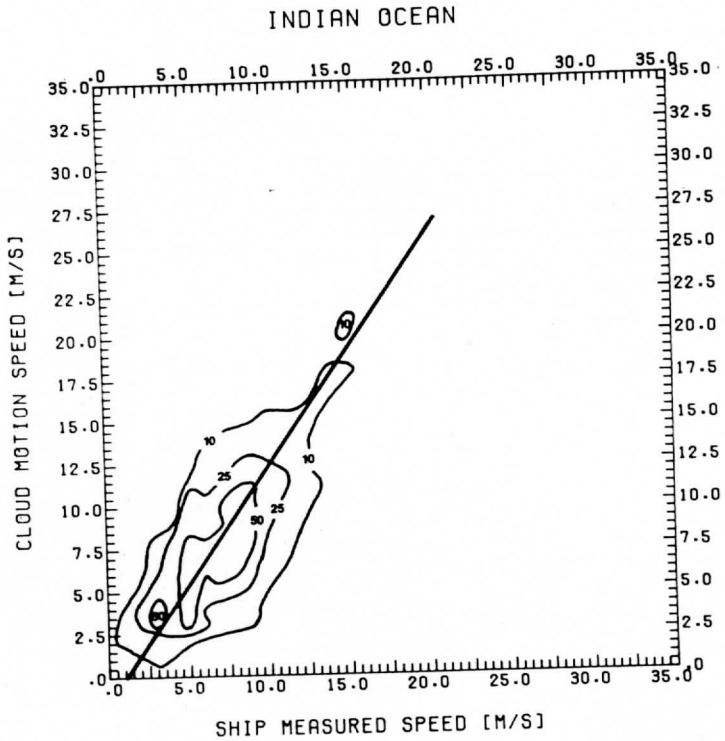

Fig. 4. Scatter plot of the scalar wind speed measurements (m s^{-1}) for ship and cloud motions for the total Indian Ocean and the entire period from 1 May to 31 July 1979. Contours indicate the number of points in 1 m s^{-1} intervals. The linear relationship is described in section 4.

boundary layer increased with wind speed as one would expect. To quantify this relationship, a linear regression was fitted to the data using the least-square method. However, the least-square method reduced the scatter of only one variable around the regression line. The independent variable was assumed to be perfectly known. In reality, neither variable was perfectly measured and scatter existed in both of them, which is typical of most data (Panofsky and Brier, 1968, p. 87). Thus two

regressions of the form $Y = A_{xy}X + B$ could be calculated: one with the cloud measurement as the independent variable (X), and another using the ship measurement as the independent variable. The 'best fit' regression lying somewhere between the two.

As an approximation of the 'best fit' regression, we chose a linear relationship with a slope equal to the ratio of the variances of the two variables.[1] The variances were taken as the root-mean-square of the deviations from the means and the regression was fitted through the means of both variables.

$$S_s = 0.72S_c + 1.2. \tag{2}$$

This regression satisfactorily fits the cloud (S_c) and ship (S_s) speed data (Figure 4). Scatter plots were drawn for separate regions of the Indian Ocean (not shown) but the plots all basically resembled Figure 4. The scatter around (2) was 2.6 m s^{-1} (root-mean-square) for all the data. Therefore we conclude that one relationship adequately describes the speed data.

3.3. Wind directions

Directional measurements were found to have different relationships which were more complicated than the speed data. Cloud ship comparisons were made by subtracting the ship measurements from the cloud measurement. Positive differences indicated frictional veering in the northern hemisphere. In the southern hemisphere frictional considerations implied negative cloud-ship relationships.

The directional differences were found to vary with geographical location, wind speed, and the direction of the basic wind. To find these relationships the Indian Ocean was divided into 6 different areas: Arabian Sea (A), Bay of Bengal (B), the Somali Coast (C), the Equatorial Latitudes (D), the Southern Hemisphere Trade Winds (E), and the Southern Mid-Latitudes (F) (see Figure 1).

The data also were stratified into two classes of wind speeds, ≤ 10 m s^{-1} and > 10 m s^{-1}. The higher wind speeds were found in the strong monsoon currents while the lower speeds were found outside of the strong currents or in the time period before the monsoon developed. The cloud-ship directional measurements for each location, speed class, and basic flow origin are presented in Table I. The data were stratified according to wind direction (direction the wind came from) at the cloud level.

The cloud-ship comparisons in all areas followed one general trend in spite of regional differences. That is, the magnitudes of the cloud-ship differences were smaller for the high-speed group than the low-speed group. This result was expected because the increased shear in the boundary layer found at the higher speeds (Figure 4) increased the turbulent mixing and diminished the secondary circulations. The mixing would tend to couple the cloud levels with the lower level winds.

[1] This procedure was originally used by H. V. Sverdrup, 1916: Druckgradient, Wind und Reibung an der Erdoberfläche. Ann. Hydrogr. U. Marit. Meteorol. 44, 413–427, as indicated by a reviewer of this manuscript.

TABLE I

The directional differences between cloud and ship reports for the Indian Ocean during the period 1 May to 31 July 1979. The cloud-ship comparisons were grouped into quadrants (N, E, S, and W) according to the direction the wind was coming from as defined by the cloud motions. Speed classifications were also based on the cloud motions. The r.m.s. scatter is indicated by ±, and the number of cases in each interval is shown by ( ). Intervals with < 20 cases were left blank.

	Cloud Motion Dir. – Ship Wind Dir.						
	≤ 10 ms^{-1}				> 10 ms^{-1}		
Location	N	E	S	W	E	S	W
A. Arabian Sea	47° ± 58° (72)	33° ± 85° (26)	−5° ± 36° (76)	21° ± 29° (338)	—	—	12° ± 19° (496)
B. Bay of Bengal	—	—	—	33° ± 25° (18)	—	—	10° ± 16° (9)
C. Somali Coast	—	1° ± 48° (37)	−8° ± 30° (243)	11° ± 31° (114)	—	−2° ± 22° (111)	3° ± 13° (108)
D. Equatorial Lat.	24° ± 43° (23)	−13° ± 59° (80)	−8° ± 44° (134)	14° ± 29° (515)	—	—	10° ± 20° (335)
E. Southern Trades	—	−19° ± 24° (380)	−5° ± 23° (279)	—	−14° ± 20° (258)	−5° + 19° (71)	—
F. S. Mid-Latitudes	−39° ± 49° (66)	−12° ± 34° (148)	2° ± 49° (110)	13° ± 89° (56)	−10° ± 18° (34)	3° ± 16° (44)	−3° ± 43° (36)

In general the cloud-ship relationships were indicative of frictional veering as expected. This was the case for the majority of comparisons made, which were westerly winds (wind from the west blowing to the east) in regions (A) and (B). Backing conditions were found in the southern hemisphere in (E) and (F) and for southerly winds that crossed the equator in (C) and (D). Halpern (1979) found similar relationships for the southern hemisphere trades in the Pacific. For winds crossing the equator, Mahrt (1972) has indicated that the southern hemisphere frictional characteristics (backing) are carried acrossed the equator. It also should be noted that the easterlies defined at the cloud level with boundary-layer backing essentially represented a southeasterly flow in the boundary layer. Thus most of the easterlies in (C) and (D) probably represented air of southern hemisphere origin.

3.4. Directional Scatter

The scatter in the cloud-ship direction comparisons was generally under 20° (r.m.s.) for the high-speed group with only one exception where a small number of comparisons were made. For the low-speed group the scatter was higher ranging from 23° to 89°. However, for the quadrants where the predominant wind directions occurred, the westerlies in (A) and (B), the southerlies in (C) and (D), and the easterlies in (E) and (F), the scatter was generally of a reasonable magnitude, ≤ 30° (r.m.s.). These directional quadrants contained the mean winds of the summer

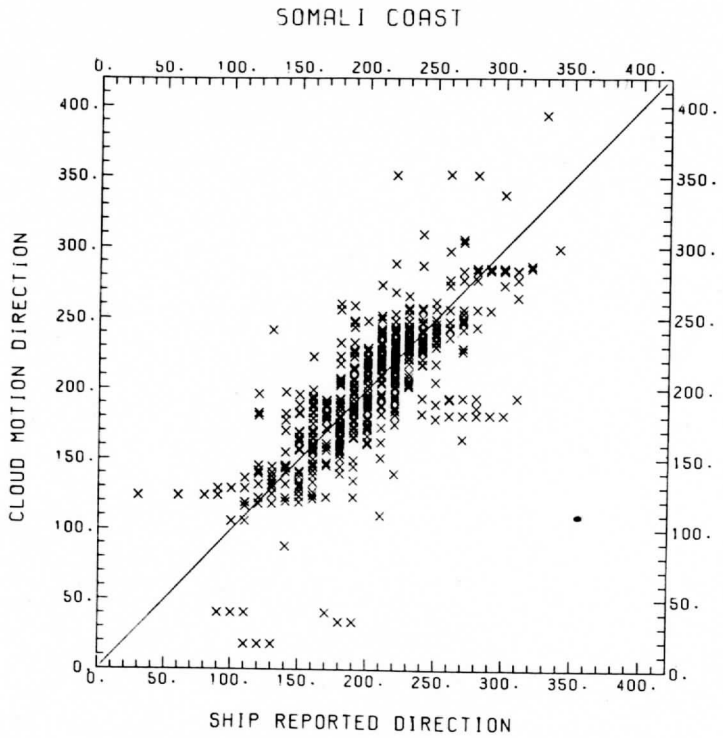

Fig. 5. Scatter plot of the cloud and ship measuted wind directions for the Somali Coast area (see Figure 1). The line is a 1 : 1 relationship.

monsoon (Young *et al.*, 1980) and thus they had a large number of cloud and ship data while the other quadrants had considerably less data.

Scatter plots of wind directions in the Somali Coast area (Figure 5) and the Bay of Bengal (Figure 6) indicate good agreement between cloud and ship measurements for the majority of cases, with a few radical departures. For all of the areas and wind directions, the cloud-ship comparisons average 22° (r.m.s.) of scatter for the high-speed group and 42° (r.m.s.) for the low-speed group.

4. Discussion and Conclusions

It appears that the cloud motion data can be used to estimate surface winds with reasonable accuracies after the mean shear has been removed. The best cloud-ship comparisons were found where the winds exceeded 10 m s^{-1}. This occurred in 20% of the ship data and 36% of the cloud data. This result is encouraging because the higher speeds are more important to the stress analyses. For these conditions we would expect estimations of the surface winds from cloud motions to have accuracies of 22° in direction and 2.6 m s^{-1} in speed.

In general, the accuracy of measuring wind speeds over oceans has usually been between 1.5 and 2.5 m s^{-1}. Using scientific ship measurements, Pierson *et al.* (1980)

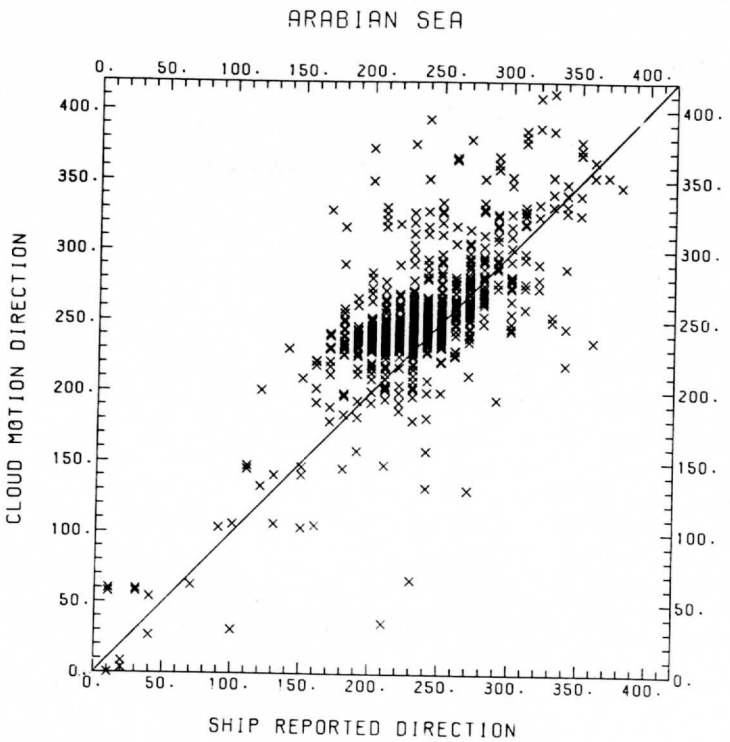

Fig. 6. Scatter plot of the cloud and ship measured wind directions for the Arabian Sea area. The line = 1:1.

found that bridge-measured winds averaged over 2 min deviated from 30 min averages by 1.5 m s^{-1}. This is a result of turbulence in the boundary layer. Wylie *et al.* (1980) also found a 1.5 m s^{-1} r.m.s. difference between wind measurements made by sun glitter reflections off the sea surface and cloud motions. Cloud motions differed from SEASAT microwave surface wind measurements by 1.9 m s^{-1} in the same study. An analysis of 52 soundings made in the Caribbean by the same authors displayed a 2.3 m s^{-1} r.m.s. difference between the 914 m level and the surface even after a mean shear of 1.7 m s^{-1} was removed.

The cloud data also displayed a higher degree of horizontal uniformity (spatial correlation) than the ship data. This probably resulted from the clouds being organized into areas which displayed homogeneous characteristics. The manual method of cloud selection used by the Wisconsin cloud trackers also tended to be weighted toward areas where uniform characteristics were present. The cloud trackers generally avoided areas where chaotic cloud motions existed because the ability of those clouds to represent the synoptic wind field was in doubt. Thus, the cloud data provided a good representation of the general flow.

For the analyses of the stress, we intend to combine both the cloud and ship data. The two will complement each other. The cloud data set is weak near the Arabian coasts because of the lack of clouds, although ship observations were numerous in

the same area. On a few days large directional veering angles between the cloud motions and ship observations were found. The clouds indicated northeasterly motions while the ships reported northwesterly winds. The ship observations can be used to strengthen the stress analysis where observations were abundant.

The clouds in turn provided a wealth of data for the majority of the Indian Ocean which had few or no ship observations. The trade winds and most of the ocean south of the equator and east of Africa were rarely sampled by the ships. The statistics presented in this paper will be used for providing surface wind information in these areas by correcting the cloud motion data for boundary-layer shear.

Acknowledgments

This work would not have been possible without the efforts of Dr Verner E. Suomi in obtaining a geostationary satellite for the MONEX program. His encouragement and advice during the data analysis phase of MONEX is gratefully acknowledged. The authors also appreciate the efforts of Hassan Virgi, Cecil Lo, John A. Young, and many others at the University of Wisconsin who assisted in the analyses of cloud motions during the summer of 1979. This work was supported by grant ATM-79-13097 from the National Science Foundation.

References

Endlich, R. and Mancuso, R.: 1968, 'Objective Analysis of Environmental Conditions Associated with Thunderstorms and Tornadoes'. *Monthly Weather Rev.* **96**, 342–350.

Halpern, D.: 1979, 'Surface Wind Measurements and Low-Level Cloud Motion Vectors near the Intertropical Convergence Zone in the Central Pacific Ocean from November 1977 to March 1978'. *Monthly Weather Rev.* **107**, 1525–1534.

Hasler, A. F., Shenk, W. E., Skillman, W. C.: 1976, 'Wind Estimates from Cloud Motions: Preliminary Results from Cloud Motions-Phase I of an Aircraft Verification Experiment', *J. Appl. Meteorol.* **15**, 10–15.

Hasler, A. F., Skillman, W. C., Shenk, W. E., and Steranka, J.: 1979, 'In Situ Aircraft Verification of the Quality of Satellite Cloud Winds over Oceanic Regions'. *J. Appl. Meteorol.* **18**, 1481–1489.

Hasthenrath, S., and Lamb, P. J.: 1979, 'Climatic Atlas of the Indian Ocean, Part I: Surface Climate and Atmosphere Circulation'. Univ. of Wisc. Press, Madison, Wisc. 97 pp.

Mahrt, L. J.: 1972, 'A Numerical Simulation Study of the Influences of Advective Accelerations in an Idealized Low-Latitude Planetary Boundary Layer'. *J. Atmospheric Sci.* **29**, 1477–1484.

Panofsky, H. A., and Brier, G. W.: 1968, 'Some Applications of Statistics to Meteorology'. Penn. State Univ. Press, University Park, Pa. 224 pp.

Pierson, W. J., Peteherych, S., and Wilkerson, J. C.: 1980, 'The Winds of the Comparison Data set for the Seasat Gulf of Alaska Experiment'. *IEEE J. of Oceanic Eng.* **OE–5**, 169–176.

Ramage, C. S., Adams, C. W., Hori, A. M., Kilonsky, B. J., and Sadler, J. C.: 1980, 'Meteorological Atlas of the 1972–73 El Nino., Dept. of Meteorology, Univ. of Hawaii, Honolulu, Hawaii, 101 pp.

Wylie, D. P., Hinton, B. B., and Millett, K. M.: 1980, 'A Comparison of Three Satellite Based Methods for Estimating Surface Winds over Oceans'. *J. Appl. Meteorol.*, in press (April issue).

Young, J. A., Virji, H., Wylie, D. P., and Lo, C.: 1980b, 'Summer Monsoon Windsets from Geostationary Satellite Data'. Space Science and Engineering Center, Univ. of Wisconsin-Madison, Madison, Wisc. 53706, 127 pp.

Attachment 3

Reprinted from MONTHLY WEATHER REVIEW, Vol. 109, No. 8, August 1981
American Meteorological Society
Printed in U. S. A.

Some Statistical Characteristics of Cloud Motion Winds Measured over the Indian Ocean during the Summer Monsoon

DONALD P. WYLIE AND BARRY B. HINTON

Some Statistical Characteristics of Cloud Motion Winds Measured over the Indian Ocean during the Summer Monsoon

DONALD P. WYLIE AND BARRY B. HINTON

Space Science and Engineering Center, University of Wisconsin–Madison, Madison 53706

14 November 1980 and 21 April 1981

ABSTRACT

Cloud motions over the Indian Ocean for May–July 1979 were used to obtain spatial auto correlations of the deviations of the wind components from local means. Best correlations were associated with u', low altitude clouds and alongwind displacements. Worst correlations arose from v', high clouds and crosswind displacements. The crosswind anisotropy was ~15%. All correlations were 0.49 or greater at 5° separation or less.

1. Introduction

We have examined the spatial correlations of the cloud motion observations made at the University of Wisconsin for the FGGE data set.[1] Our purpose was to determine what scales of atmospheric motion the cloud motions represented and the noise level in these data. Our results provide information useful for developing objective interpolation schemes that will treat these data properly.

The shape of the weighting function is important in the design of an interpolation scheme. Exponential functions, or functions that are close approximations over short distances, are usually used. Endlich and Mancuso (1968) provided for anisotropy by using weighting functions that were elongated in the direction of the wind. But it has been convenient to assume that wind fields are isotropic (Ogura, 1958). A recent study of cloud motions in a limited region by Maddox and Vonder Haar (1979) indicated that they were not. Therefore, we decided to calculate the spatial correlations for a part of the FGGE data set and to test for isotropy.

2. Data used

Cloud motions were measured over the Indian Ocean for the FGGE year at the University of Wisconsin using images from the geostationary satellite positioned near 58°E longitude. The Man Computer Interactive Data Analysis System (McIDAS) was used for tracking the cloud features on the images (Smith, 1975). The technique used at Wisconsin involved a manual selection of the cloud features by an operator viewing the picture who also provided a first guess of the feature's motion. Then the McIDAS software defined the motions more precisely using a cross-correlation algorithm applied to the digital satellite images (Smith and Phillips, 1972). Infrared (IR) geostationary satellite images were used to derive the altitudes of the cloud features. Because of an equipment failure there were periods when the geostationary IR images were not available and the IR sensors on the TIROS-N satellite were used. Other details on the data processing procedures used during FGGE are given by Mosher (1979).

The cloud motions were divided into two groups: low-level clouds with tops below 700 mb altitude (mostly shallow cumuli), and high-level clouds with heights measured from 300 to 100 mb (cirrus or cirrus anvils emanating from cumulonimbi). All cloud features tracked at levels between these two groups were ignored in this study.

Special attention was given to the summer monsoon period from 1 May to 31 July 1979. During this time the wind-tracking effort was doubled to increase the density of observations made over the Indian Ocean. From 600 to 2000 observations were made each day by two groups, one at the Madison campus of the University of Wisconsin and the second at the Milwaukee campus.

We chose to restrict our analyses to the images taken during the daylight hours. A second analysis was made after dark, 12 h later, using only IR images. However, the IR sensor malfunctioned during the summer of 1979 causing a loss of about 60% of the geostationary IR images.

The daytime analysis, in effect, contained cloud motions that were tracked on both visible and IR images, when the IR images were available. The low clouds were best defined on the visible images while high cirrus clouds often appeared to be very dim in the visible images. Where the cirrus clouds existed

[1] FGGE is an acronym for the First GARP Global Experiment where GARP represents the Global Atmospheric Research Program. FGGE is sometimes referred to as the Global Weather Experiment.

0027-0644/81/081810-03$04.75

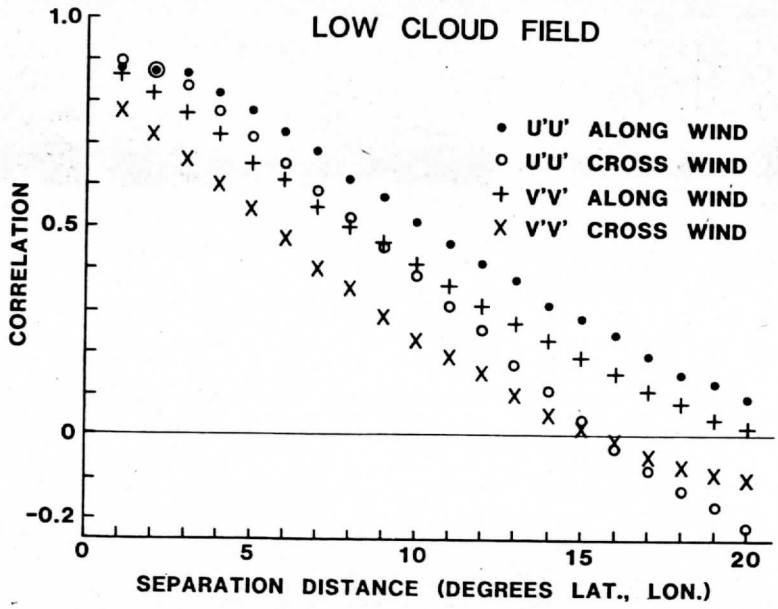

FIG. 1. The correlation of low-cloud motions (below 700 mb) measured over the Indian Ocean during the summer monsoon, 1 May–31 July 1979.

the operators had the option of tracking them on the IR images if they could be more clearly identified. Thus to make the cloud motion analyses the operators switched to the image type that best defined each cloud tracer.

From these cloud motion observations we calculated the spatial autocorrelations for each day available from

$$C = \frac{\Sigma U'U'(d)}{\Sigma U'^2} . \quad (1)$$

The correlations (C) were calculated for both the zonal (U) and meridional (V) components of the wind after removing the means of the data for each day, i.e., $U' = U - \bar{U}$. The zonal and meridional means ($\bar{U}$ and $\bar{V}$) were derived separately for each day's wind analysis. The correlations were calculated as functions of the distance (d) between observations. Each correlation was normalized by the total variance of the variable ($\Sigma U'^2$ or $\Sigma V'^2$) on a daily basis.

To determine the degree of anisotropy displayed by these data we divided the correlations [$\Sigma U'U'(d)$ or $\Sigma V'V'(d)$] into two groups: those displacements (d) aligned within ±20° of the mean wind direction, and those aligned within ±20° normal to the wind. The direction was defined for each $U'U'$ or $V'V'$ pair using the gridded value presented in the atlas of Young *et al.* (1980), at a location half-way between the two observations. The gridded values were derived from 2–10 winds within 6° radius of each grid point using the method of Endlich and Mancuso (1968). Grids were calculated at 2° latitude and longitude spacing.

3. Discussion

The spatial correlations for each of the 91 days examined were averaged to form the mean correlations for the 3-month period (Figs. 1 and 2).

It is apparent from the figures that the cloud motion data contain a high degree of horizontal consistency. The spatial correlations decreased slowly with distance between observations. This factor is partially the result of the method of analysis used at Wisconsin. The analysts who manually selected cloud tracers and edited the motion calculations tended to emphasize the large-scale characteristics of the wind fields. They were inclined to select only clouds that conformed to their view of the large-scale pattern.

The correlations show that the data are slightly anisotropic. The cross-wind correlations were 10–15% less (in variance) than the along-wind correlations. This difference was most notable at separation distances > 4°. The high-level winds exhibited slightly less difference between the along-wind and cross-wind directions.

The high-cloud fields had lower correlations than the low-cloud fields, in general. This result may have been an effect of the type of clouds tracked at each level. Low-cloud fields consisted primarily of trade wind cumulus or similar small cumulus clouds which were abundant over large areas and moved with uniform characteristics. The high-cloud tracers, on the other hand, were mainly cirrus fragments moving away from cumulonimbi cells or detached cirrus patches. Their organization was different than the low clouds because of the divergence caused by expanding anvils in large-cloud systems. It is sus-

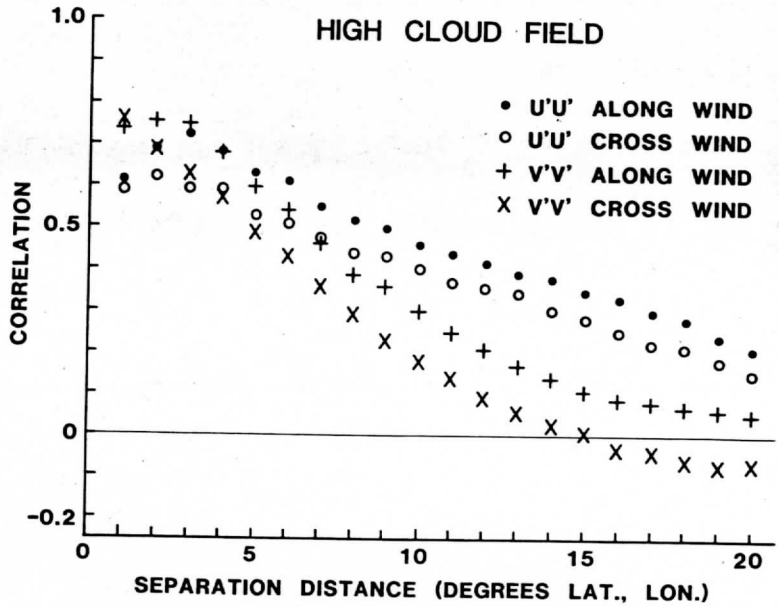

FIG. 2. The correlation of high-cloud motions (300–100 mb) measured over the Indian Ocean 1 May–31 July 1979.

pected that the true level of the winds that each high-cloud tracer represented also varied over the high-cloud field. This would have decreased the correlation because our definition of the high clouds included a deep layer, 300–100 mb.

The overall variances in the wind components at $<1°$ separation distance were considerably larger for the high clouds than the low clouds. These were 164 $m^2\ s^{-2}$ for U and 58 $m^2\ s^{-2}$ for V in the high clouds and 61 $m^2\ s^{-2}$ for U and 21 $m^2\ s^{-2}$ for V in the low clouds. Thus the high-cloud data contained more variable structure or noise than the low-cloud data.

4. Conclusions

From these statistics we conclude that the degree of anisotropic behavior of the cloud data was small. Anisotropic weighting functions are not necessary for these data if synoptic-scale flows only are considered. The cloud motions in general displayed a high degree of consistency between observations within 5° of latitude or longitude as evident from the shape of the correlations. Thus for defining the synoptic-scale wind fields the cloud motion observations can be directly used without extensive smoothing or editing procedures.

Acknowledgments. The authors appreciated the advice of Dr. J. H. Chu on the interpretation of statistical functions. This work was funded by NSF Grant ATM-79-13907.

REFERENCES

Endlich, R., and R. Mancuso, 1968: Objective analysis of environmental conditions associated with thunderstorms and tornadoes. *Mon. Wea. Rev.*, **96**, 342–350.

Maddox, R. A., and T. H. Vonder Haar, 1979: Covariance analyses of satellite-derived mesoscale wind fields. *J. Appl. Meteor.*, **18**, 1327–1334.

Mosher, F. R., 1979: Cloud drift winds from geostationary satellites. *Atmos. Tech*, No. 10, 53–60. [NCAR, unpublished].

Ogura, Y., 1958: On the isotropy of large-scale disturbances in the upper atmosphere. *J. Meteor.*, **15**, 375–382.

Smith, E. A., and D. R. Phillips, 1972: Automated cloud tracking using precisely aligned digital ATS pictures. *IEEE Trans. Comput.*, **C-21**, 715–729.

Smith, E. A., 1975: the McIDAS system. *IEEE Trans. Geosci. Electron.*, **GE-13**, 123–136.

Young, J. A., H. Virgi, D. P. Wylie and C. Lo, 1980: Summer monsoon wind-sets from geostationary satellite data. Space Science and Engineering Center, Madison, 127 pp.

Attachment 4

The Wind Stress Patterns over the Indian Ocean During the Summer Monsoon of 1979

Donald P. Wylie
Barry B. Hinton

Space Science and Engineering Center
University of Wisconsin-Madison
Madison, Wisconsin 53706

March 1981

Abstract

A detailed analysis of the wind stress patterns over the Indian Ocean were made from 1 May to 31 July 1979. A combination of cloud motion and ship data were used to diagnose the surface wind patterns to a degree of detail that was not possible in the past for one individual season. These data showed how the monsoon developed and the fluctuations of the Somali Jet and the southern hemispheric tradewinds. Also discussed are the wind stress patterns exerted by two traveling tropical storms which combined together to exert an abnormally high westerly wind stress on the equator before the monsoon developed.

1. Introduction

To quantitatively understand and model ocean circulations, detailed data on the wind stress, the primary forcing mechanism, are needed. During the World Weather Watch of FGGE[1] and the joint summer MONEX programs a (Fein and Kuettner, 1980) unique set of wind observations were obtained from tracking cloud motions (Young et al., 1980) over the Indian Ocean. Thus a logical use of these data would be to estimate the patterns of wind stress on the ocean. This is precisely the intent of this paper.

Previous studies of wind stress patterns have been limited because of the lack of data. Ship observations and scientific expeditions have provided a sparse collection of wind data from which wind patterns can be inferred but not at a density for detailed studies of the patterns over whole ocean basins. Perhaps the best data on stress patterns over the Indian Ocean are the climatologies that were compiled by Hastenrath and Lamb (1979), Hellerman (1967), and Bruce (1978) by compositing many years (approximately 20 to 60) of merchant observations. While these climatologies depict the general nature of the wind patterns, they can not give quantitative details on the events of one season in one year.

The FGGE and MONEX experiments provided large volumes of atmospheric and oceanic data over the Indian Ocean during the summer monsoon of 1979. In this paper we will focus on the development of the summer monsoon. We have made wind stress analyses on a daily basis from 1 May to 31 July 1979. The intent of this exercise was to provide a quantitative wind stress data set for the benefit of other studies, both diagnostic and modelling, of the Indian Ocean that will use the MONEX data.

---

[1] FGGE stands for the First Garp Global Experiment where GARP stands for Global Atmospheric Research Program.

2. The data used

For our stress analyses we have combined data from two complimentary sources: the cloud motion observations and the merchant ship reports. This combination was made to alleviate the problems caused by the weaknesses in each type of data and to provide a composite analysis that depicted the strengths of each data. For example, the cloud motions provide good coverage over most of the Indian Ocean except for the northern parts of the Arabian Sea and the Bay of Bengal. In the beginning of the study period, the first two weeks of May, there were few clouds in these areas and thus we did not obtain a good analysis of the wind fields during that time.

The merchant ship routes, fortunately, crossed the areas where the cloud motion coverage was poor. Thus by combining these data we were able to better define the wind patterns above what could have been obtained from either data source by itself. The methods used for compositing these data and correcting the cloud motions for wind shear in the atmospheric boundary layer are described as follows.

a. The cloud motion data

Cloud motions were tracked on the images made by the geostationary satellite (a standard United States GOES model) positioned over the Indian Ocean at approximately 57° East longitude. All cloud motion data were obtained by manual operators selecting cloud tracers at the Madison and Milwaukee campuses of the University of Wisconsin using the Man-Computer Interactive Data Analysis System (McIDAS).

For cloud tracking, a series of three satellite images were used taken at 0.5 h intervals in the time period from 830 to 1100 GMT. This period was during the daytime when the visible satellite images could be used. A second cloud motion analysis was made 12 h later using infrared

images, however, a malfunction in the sensor caused the loss of the infrared images during approximately 60% of the days studied. Because the infrared analysis was incomplete, we used only the once per day cloud motion analysis obtained from the visible data.

For each cloud tracer tracked, two motion vectors were calculated using the three pictures in the sequence. The cloud displacements were derived from correlation algorithms using the digital satellite data and a first guess of the cloud's movement provided by the operator. Quality control editing was automatically applied in the correlation algorithm. In addition, the two vectors derived for each cloud were compared for a consistency check on the algorithm. Additional data quality checks were manually made by the target selection operator who inspected each calculation with the satellite image sequence immediately after it was made. In the final analysis all vector pairs that passed all the quality controls were averaged together to form one motion vector for each cloud tracer. More details on the Wisconsin wind analysis system are given in Mosher (1979).

During the period 1 May to 31 July 1979 approximately 800 motion vectors per day were extracted from the low level cloud fields. The area cover by the cloud tracking system was from 40°E to 110°E longitude and 40°N to 40°S latitude. These vectors were interpolated to a 2° latitude by 2° longitude grid inside this area using the method of Endlich and Mancuso (1968). The resulting grids were presented in an atlas by Young, et al., (1980).

The method of interpolation used weighting functions for each motion vector that were a function of the distance from the vector to the grid point (R in °).

$$w = 4./(4. + R^2) \qquad (1)$$

This function approximated a gaussian low pass filter with a 50% or less value given to all vectors that were more than 2° from the grid point. Only the vectors within 6° of each grid point were used. Where less than 2 vectors inside this area were found, the grid points were not filled.

For the wind stress analyses, the study area was restricted to the central Indian Ocean from the East African coast to 96°E longitude and from the Southern Asian coast to 32°S latitude. The Red Sea and the Persian Gulf also were excluded from this study.

b. The ship data

The marine deck compiled by the FGGE level IIb mobile ship data center in Hamburg, FRG was used as the source of ship data for this analysis. An average of 177 observations per day were found in the Indian Ocean. For the daily surface wind analysis all ship reports taken from 00 to 2100 GMT on each day were used. The satellite analysis was made in the middle of this time period.

To weed out the bad ship reports an automatic editing function was applied to the ship data on a daily basis. Each ship report was compared to the average of all of the other ships within 5° of latitude or longitude. If the ship report differed by more 45° in wind direction or 5 m s^{-1} in speed from the vector average of the other ships, than the report was eliminated from the data file. A minimum of two external reports were required to define the wind average around each individual report being examined. In areas where less than two neighboring reports were found, the report also was deleted. This editing procedure eliminated an average of 13% of the ship reports on each day studied.

3. The method of data combination

In order to use the cloud motion data as estimates of the surface

winds, corrections had to be applied for the wind shear in the atmospheric boundary layer below the clouds. These corrections were empirically derived by comparing co-located ship and cloud observations (see Wylie and Hinton, 1981). Each ship observation that passed the editing procedure was compared to the cloud motion analysis at the nearest grid point. A total of 4293 cloud-ship comparison pairs were found for the three month period. From these intercomparisons statistical relationships between the cloud motion and ship reported winds speeds and directions, were derived.

For the wind speeds a linear relationship was used to account for the sub-cloud shear.

$$S_{sfc} = 0.72S_{cld} + 1.2 \qquad (2)$$

This relationship fit the cloud-ship comparisons with an average root mean squared scatter of 2.6 m s^{-1}.

The cloud-ship directional relationships were found to be more complicated. They varied with latitude, direction of the basic flow, and wind speed. The corrections for the cloud direction were derived in six geographical areas that were mainly divided by latitude. Distinctions as to which of four quadrants the winds were coming from also were made, however, in some areas the wind directions were mostly in one quadrant and a meaningful statistic for the other quadrants could not be obtained. Where this situation occurred, the directional corrections were assumed (see Table 1).

The directional corrections applied ranged from -47° in the northern hemisphere to +14° in the southern hemisphere. For the higher wind speeds, cloud motions >10 m s^{-1}, the directional corrections were smaller ranging from -12° in the Arabian Sea to +14° in the southern hemisphere trades. In general, the cloud-ship directional scatter also was lower for the

intercomparisons made under the higher wind conditions (see Wylie and Hinton, 1981). Thus we feel our analyses are more accurate in the areas where high winds occurred than where light winds were found.

After correcting the cloud motion grids for boundary layer shear, the ship data were added. The ship reports were interpolated to the grid points using the same weighting function as used to make the cloud motion grids (1). The cloud motion value at each grid point was added to the interpolated sum with a relative weight of 0.5. Thus for grid points where only one ship report at 2° distance were found, the ship report and the cloud motion analysis were weighted equally. For grid points where one or more ship reports closer than 2° distance were found, the ship reports dominated the interpolated value. Where no ship reports within 6° of latitude or longitude were available, the cloud motion analysis (corrected for shear) was used exclusively.

The ship reports were concentrated along the lines of the main merchant routes. Most of the reports were found along a line from Malaysia to Sri Lanka to the Red Sea acrossed the Northern Indian Ocean. Several reports also were obtained north of this line in the Arabian Sea. A second route along the East African Coast also contained several reports each day. A minor trade route from Malaysia to South Africa through the center of the Indian Ocean occasionally contained reports on some of the days analyzed. Outside of these areas few ship data were found and the wind analyses made were primarily from the cloud motion data. More details on the locations of the ship data can be found in Wylie and Hinton (1981).

The daily surface wind analyses produced from the cloud-ship combination were converted to surface stress (τ) estimates using the bulk aerodynamic

formula.

$$\tau = \rho C_d U^2 \qquad (3)$$

Where (U) is the wind speed and (ρ) is the air density which was assumed to vary with latitude from 1.16 kg m^{-3} at 20°N to 1.21 kg m^{-3} at 30°S. A drag coefficient that was a linear function of wind speed, $C_d = (0.8 + 0.065U)\ 10^{-3}$, was used following the recommendation of Wu (1980).

4. Monthly mean patterns

a. May 1979

During May the easterly tradewinds from 5°S to 25°S were strong throughout the entire month (Fig. 1). Two areas of noticeably high winds were: off the north coast of Madagascar and on the eastern side of the Indian Ocean at 15°S and 90°E. North of Madagascar, the winds were consistently from the southeast while upwind on the eastern side of the study area the winds were somewhat enhanced by a travelling vortex that appeared early in May. This vortex will be discussed in further detail in the next section.

In the Arabian Sea the winds were very weak throughout the month. Although the wind direction had shifted to approximately the expected direction of the monsoon, from the southwest (Hastenrath and Lamb, 1978) little stress on the ocean was apparent over entire Arabian Sea.

In the Bay of Bengal the wind directions corresponded to the mean of the summer season also with very low magnitudes. However, convective disturbances were present in this area which caused a large variability in the wind directions resulting in a weak mean stress.

In comparison to the Hastenrath and Lamb (1979) climatology we found

the May 1979 trades to be nearly the same strength. In the Arabian Sea, however, the climatology indicated substantially strong ($\simeq$7 m s^{-1} maximum) southwest winds while our analysis found only light winds during the month. This could be a reflection of the later than normal onset of the monsoon during the 1979 season (Fein and Kuettner, 1980).

b. June 1979

During June the monsoon developed to nearly full strength (Fig. 2). The southwesterly winds in the Arabian Sea developed into the very strong "Somali Jet" with cloud motions often in excess of 25 m s^{-1}. At the surface our analysis estimated the stress to be in excess of 0.3 N m^{-2} (3 dynes cm^{-2}).

The Somali Jet appeared more vividly in our stress analyses than our surface wind analyses because the stress was, in effect, a cubic function of the wind speed. When the quadratic aerodynamic stress parameterization (3) was combined with a drag coefficient that was a linear function of wind speed, the stress increased with the cube of the speed. Hence, the areas of strong winds exerted a larger force on the ocean than was apparent from looking at the wind analyses by themselves.

The stress exerted by the trade winds south of the equator was also stronger in June than in May. Most of the area had an average stress $\geq$ 0.1 N m^{-2} ($\geq$ 1 d cm^{-2}).

The June 1979 tradewinds were approximately the same strength as the Hastenrath and Lamb climatology. The Somali Jet , however, was weaker than the climatology partly due to the late development of the monsoon.

c. July 1979

During July the Somali Jet was even stronger than in June with the maximum stress exerted being >0.45 N m^{-2} (4.5 d cm^{-2} see Fig. 3). A clear

"S" shaped pattern of the winds over the Indian Ocean was present. Below 20°S the winds came from a southerly direction, than turned toward the west in the trades. The trades curved toward the north at the equator and turned to the northeast in the Arabian Sea and Bay of Bengal. The average stress exerted by the trades also increased east of Madagascar to >0.15 N m^{-2}.

The "S" shaped pattern was very similar to the climatological wind pattern shown in Hastenrath and Lamb (1979). The magnitude of the July averaged Somali Jet also was close to the climatological average. The only area where the July 1979 analysis noticeably differed from the climatology was the southern hemisphere trades which were slightly weaker.

5. Temporal changes in the stress patterns

To present a record of the temporal variations of the stress we have compiled a series of 10 day average stress maps (Figs. 4-12). Each 10 day average was made from the daily calculations of the stress on the 2° x 2° grids as previously discussed.

In the first 10 day period in May two storm systems were present in the eastern Indian Ocean. A tropical storm in the northern hemisphere moved along a track from a position at 4°N and 92°E on 1 May toward the northwest reaching India on 11 May at 13°N and 80°E. At the same time a companion vortex moved westward very slowly from a position of 5°S and 92°E on 1 May to a position of 6°S and 88°E on 8 May.

The northern storm system exhibited many cirrus anvils on the satellite images (see the Young, et al., 1980, atlas, or the note by Rao, 1980) indicating that many cumulonimbus clouds were present. In contrast to the northern storm, the southern storm had far fewer cirrus anvils associated with it.

From 8 May to 17 May the cirrus clouds associated with the southern vortex disappeared but the vortex moved westward and at a faster speed. It was last diagnosed as a vortex on the wind analyses on 17 May at 4°S and 68°E.

As a result of having two large vortexes positioned approximately 10^{o} of latitude appart in two different hemispheres, a strong westerly wind developed between the storms. The two vortexes rotating in opposite directions, added in strength at the equator. A westerly jet appeared on the wind analyses at the equator and 82°E reaching a maximum strength of 12 m s^{-1} on 5 May. Some variance in the diagnosis of the jet and the vortex from day to day was present in our analyses because of sampling problems. Obscurations of the low cloud motions by cirrus clouds prevented detailed analyses on some of the days during this period. Thus the 10 day averaged stress of 0.15 N m^{-2} shown in Figure 4 may have been a slight under estimate of what actually occurred.

Outside of these storm systems, the wind analyses were seldom obscured. The trade winds in the southern hemisphere, in particular, were well diagnosed by a large sample of low level clouds and the Arabian Sea was adequately covered by the merchant ship reports.

In the second 10 day period (11-20 May, Fig. 5) the trade winds remained strong on the eastern side of the ocean along a line from 80°E to 90°E, at 18°S. This area was south of the southern vortex and thus it probably was enhanced by the vortex. In the Bay of Bengal a stronger southwesterly flow also appeared from 11 to 20 May. Prior to this time the flow a appeared to be unorganized in this area.

From 21 to 30 May (Fig. 6) the trade winds diminished in strength compared to the previous 10 days. The vortex in the southern hemisphere was no longer

found on the daily analyses. Along the equator southerly and southeasterly winds were found where southwesterly winds were present, east of 65°E, in the preceding period. In the Arabian Sea a weak anticyclonic vortex continued while in the Bay of Bengal the southwesterly winds diminished in strength.

From 31 May to 9 June (Fig. 7) the stress pattern was similar to the preceding periods. The trade winds appeared to increase slightly over the previous 10 day period.

The strong southwesterly winds of the Somali Jet first appeared on 12 June (Fig. 8). The 10 to 19 June period depicted the full monsoon pattern with a very strong jet east of Africa at 8°N and 52°E, with stress > 0.35 N m^{-2}. The southwesterly winds in the Bay of Bengal also appeared to increase in strength. South of the equator, the trades remained at nearly the same strength.

The period from 20 to 29 June (Fig. 9) exhibited the highest wind stress in the Somali Jet, 0.6 N m^{-2} at 12°N and 60°E. The center of the jet moved northeast (downwind) from its position in the previous period. The entire Arabian Sea was dominated by strong southwesterly winds. The southwesterly winds in the Bay of Bengal also peaked in strength during this period exerting a maximum stress of 0.3 N m^{-2}.

In contrast to the high winds in the northern hemisphere, the southern hemisphere trades weakened in intensity.

From 30 June to 9 July (Fig. 10) the trades increased in strength while the winds in the northern hemisphere decreased in strength. During the period of strong trade winds, the highest stress values were found to the east of Madagascar. In all the previous analyses the trade winds peaked in two locations: north of Madagascar, and on the eastern side of the Indian Ocean. This period exhibited a change in the pattern of the trades with the strongest winds being on the western side of the ocean.

From 10 to 19 July (Fig. 11) the trades weaken in strength. However, the largest change was in the Bay of Bengal where the southwesterly winds dropped to the intensity levels that existed before the monsoon developed. The Somali Jet exhibited only a slight decrease in strength during this period.

From 20 to 29 July (Fig. 12) the Somali Jet increased in strength and its center shifted slightly to the southwest (upwind) by 2° of latitude and longitude to 10°N and 56°E. Also of important was the extension of the westerly winds in the northern hemisphere acrossed the equator in the center of the ocean from 70°E to 80°E. The east-west line that separated the easterly trades from the westerlies appeared to migrate south during this time. The trades south of the equator increased in strength from 20 to 29 July inspite of the shift of the westerlies.

6. Curl of the stress

The curl, $\nabla \times \tau$, of the stress fields was evaluated on each daily analysis made. Monthly averages of the curl patterns are presented here which were made by averaging the daily analyses.

a. May 1979

During May the curl was strongest in the area of the vortex that was found in the southern hemisphere as previously discussed (see Fig. 13 at 6°S and 88°E). A persistent band of negative curl extended acrossed the whole width of the southern hemisphere from the equator to 12°S. This was a reflection of the turning of the trade winds toward the north shown in Fig. 1.

Around the eastern coast of India a strong positive curl was found resulting from the southwesterly winds in the Bay of Bengal which were

strongest near the center of the Bay.

In the Arabian Sea the curl was extremely small because of the light wind conditions that existed there during the entire month.

b. June 1979

During June the dominant feature was the Somali Jet as shown in Fig. 2. The curl depicted strong anti-cyclonic values (-) to the southeast and strong cyclonic values (+) to the northwest (Fig. 14). The contours between these extremes depicted the axis of the Jet.

An area of strong (-) curl also was found at 3°S and 82°E where the easterly trades turned toward the north. The belt of turning winds (to the north) in general exhibited moderate values over most of the area between the equator and 12°S.

Also of importance was the increase in (+) curl along the eastern coast of India which resulted from the strengthening of the winds in the Bay of Bengal.

c. July 1979

In July the (-) curl southeast of the Somali Jet was even stronger than in June. On both sides of this jet the gradient in wind speeds was larger than in the previous month as evident by the curl patterns.

The latitudinal belt where the trades turned north exhibited a near uniform curl acrossed the whole ocean with no obvious areas of maxima.

The (+) curl on the eastern coast of India also decreased reflecting the weakening of the winds in the Bay of Bengal during the month.

7. Summary and discussion

By comparing our analyses for the monsoon of 1979 with the Hastenrath

and Lamb (1979) climatology, areas where major differences from the long term mean became apparent. The most notable differences were found in May. The Somali Jet was completely absent during May of 1979 which deviated from other years when early onsets of the monsoon occurred.

The second major deviation from the climatology was the strength of the trades in the eastern Indian Ocean, also during May and the strong westerly Jet that occurred on the equator in the early part of the month. The strong vortex in the southern hemisphere that was found was not as evident in the climatological average.

Also worth noting was the strengthening of the southern hemispheric trades that occurred when the Somali jet decrease slightly from 30 June to 9 July (Fig. 10). Later when the jet was at it strongest intensity, 20-29 July (Fig. 12), the trades had weakened slightly. This indicates a possible opposite phase oscillation between the two hemispheres.

As a final note, the extremely high stress values exerted by the Somali Jet are a marvel in themselves. Because of the cubic relationship between wind speed and surface stress, the jet exerted over 3 times the stress of the southern hemispheric trades.

Acknowledgements

The authors are grateful to the FGGE wind trackers at Wisconsin for their conscientious efforts in interpreting the satellite imagery into meaningful wind analyses. Without their efforts the stress analyses would have been more difficult. The help of Cecil Lo and Hassan Virgi in developing the gridding techniques was also appreciated. This reasearch was funded by NSF gout ATM79-13097.

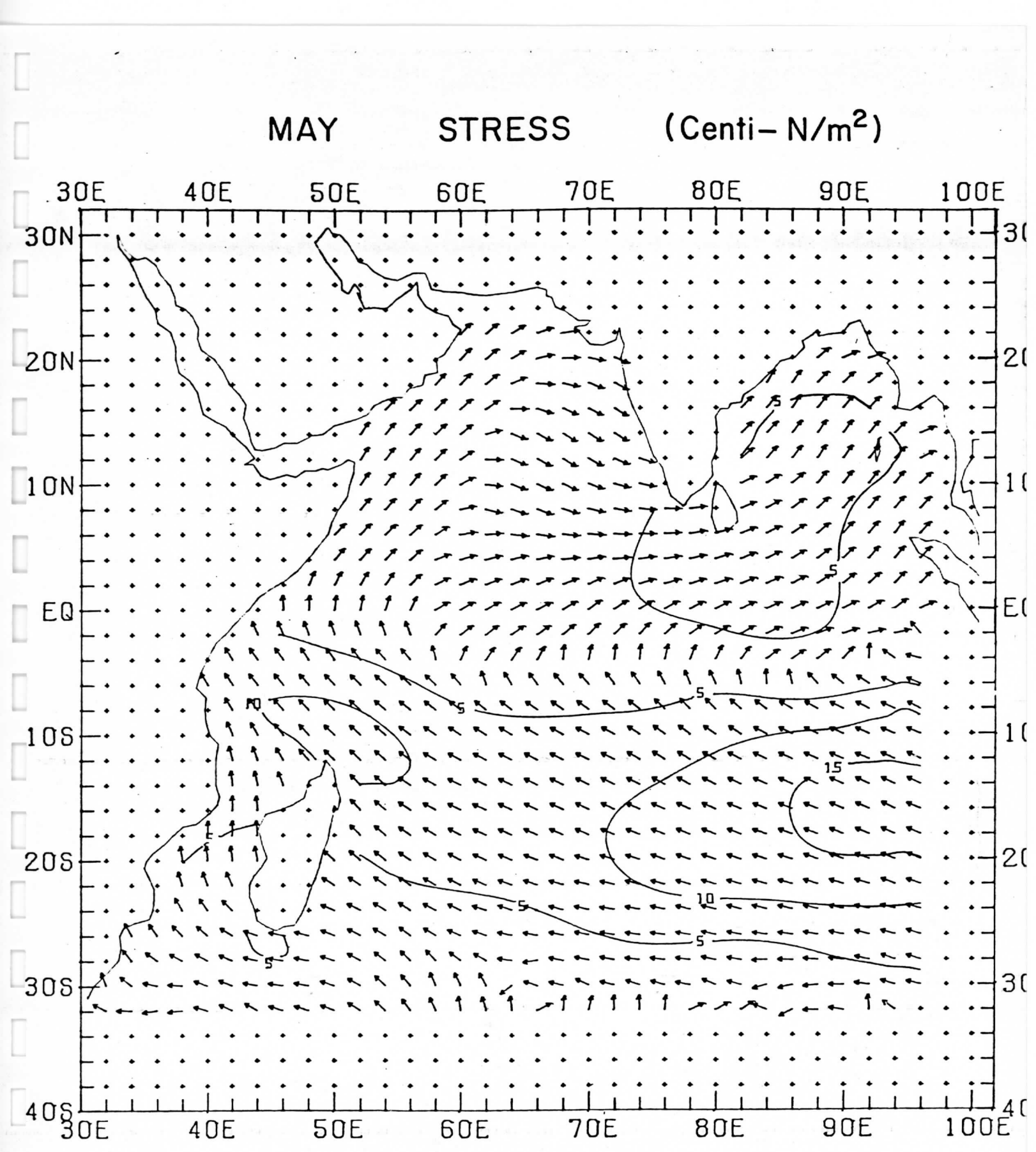

Figure 1: The average wind stress for the month of May 1979. The vectors indicate the directions of the surface winds at 2° grid spacings. The contours indicate magnitudes of the stress in units of 0.01 N m^{-2} (0.1 dynes cm^{-2}).

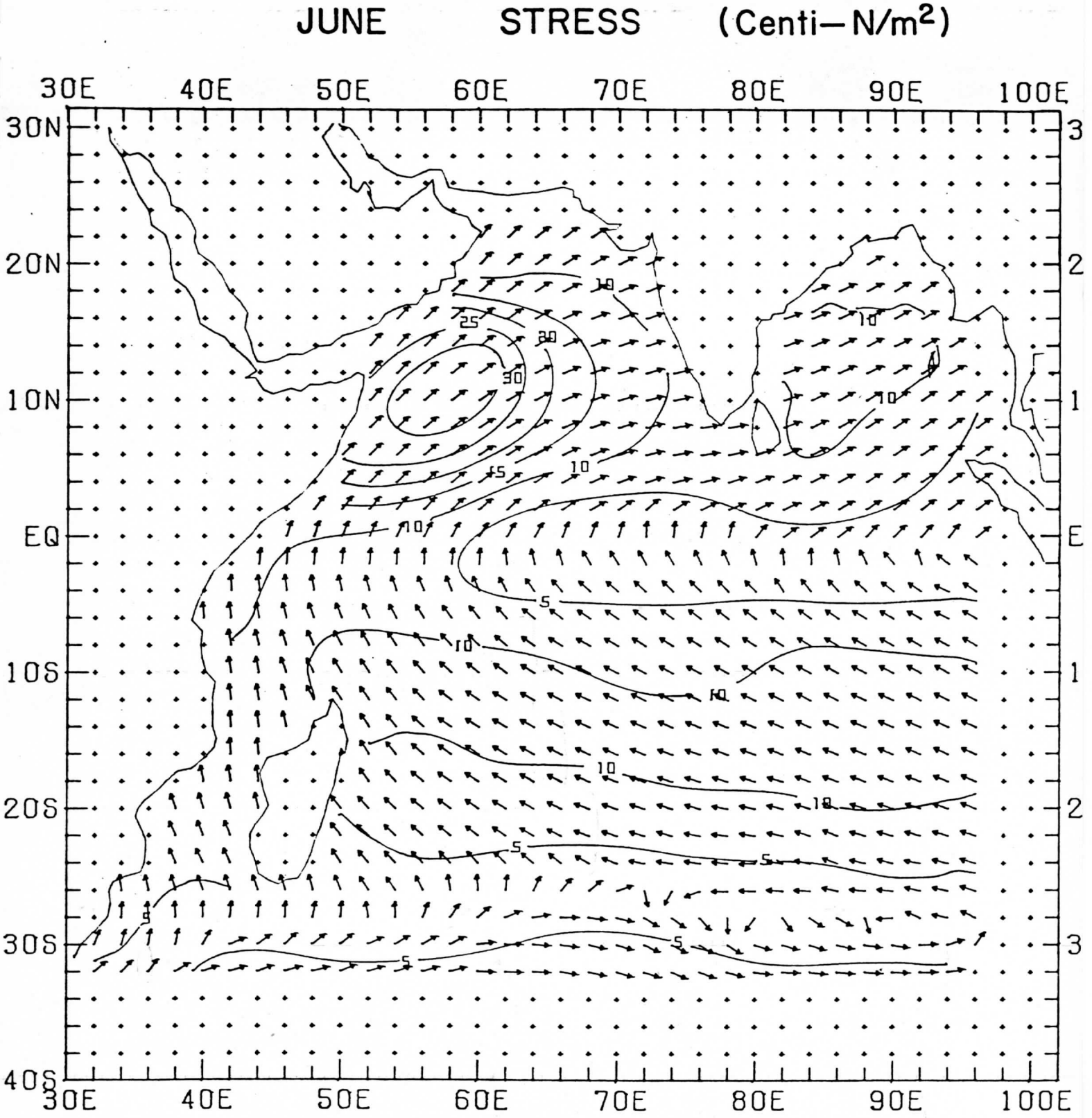

Figure 2: The average wind stress for June 1979.

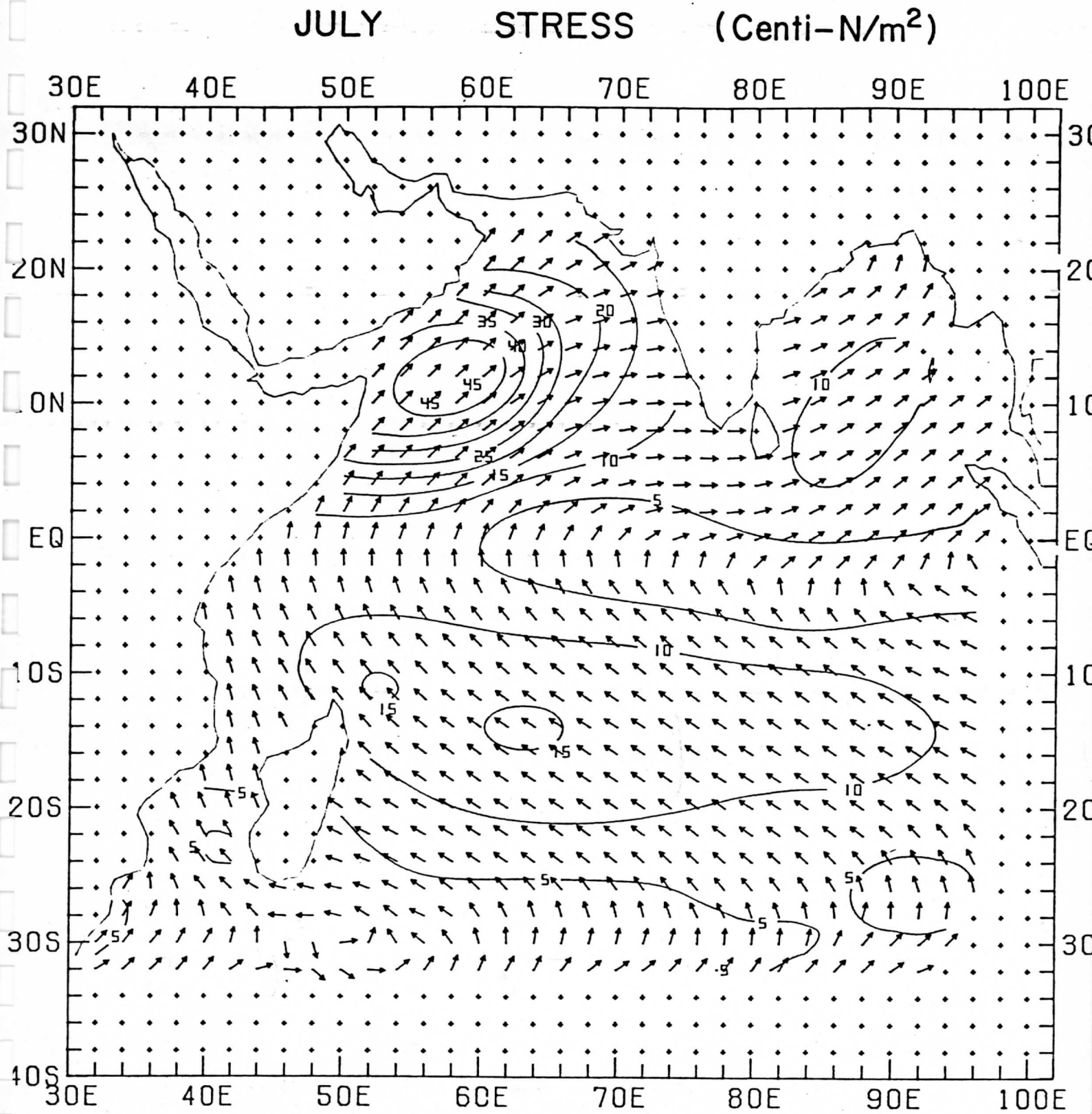

Figure 3: The average wind stress for July 1979.

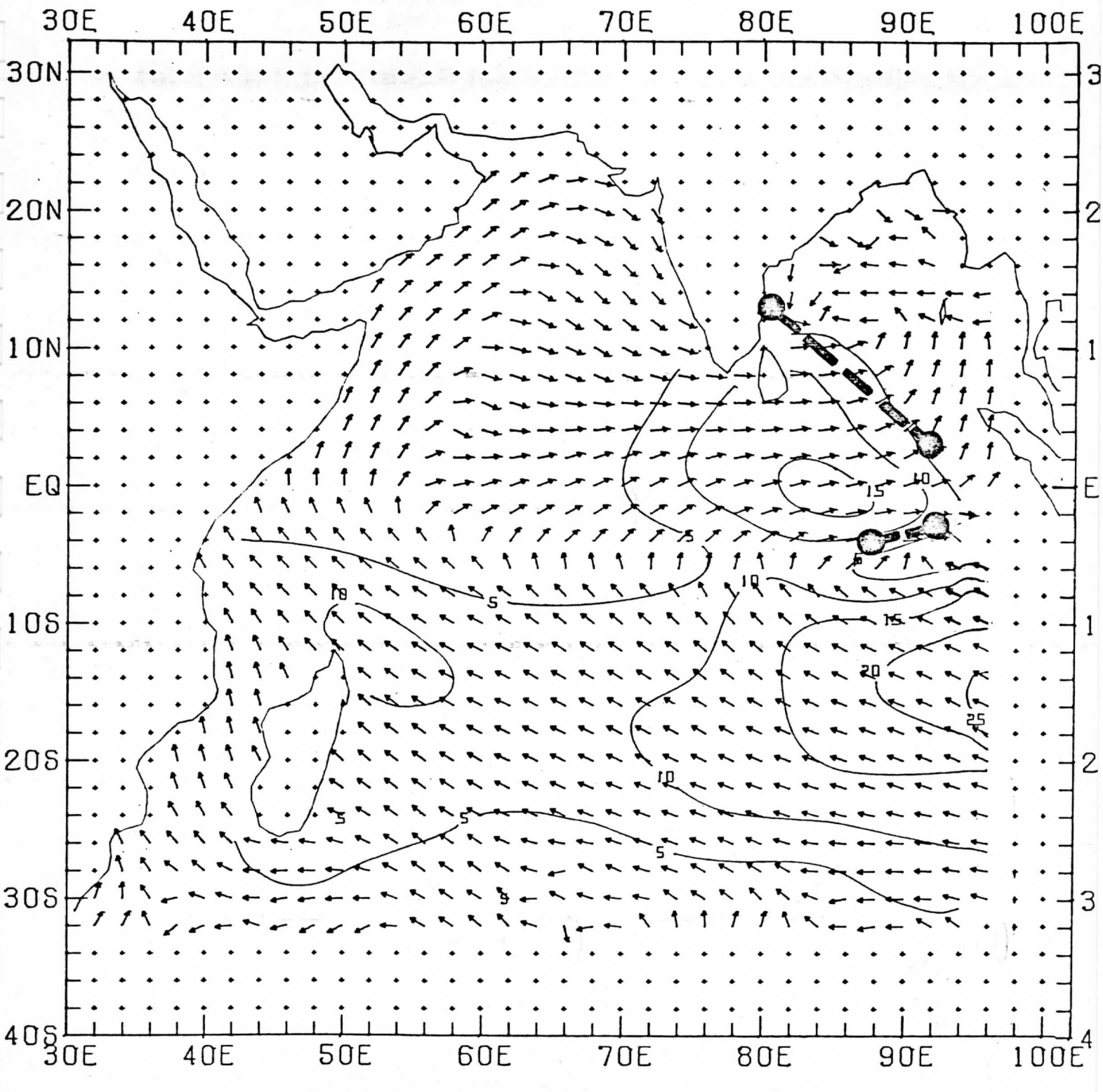

Figure 4: The average wind stress from 1 to 10 May 1979. The tracks of two tropical storms in both hemispheres are shown by dashed lines, see text.

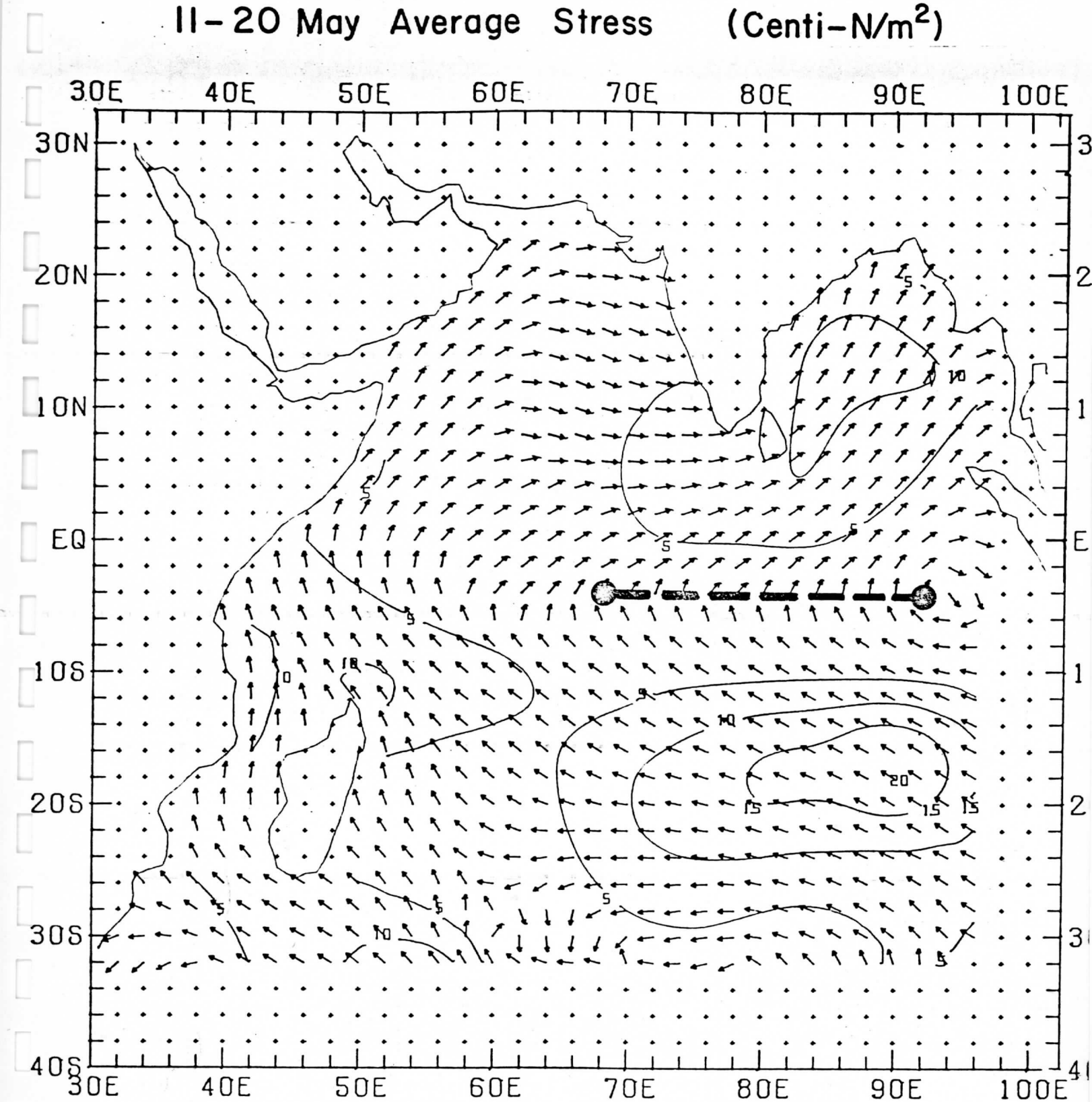

Figure 5: The average wind stress from 11 to 20 May 1979. The track of the southern hemisphere vortex is indicated by the dashed line.

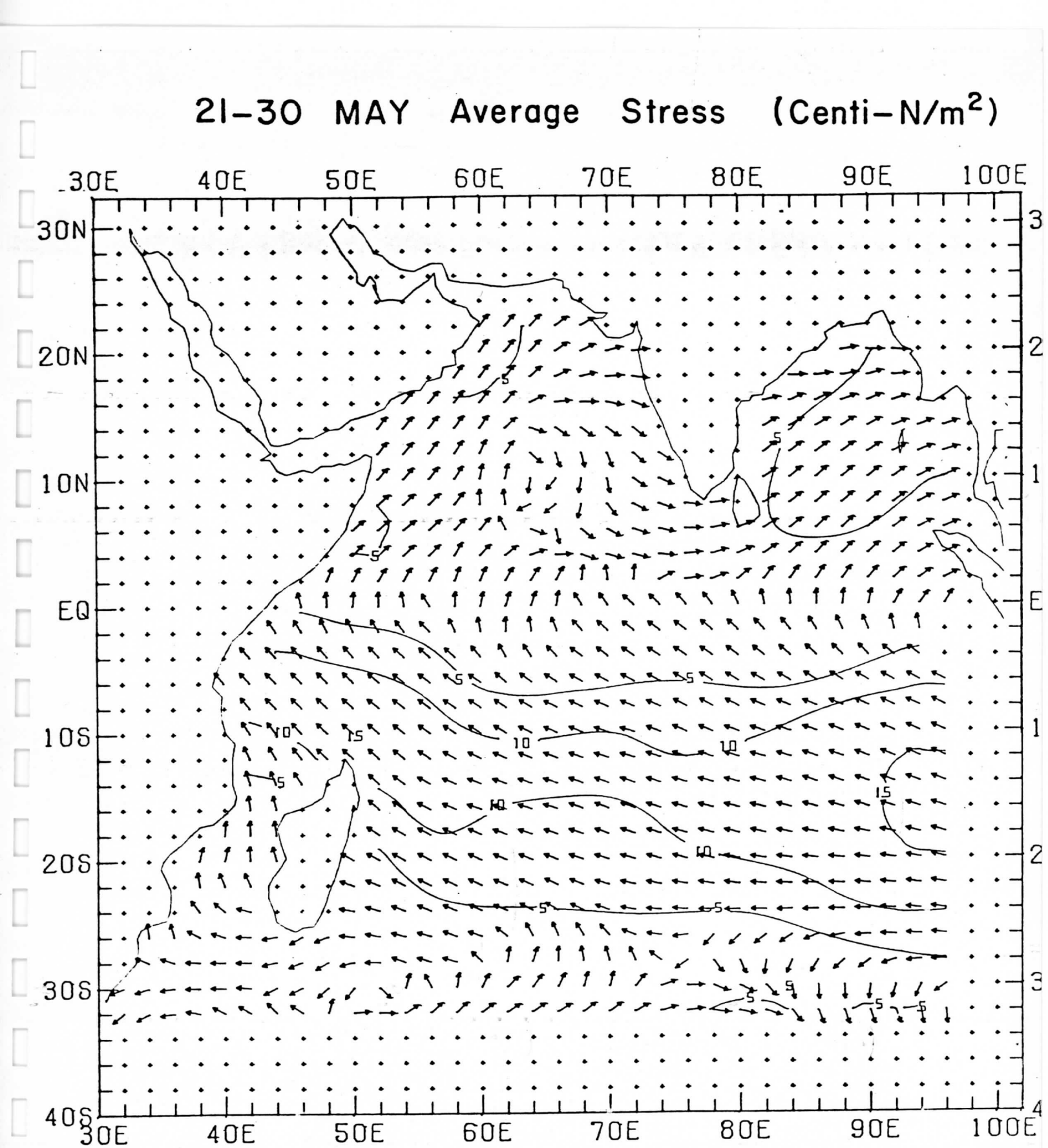

Figure 6: The wind stress from 21 to 30 May 1979.

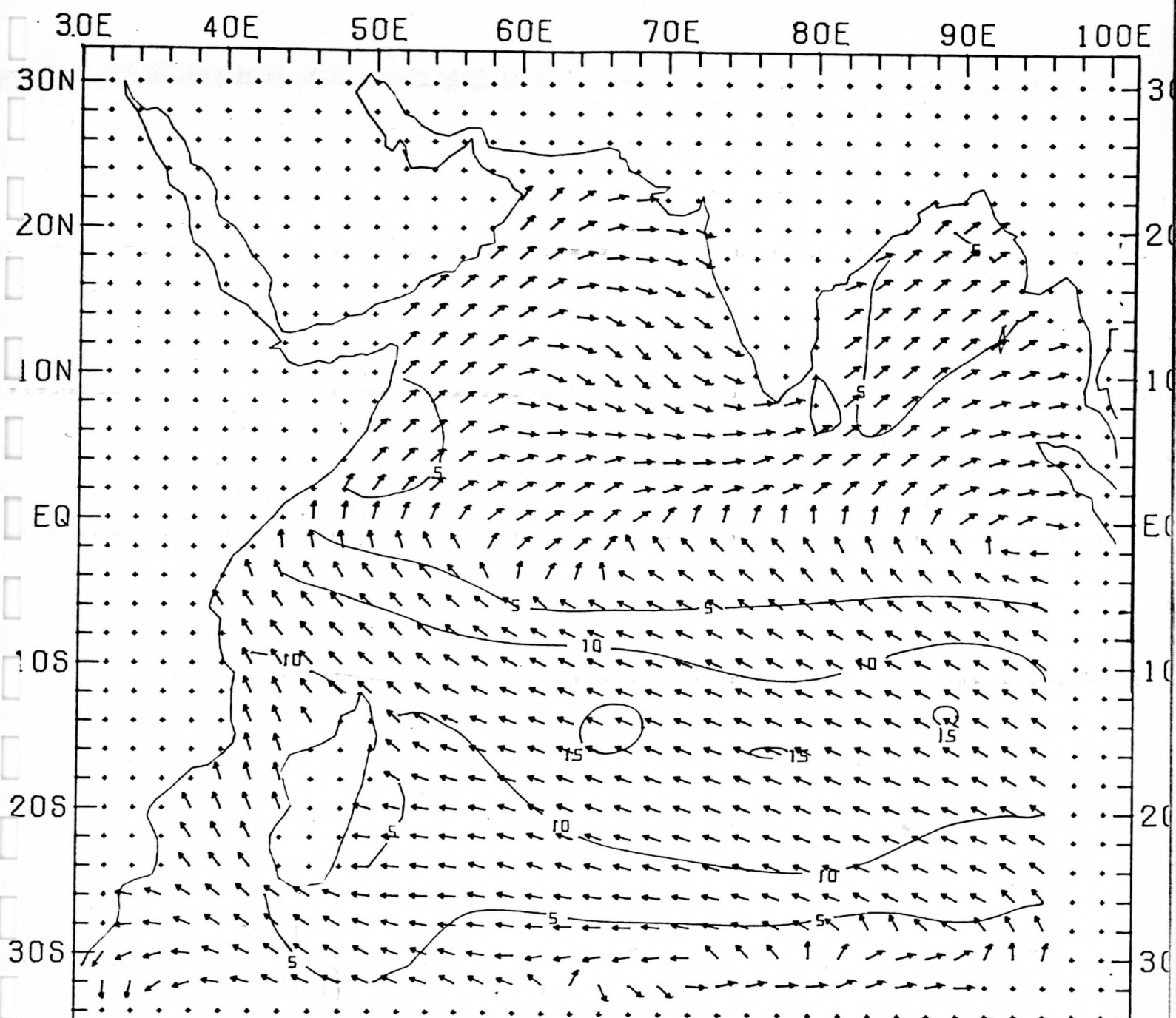

Figure 7: The wind stress from 31 May to 9 June 1979.

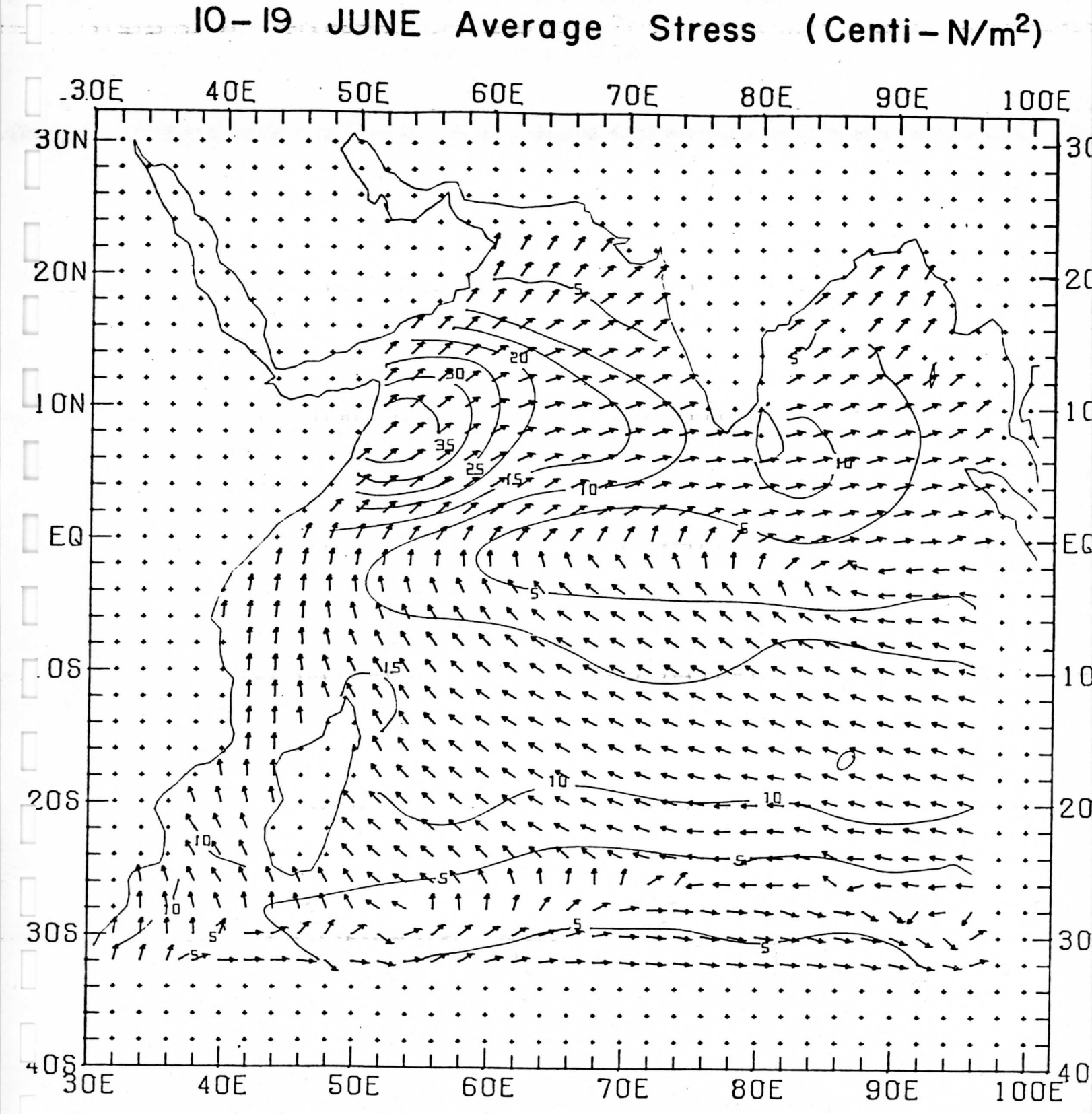

Figure 8: The wind stress from 10 to 19 June 1979.

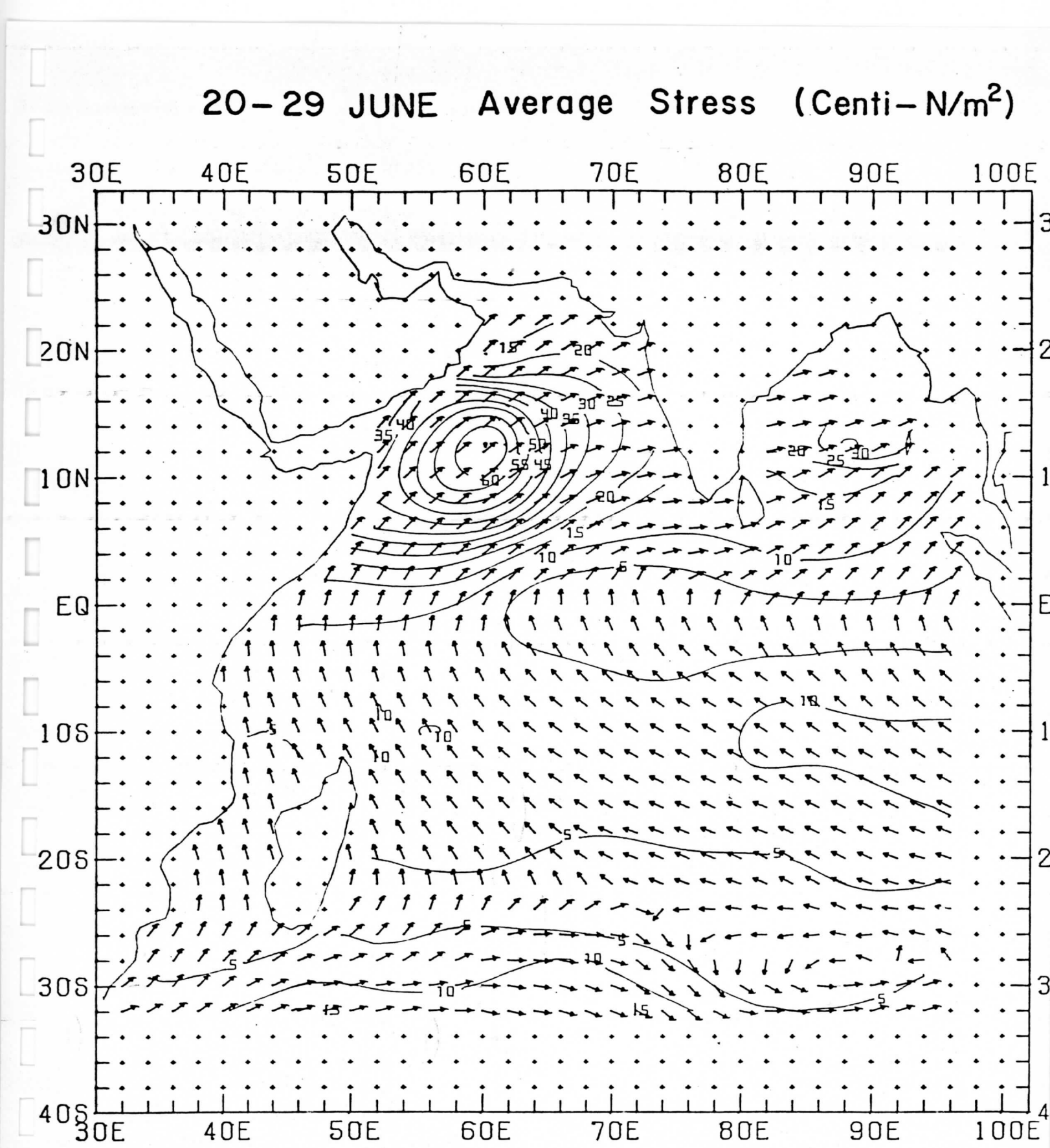

Figure 9: The wind stress from 20 to 29 June 1979.

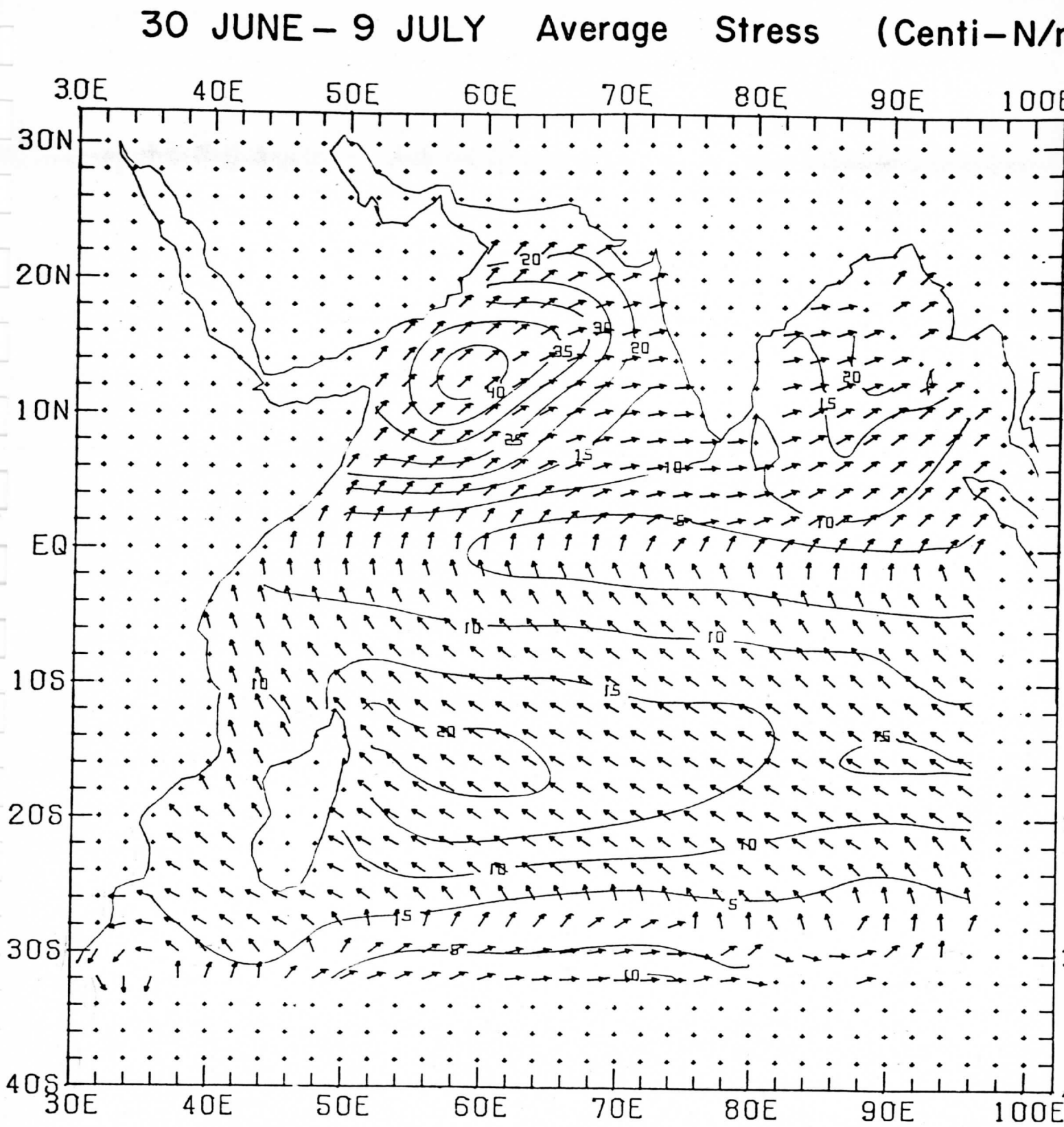

Figure 10: The wind stress from 30 June to 9 July 1979.

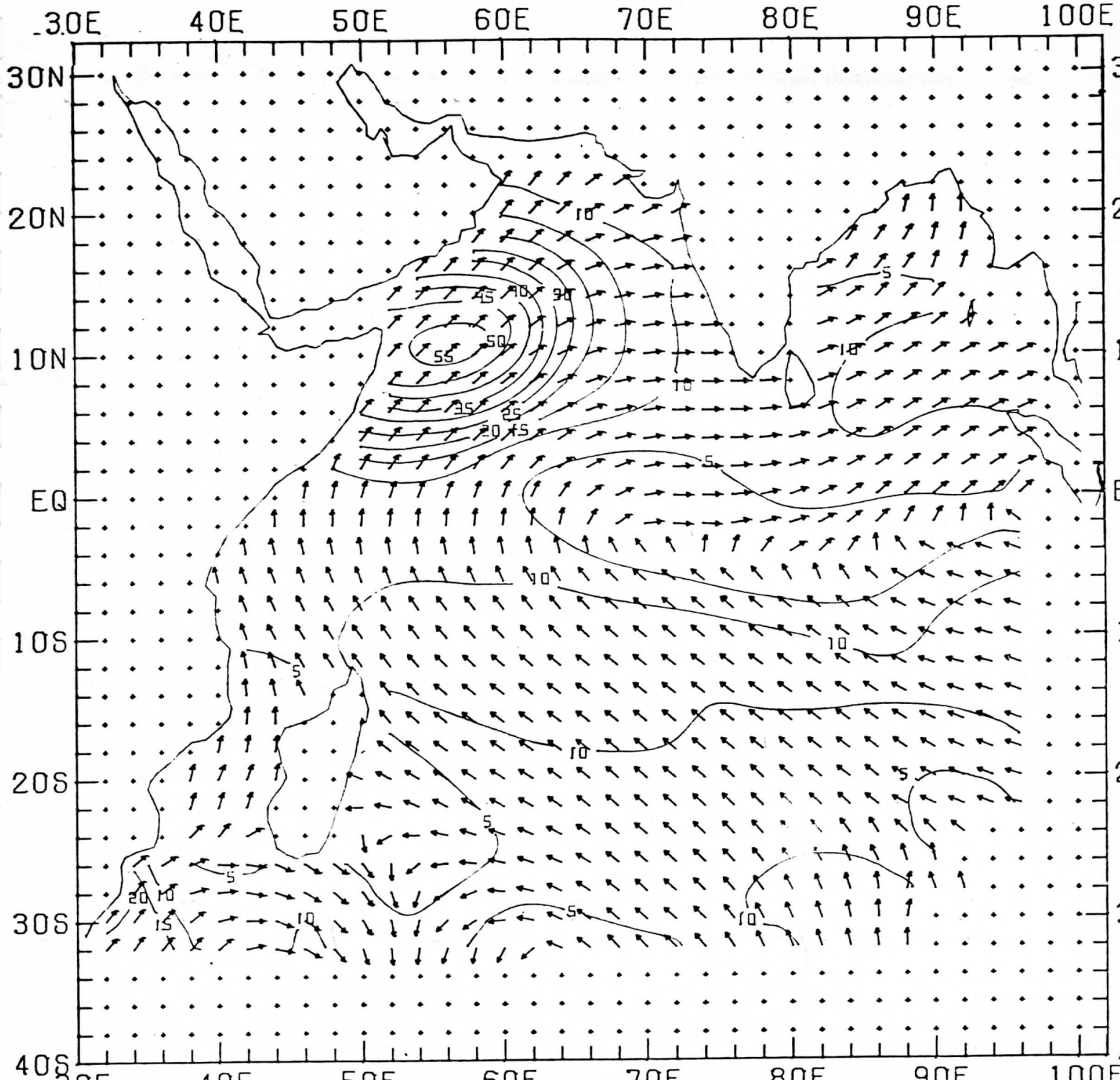

Figure 12: The wind stress from 20 to 29 July 1979.

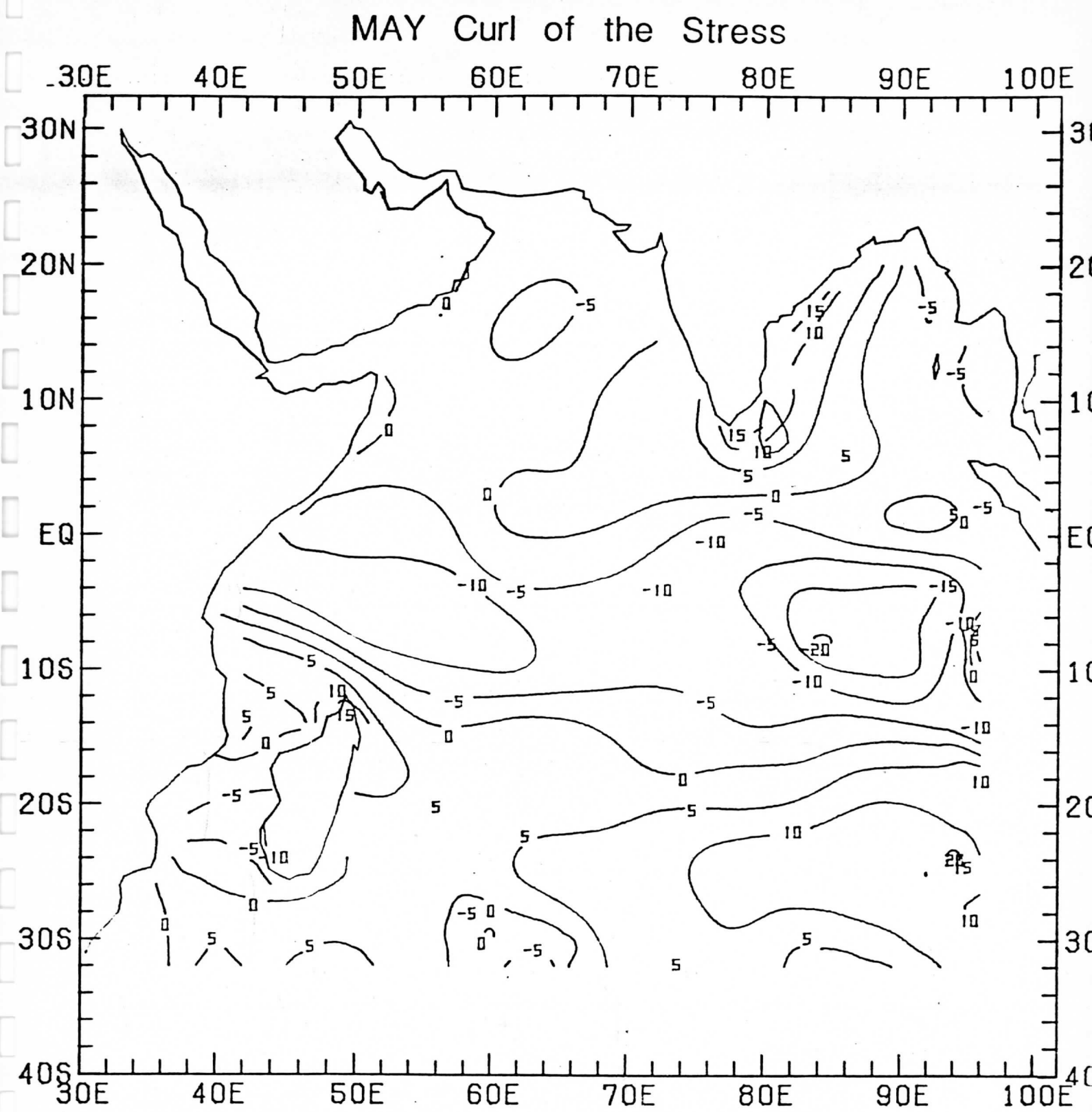

Figure 13: The average $\nabla \times \tau$ for the month of May 1979 calculated from 2° latitude x 2° longitude grids on a daily basis.

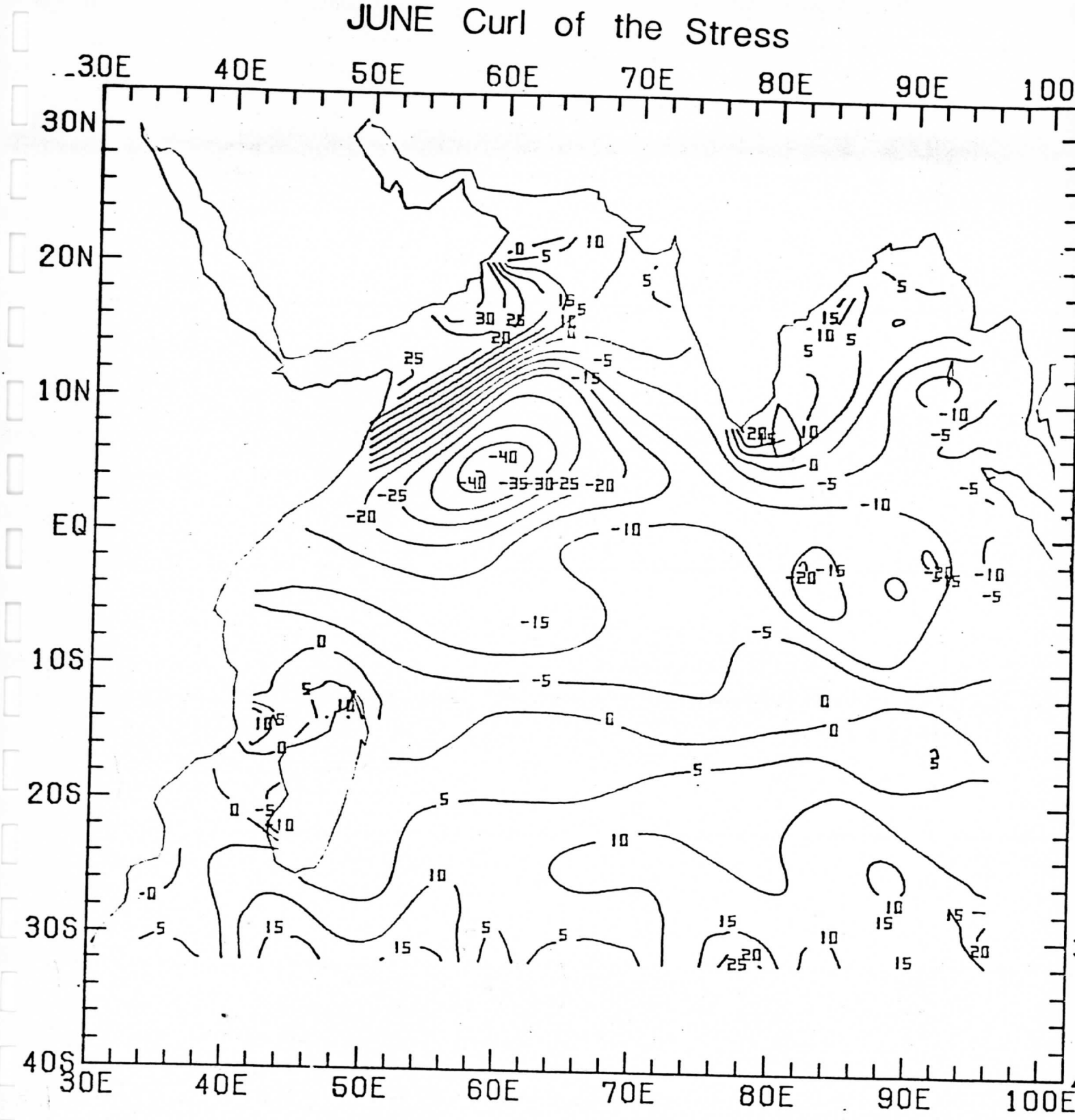

Figure 14: The average $\nabla \times \tau$ for July 1979.

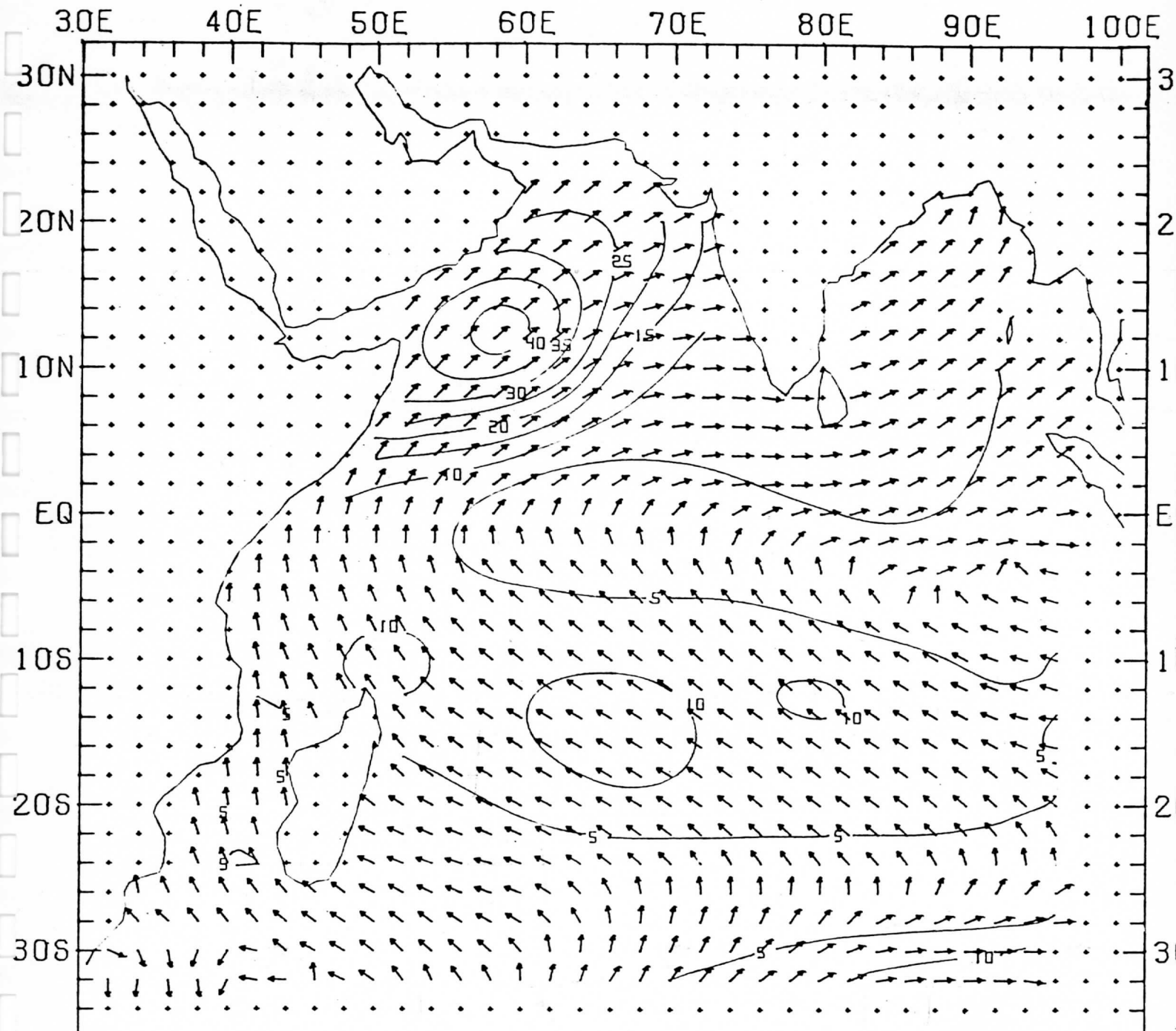

Figure 11: The wind stress from 10 to 19 July 1979.

Attachment 5

A COMPARISON OF CLOUD MOTION AND SHIP WIND OBSERVATIONS OVER THE INDIAN OCEAN FOR THE YEAR OF FGGE

by

Donald P. Wylie

Barry B. Hinton

Space Science and Engineering Center
University of Wisconsin-Madison
Madison, Wisconsin 53706

November 1981

ABSTRACT

Cloud motions over the Indian Ocean were compared to ship observations for the FGGE year. The statistics of this comparison show seasonal changes in the cloud-ship relationship as well as geographical and wind pattern dependent fetch history changes. Most of these changes follow simple boundary layer relationships governed by friction and temperature advection. The most significant result is the improvement of the cloud-ship directional shear with wind speed. The mean veering angle between the cloud and ship measurements decreased at higher wind speeds along with scatter of the shearing angle. This implies that the ability of cloud motion measurements to indicate the wind stress on the ocean improves for the important situations when the winds are strong.

1. Introduction

In a previous paper (Wylie and Hinton, 1981a) satellite derived cloud motion measurements were statistically compared to ship wind observations to lay the basis for combining the two data sources into a detailed surface wind analysis of the Indian Ocean summer monsoon of 1979. This was part of the Global Atmospheric Research Program's (GARP) First GARP Global Experiment (FGGE) which has also been called the Global Weather Experiment. Wylie and Hinton (1981a) compared cloud motion and ship observations for the months of May, June and July, 1979. The resulting wind and sea surface stress analyses were reported in Wylie and Hinton (1981b). We have now developed similar statistics for the other months of the FGGE year, which are the subject of this paper.

One year has been analyzed for the cloud motion-ship observation statistics. FGGE observations started on 1 December 1978 and were made for 12 months covering most of the calendar year of 1979. Both the summer monsoon and the opposite wind patterns of the winter monsoon were included.

We have divided the FGGE observations into four periods: 1) the northern summer from 1 May to 31 July, 1979, 2) the fall 1 August to 31 October, 1979, 3) the winter from 15 November 1978 to 31 January 1979, and 4) the spring 1 February to 30 April, 1979. (The data from 1-14 November were not used because they were lost from our archive of cloud motion data.) We will discuss the similarities and differences in the cloud motion-ship wind observations that occurred over the year of FGGE and summarize in tabular form the relationships of cloud motions to surface winds.

2. Data

The cloud motion measurements were made at the University of Wisconsin using satellite imagery from the geostationary satellite positioned over the Indian Ocean at 57°E longitude for the FGGE program. From these pictures cloud motions could be tracked from central Africa nearly to Malaysia. The methods used for tracking cloud motions on these images have been described several times in past papers by Wylie and Hinton (1981a), Wylie, Hinton, and Millett (1981), Wylie and Hinton (1981b), and Mosher (1979). Only a brief description will be given here.

A series of 3 satellite images spaced at 0.5 h intervals were used for tracking clouds over a 1.0 h time period. One cloud motion analysis for the Indian Ocean was made each day for most of the FGGE data set. The analysis time was nominally 900 GMT or, in a few cases, within 1.0 h of that time when most of the viewing area of the satellite was under sunlight. Both the visible and infrared pictures were used for tracking the clouds, however, the lowest level clouds (below 700 mb) which we are concerned with here were tracked primarily on the visible images. The infrared images were employed for tracking cirrus clouds which were not used in our comparison with ship observations.

The cloud motion measurements were objectively analyzed on uniform grids of 2° latitude and longitude spacing. A distance weighted summation of all cloud motion measurements within 6° of arc (i.e., about 660 km) from each grid point was used. Where less than two cloud measurements were available within 6° of a grid point, no value was given to the point.

The gridded cloud motion analyses were compared to co-located ship wind observations from the Marine Deck compiled by the FGGE Level II-b Mobile Ship

Data Center, Hamburg, Federal Republic of Germany. From 500 to 1000 cloud motion measurements were made daily. This was considerably more than the 80 to 120 ship observations for the same area that were available from four synoptic observation times during each day. In the summer monsoon analysis (Wylie and Hinton, 1981a), neighboring cloud motion measurements were found to be highly correlated over 2° of latitude or longitude. For this reason we gridded the high density observations before making comparisons with the low density observations.

All ship observations were edited against neighboring ship observations to eliminate the obviously bad data. Each ship was compared to the average of all the other ship observations within 5° of arc for the same day, all four observations periods. Any ship report that differed more than 45° in direction or 5 m/s in wind speed from the vector average of its neighbors was eliminated. In data sparse areas, where less than 2 neighboring ships were available, the ship observation was eliminated. This conservative approach to editing favored the elimination of an observation rather than risking the use of an unsubstantiated one.

The areal density of the ship observations was concentrated primarily along the major trade routes from Malaysia to Sri Lanka to the Red Sea or Persian Gulf and along the east African coast from the Red Sea to South Africa. A minor route between Malaysia and South Africa across the center of the Indian Ocean also contained a few ship observations each day. The number densities of the ship observations throughout the year were similar to the May-July period shown in Wylie and Hinton's (1981a) Figure 3.

3. Wind speed comparison

The relationship between the scalar cloud motion speeds and the ship reported wind speeds exhibited small changes during the FGGE year (see Figure 1). There was a lack of high wind speed observations (>20 m/s) during the northern winter and spring months from December through April. After the summer monsoon developed in June, many examples of cloud motion speeds greater than 20 m/s were found in the Arabian Sea and along the Somali coast.

A linear regression was fit to the cloud and ship wind speed data to make a statistical relationship that could be used for correcting cloud motions for sub-cloud wind shear. This regression was derived from the means of each observation set (cloud and ship) and the ratio of their variances as described in Wylie and Hinton (1981a). The regression was designed to pass through the means of each data set with a slope equal to the ratio of their standard deviations. This method was used in place of the usual "least squares fit" because of the scatter (and presumably errors) in both measurements. This procedure minimizes the distance of each observation from the regression line. For a longer discussion see Wylie and Hinton (1981a).

The regressions obtained for the four periods are summarized in Table 1 and shown in Figure 1. The main features of the cloud-ship relationship described by the regressions are that the ship level wind speeds were usually slightly less than the cloud motions (72 to 82%) from May through October, while for the other months, December-April, they were nearly the same. The slope of the regressions illustrate the sub-cloud shear. From December through April no mean shear was found. However, the scatter of the ship measurements around the regression was higher during the December-April period averaging 2.9 m/s (r.m.s.). In the May-October period it averaged 2.6 m/s (r.m.s.).

4. Wind directions

The wind direction comparisons were divided into four directional quadrants and six geographical areas as in Wylie and Hinton (1981a). The geographical areas were chosen based on the density of cloud-ship comparison available and the different wind patterns (see Figure 2). We classified the Arabian Sea and Bay of Bengal into separate areas from the south Asian coast to 11°N latitude. A second latitudinal belt spanned the equator from 11°N to 5°S. Since this belt contained numerous ship observations along the African coast, it was divided into a western section we labelled "The Somali Coast" and an eastern section we called "the Equatorial Latitudes." The longitude of 65°E was selected to divide the monsoon flow along the African coast (toward the northeast in summer and the southwest in winter) from the rest of the equatorial area in which a strong turning of the wind occurs. In this area the easterly (flowing toward the west) trade winds south of the equator turned across the equator to become westerly winds in the summer. In the winter the opposite pattern occurs. Easterlies north of the equator turn to westerlies south of it. The fifth region isolated the southern hemisphere trade winds from 5°S to 21°S latitude and the sixth region contained the remainder of the cloud motion analysis from 21°S to 35°S (southern mid-latitudes).

The predominant wind directions for each season are indicated by the number of cloud-ship comparisons found in each directional quadrant shown in Table 2. Over the Arabian Sea 338 westerly wind cloud-ship pairs were found from May through July, while from December through April the predominant direction was from the east or north; 556 easterly pairs and 294 northerly pairs in December and January, and 480 easterly and 253 northerly pairs from

February through April. A similar reversal of direction was found along the Somali coast and the equatorial latitude region. The southern hemisphere trade wind area and the mid-latitude area did not have any reversal of direction. The largest groups of cloud-ship pairs were the easterly and southerly winds during all seasons.

The average veering angles between the cloud and ship observations (cloud direction-ship observation direction) are shown in Figure 2 for all speeds and for two different speed classifications in Table 2. The veering angles ranged from +50° in the Bay of Bengal (February-April) to -44° in the southern mid-latitudes (December-January). These extremes generally corresponded to the different frictional effects of the northern and southern hemispheres--veering in the north and backing in the south.

The cloud-ship wind relationships also reflected the temperature advection conditions expected in each area from the wind fetch histories. For example, the largest seasonal changes were found in the Arabian Sea and the equatorial belt of the Somali Coast and Equatorial Latitude areas. The northerly winds in the Arabian Sea changed from a large summertime veering angle of 47° to a backing of -6° in winter. This change reflected the land-water temperature relationship which also changed with the seasons. During the summer the Arabian land mass usually is warmer than the ocean. An air parcel would thus cool as it crossed the water (in a northerly wind). A large boundary layer directional veering would be the expected result. In winter the opposite land-water temperature contrast causes backing (negative veering) in the boundary layer. The reversal of veering found for the southerly winds can be explained by the same arguments.

In the equatorial latitudes and along the Somali coast the easterly winds changed from a -13° veering in the summer to a +15° veering in the winter. The majority of the easterly cloud-ship pairs found during the summer were in the trade winds south of the equator. Directional backing was found for the trade winds in the region to the south which reflect frictional affects. During the winter months of December and January more easterly winds were sampled north of the equator because of the reversal of the monsoon. The positive veering found in December and January reflects the frictional conditions in the northern hemispheric winds. An example of seasonal changes in the opposite direction was found for the westerly winds which changed from a positive veering angle (14°) in the summer to a negative angle (-12°) in the winter. This reflected the seasonal changes in the wind patterns. The westerly winds were predominant north of the equator in the summer. In the winter the westerly winds were south of the equator. That is, the winds turned from being easterly around to westerly across the equator. The same seasonal veering changes from positive (24°) in the summer to backing in the winter (-5°) were found for the northerly directional category for the same reasons.

In the trade wind belt and the southern mid-latitudes the seasonal changes were small. The veering angles found partially reflected the affects of friction for different fetch directions without showing any large changes between seasons. For example, the northerly winds had large backing angles from -16° to -44°. A northerly wind in the southern hemisphere would advect warm air from the tropics poleward. In the southern hemisphere this enhances boundary layer backing and adds to the affects of friction.

For southerly winds the two forces would be of opposite sign. Advection of cold air equatorward would cause boundary layer veering which would oppose the frictional backing. From December to April the average cloud-ship directional change was positive (8° to 23°) for the southerly winds. During May to October when the trades blow strongly equatorward from the southwest, small backing angles (-5° to -7°) were found indicating a weakening of the temperature advection.

The scatter in the cloud-ship wind direction comparisons was found to be a function of wind speed (see Figure 3). For speeds from 0 to 5 m s^{-1} the directional comparisons had a root mean square deviation of ±50°. For higher speeds from 20 to 25 m s^{-1} the r.m.s. deviation decreased to 15°. The bounds of the r.m.s. deviation around the mean veering are indicated in Figure 3 for 5 m s^{-1} wind speed (cloud motion) groupings. This indicates that the cloud-ship relationship, or the ability to use cloud motions as indicators of surface winds, improves with higher wind speeds.

There were indications that the mean veering angles reduced or approached zero as wind speeds increased. This is evident in Table 2 where the veering angles for two speed classifications, $\leq$10 m s^{-1} and >10 m s^{-1}, are shown. For the higher speed class smaller veering angles were found than the low speed class for most of the areas where two classifications could be made.

The relationship of the boundary layer veering angle to wind speed is illustrated in more detail in Figure 4. The mean veering angles for the six examples shown in Figure 3 were computed in wind speed intervals of 5 m/s from 0 to 25 m/s. These angles decreased with speed for the two Arabian Sea examples (westerly and easterly), the equatorial eastierlies and the trade wind southerlies except for the 15-20 m/s interval where very few cloud-ship observations were obtained.

The average scatter of the cloud-ship comparisons is summarized in Figure 5 for 5 m/s cloud motion speed intervals. This scatter was large for the 0-5 m/s interval, 50° (r.m.s.). However, it decreased to 15° in the 20-25 m/s interval. This decrease in directional scatter with speed can be appoximated if we assume that each measurement, cloud and ship, has r.m.s. errors in the crosswind components of 2.5 m/s. The magnitude of the total cross wind component error would be $((2.5)^2 + (2.5)^2)^{1/2}$. If errors in the measurement of the alongwind components are ignored, then the uncertainty angle of the cloud-ship comparison would follow the dashed curve in Figure 5 which has a similar shape to the measured error.

5. Summary and conclusions

In general, the cloud-ship comparison statistics conform to simple qualitative theories governing boundary layer wind speed and directional changes. The geographical classifications separated the different frictional affects between the northern and southern hemisphere and the wind fetch directional classifications isolated the affects of temperature advection. The categorization of the cloud-ship data into speed intervals also found a reduction of directional shear for higher wind speeds. This is gratifying because a reduction of boundary layer directional veering with wind speed is predicted by similarity theory (Arya, 1975).

The implication of these statistics is that cloud motions can be used to estimate surface winds but a statistical boundary layer must be employed to reflect geographical changes, wind fetch histories and seasonal changes. The most important result is that the cloud motions have a more stable relationship with the surface winds with less scatter for the higher wind speeds where data on wind stress are more important.

TABLE 1

Summary of the regression equations derived from wind speed data obtained from cloud motion measurements and ship reports over the Indian Ocean from 1 December 1978 to 30 November 1979

Period	Regression fit to data	Scatter of ship data around regression (r.m.s.)
May to July	Ship = 0.72 cloud + 1.2	2.6 m/s
August to October	Ship = 0.82 cloud + 0.5	2.9 m/s
December to January	Ship = 1.0 cloud + 0.0	2.9 m/s
February to April	Ship = 1.0 cloud + 0.2	2.6 m/s

TABLE 2

Directional differences, cloud-ship, over the Indian Ocean from 1 December 1978 to 30 November 1979. The comparisons were grouped according to the direction the wind was coming from (N, E, S and W) and the speeds, both defined by the cloud motions.

	N	E	S	W	N	E	S	W
ARABIAN SEA		≤10 m s^{-1}				>10 m s^{-1}		
May-July	47° (72)	33° (26)	-5° (76)	21° (338)				12° (496)
August-October	25° (91)	6° (53)	2° (42)	17° (287)				15° (218)
November-January	-4° (321)	13° (556)	35° (28)	23° (26)				
February-April	10° (253)	12° (480)	18° (79)	-5° (80)				
BAY OF BENGAL		≤10 m s^{-1}				>10 m s^{-1}		
May-July				33° (18)				10° (19)
August-October								
November-January		14° (22)						
February-April				50° (24)				
SOMALI COAST		≤10 m s^{-1}				>10 m s^{-1}		
May-July		1° (37)	-8° (243)	11° (114)			-2° (111)	3° (111)
August-October		-12° (31)	-5° (108)	5° (23)			-2° (54)	8° (25)
November-January	1° (138)	15° (216)			2° (24)	14° (35)		
February-April	-11° (67)	7° (323)	17° (26)					

TABLE 2, cont.

	N	E	S	W	N	E	S	W
		<10 m s^{-1}				>10 m s^{-1}		
EQUATORIAL								
MID-LATITUDES								
May-July	24°	-13°	-8°	14°				10°
	(23)	(80)	(134)	(515)				(335)
August-October	29°	-11°	-19°	12°				9°
	(58)	(55)	(77)	(369)				(165)
November-January	-5°	10°		-12°		2°		
	(235)	(383)		(22)		(58)		
February-April	11°	15°	-24°	-15°				
	(274)	(395)	(60)	(231)				
SOUTHERN TRADES		<10 m s^{-1}				>10 m s^{-1}		
May-July		-19°	-5°			-14°	-5°	
		(380)	(279)			(258)	(71)	
August-October		-15°	-7°			-13°	-7°	
		(156)	(64)			(132)	(25)	
November-January	-25°	-12°	23°	1°				
	(57)	(311)	(41)	(28)				
February-April	-16°	-9°	8°	-10°		-16°		-8°
	(85)	(352)	(206)	(124)		(39)		(20)
SOUTHERN		<10 m s^{-1}				>10 m s^{-1}		
MID-LATITUDES								
May-July	-39°	-12°	2°	13°		-10°	3°	-3°
	(66)	(148)	(110)	(56)		(34)	(44)	(36)
August-October	-26°	-8°	7°			-17°		1°
	(47)	(62)	(48)			(25)		(21)
November-January	-44°	-6°	10°	-38°			7°	
	(77)	(148)	(90)	(62)			(26)	
February-April	-39°	-10°	9°	25°		-7°		
	(99)	(226)	(126)	(29)		(32)		

REFERENCES

Arya, S. P. S., 1975: Geostrophic drag and heat transfer relations for the atmospheric boundary layer. Boundary Layer Met., 101, 147-161.

Mosher, F. R., 1979: Cloud drift winds from geostationary satellites. Atmospheric technology, NCAR, Boulder, Colorado, December 1978-February 1979, 53-60.

Wylie, D. P., and B. B. Hinton, 1981a: The feasibility of estimating large-scale surface wind fields for the summer MONEX using cloud motion and ship data. Boundary Layer Met., 21, 357-368.

Wylie, D. P., and B. B. Hinton, 1981b: The wind stress patterns over the Indian Ocean during the summer monsoon of 1979. J. Physical Oceanography, in press.

Wylie, D. P., B. B. Hinton, and K. G. Millett, 1981: A comparison of three satellite-based methods for estimating surface winds over oceans. J. Applied Met., 10, 339-449.

LIST OF FIGURES

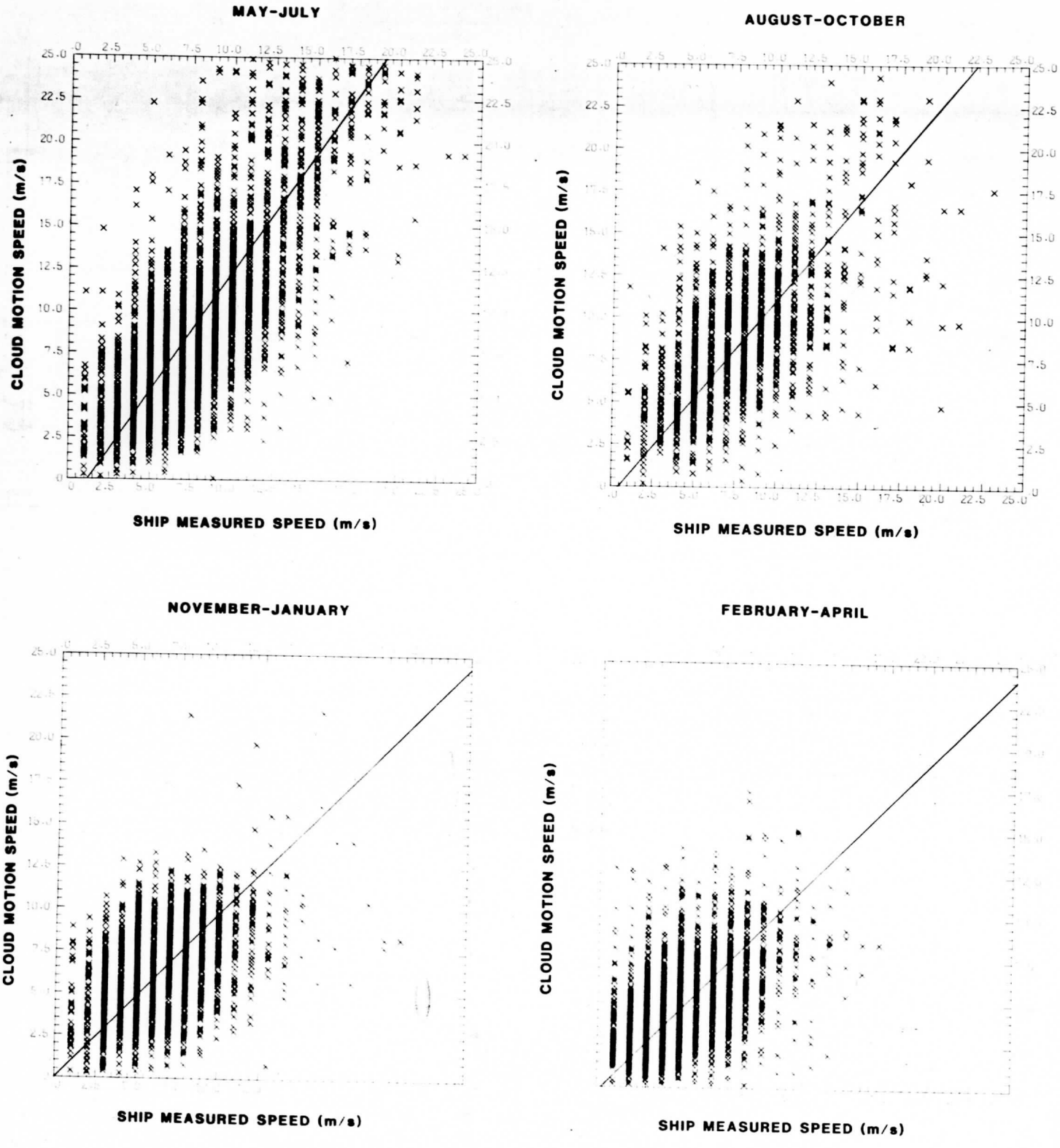

Figure 1: Scatter plots of cloud motion speeds and ship measured wind speeds (both scalar quantities) over the Indian Ocean from 1 December 1978 through 30 November 1979.

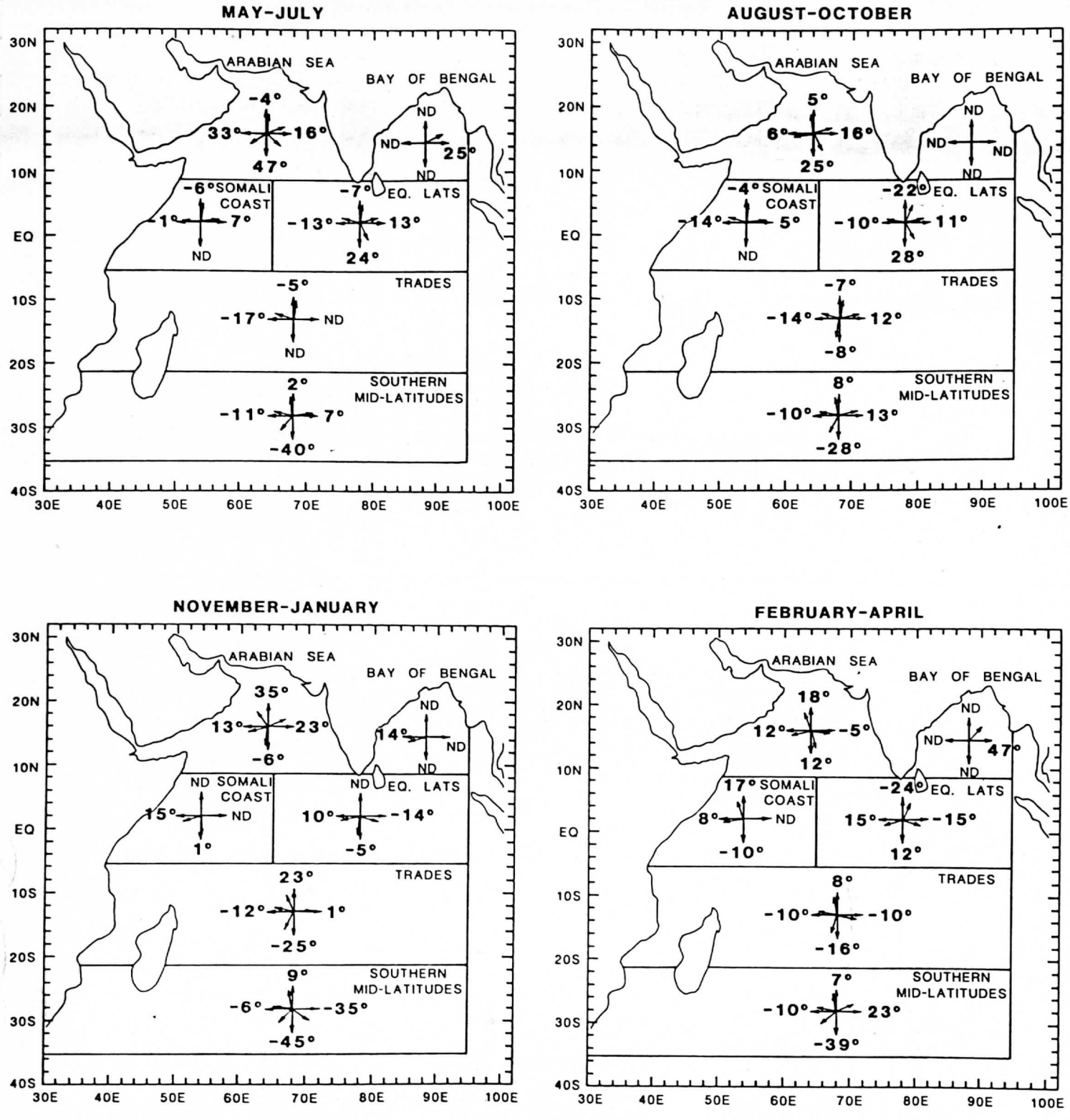

Figure 2: The mean sub-cloud wind directional veering for each season and geographical area (all wind speeds averaged together). The cloud-ship comparisons were stratified according to 4 quadrants based on the cloud motion direction. A positive angle indicates an average veering between the cloud and ship levels, cloud direction greater than ship direction.

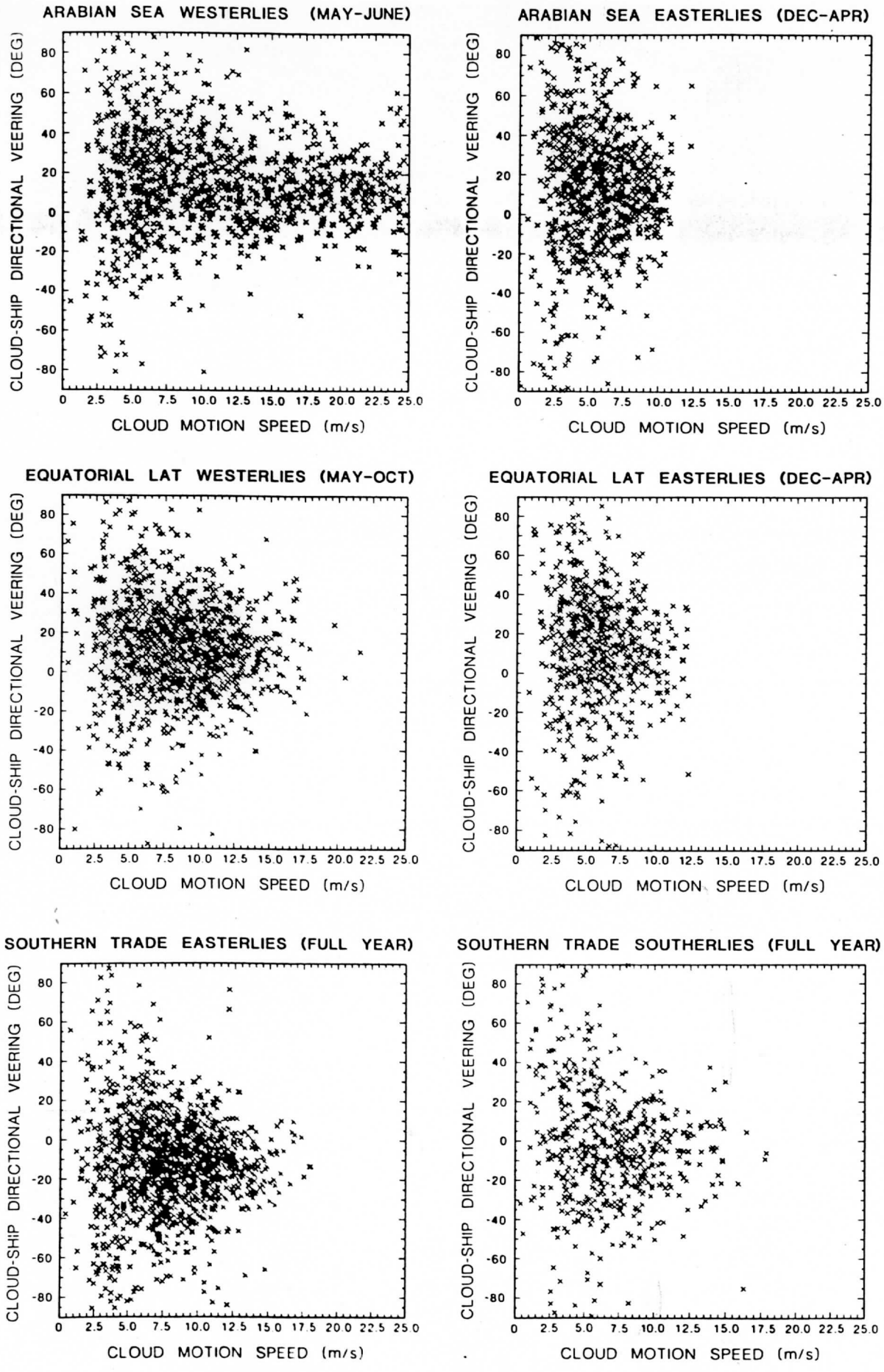

Figure 3: The cloud-ship wind directional veering as a function of wind speeds for six example regions and wind directions. The wind speeds were taken from the cloud motions without any boundary layer corrections.

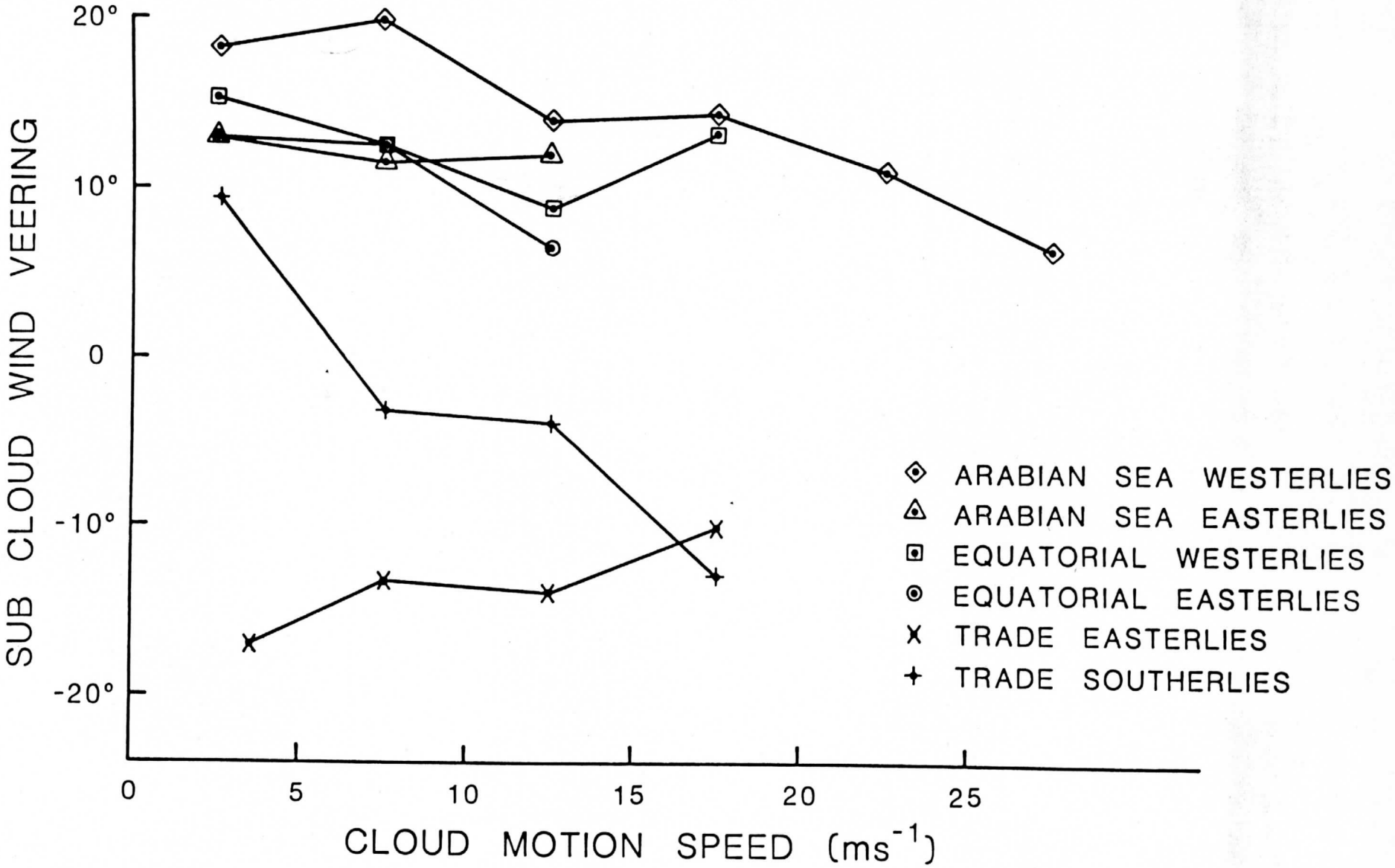

Figure 4: The mean veering angles (cloud-ship) for 5 m/s speed intervals computed from the data shown in Figure 3.

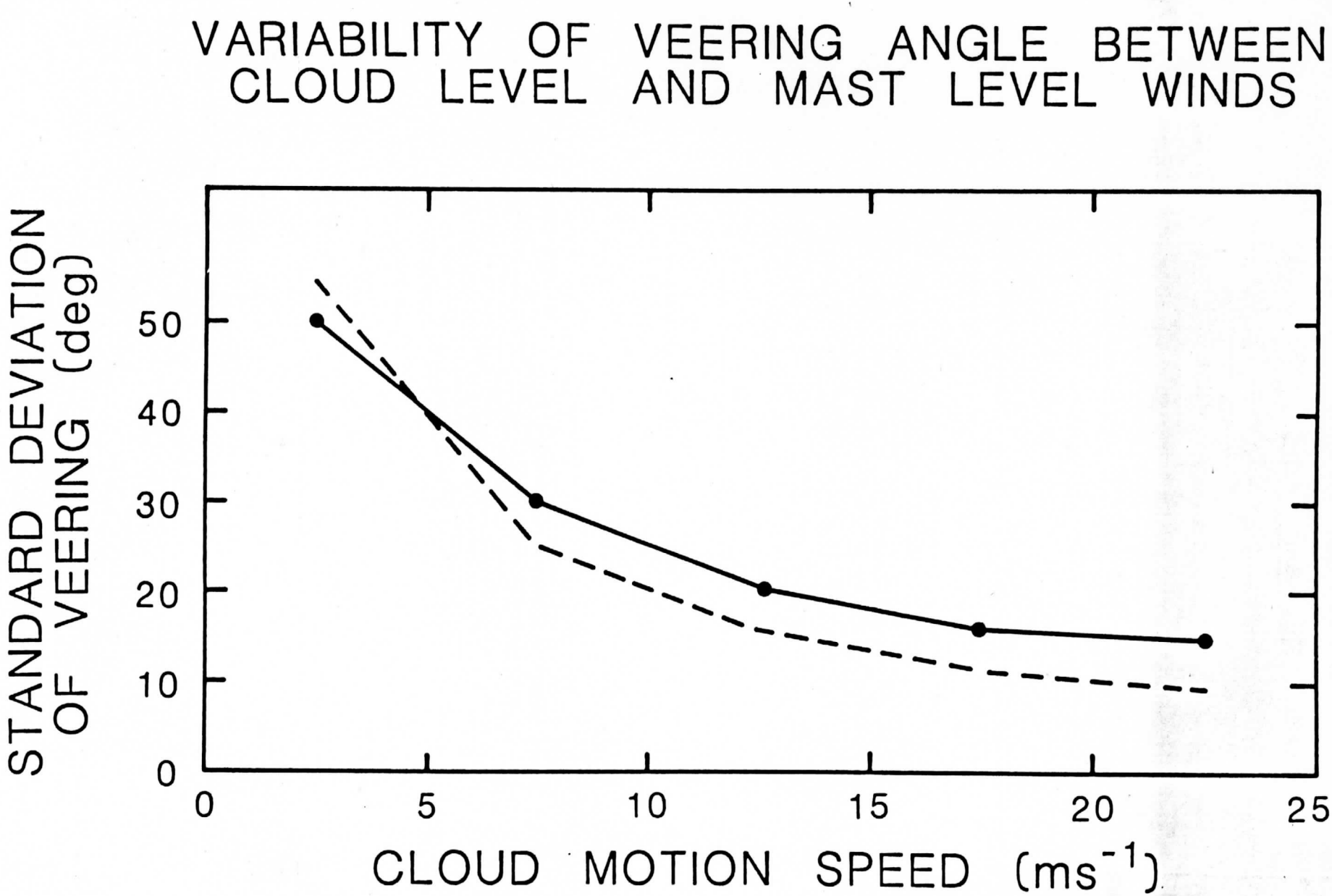

Figure 5: The average scatter (r.m.s.) of the cloud-ship directional veering as a function of speed (solid line). Computations were made over 5 m/s speed bands based on the cloud motion data. The veering angle estimated from a 2.5 m/s cross wind error for each speed interval also is shown by the dashed line.

Attachment 6

Monthly Charts of Stress on the Indian Ocean

Units are 10^{-2} Newtons per meter or 10^{-2} Pa only the charts not shown in Attachment 4 have been included. This information is preliminary and will be superseded by a more extensive publication.

78349 31-AVG

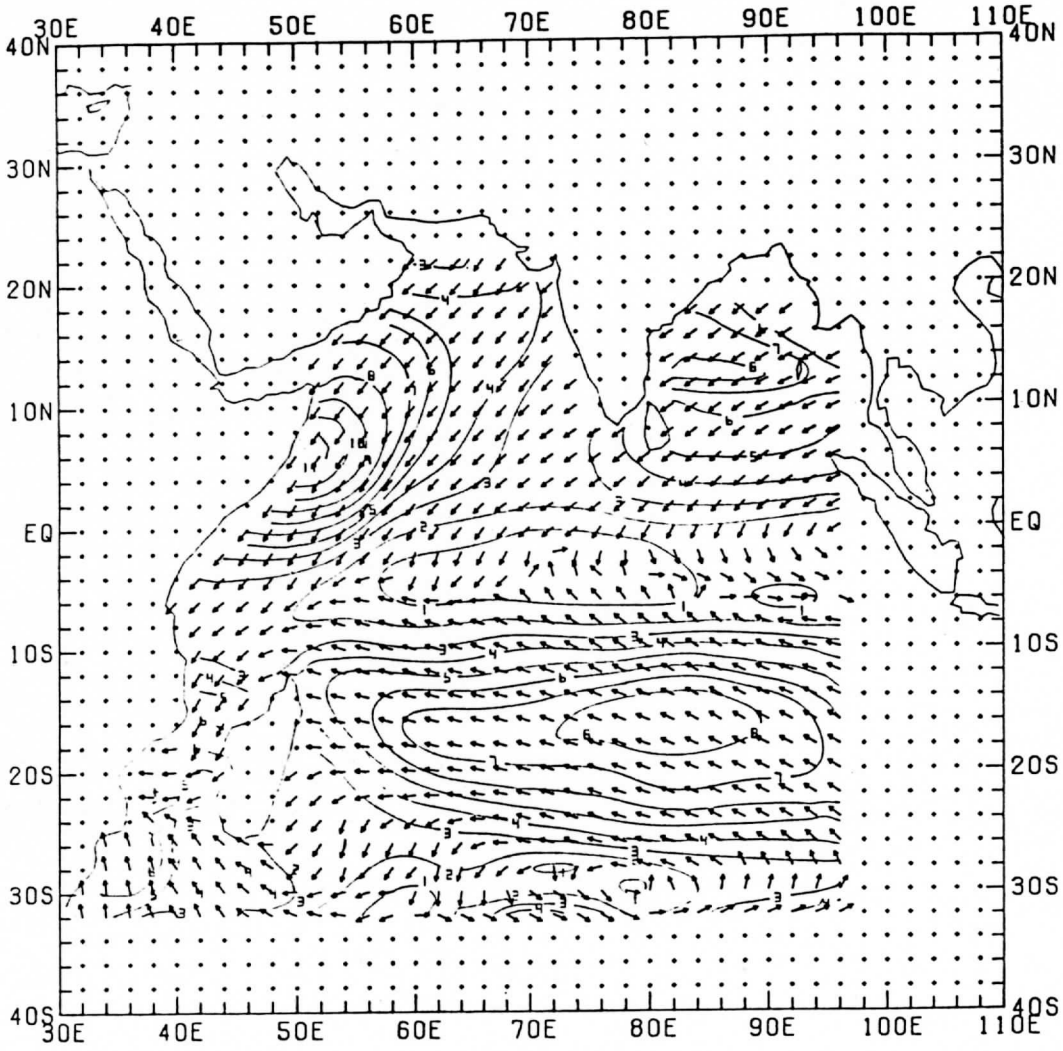
30E
40E
50E
60E
70E
80E
90E
100E
110E
40N
30N
20N
10N
EQ
10S
20S
30S
40S

79015 31-AVG

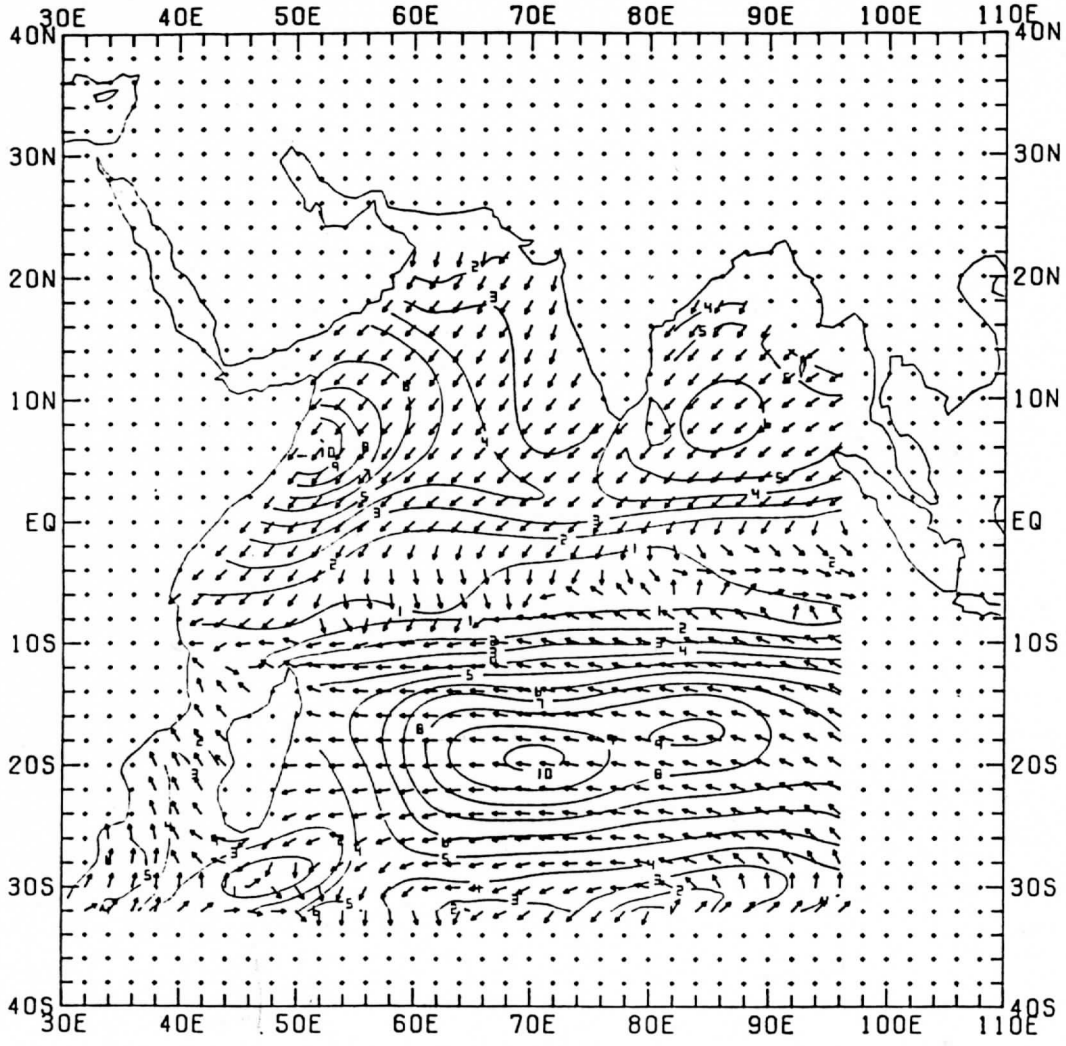
30E
40E
50E
60E
70E
80E
90E
100E
110E
40N
30N
20N
10N
EQ
10S
20S
30S
40S

79045 28-AVG

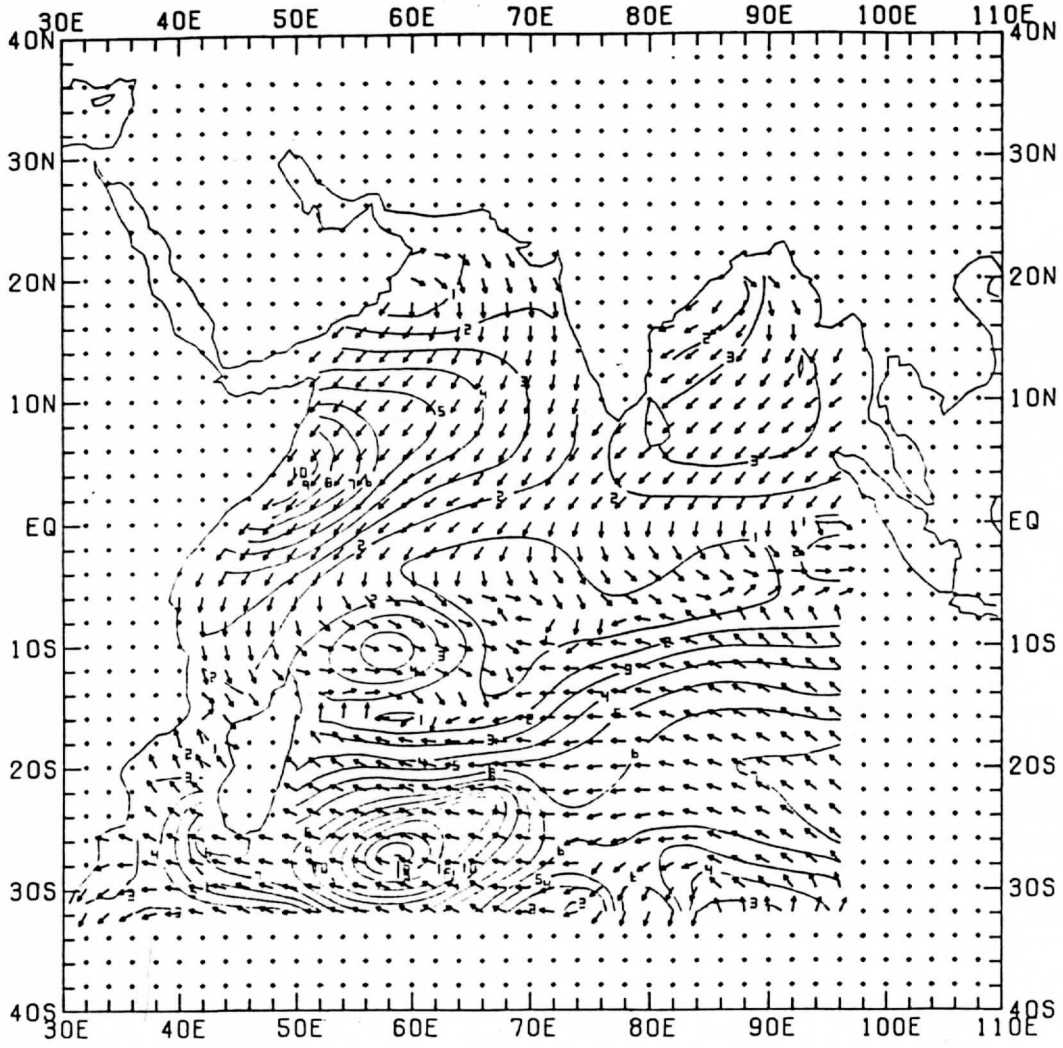
30E
40E
50E
60E
70E
80E
90E
100E
110E
40N
30N
20N
10N
EQ
10S
20S
30S
40S

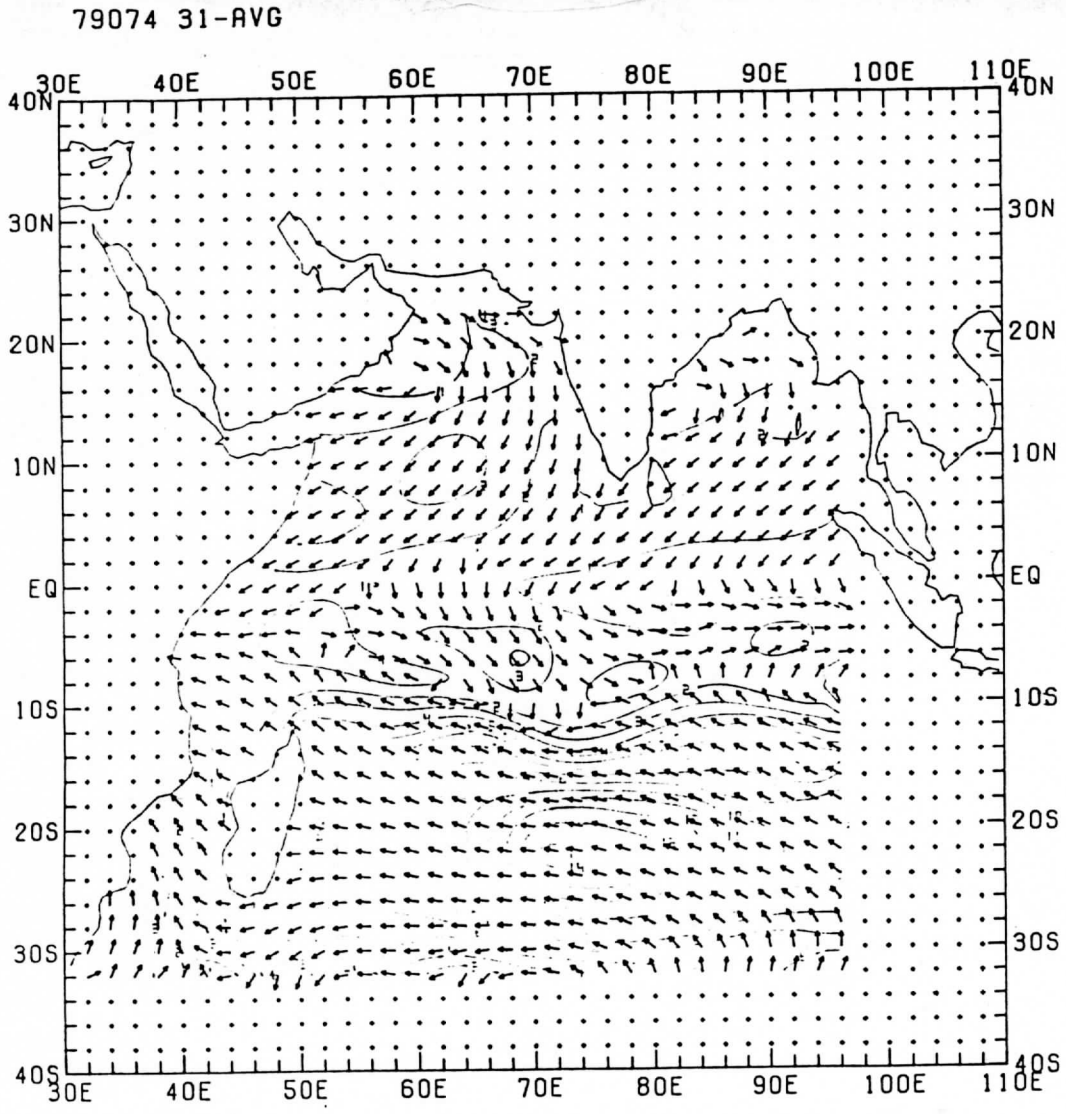
79074 31-AVG
30E
40E
50E
60E
70E
80E
90E
100E
110E
40N
30N
20N
10N
EQ
10S
20S
30S
40S

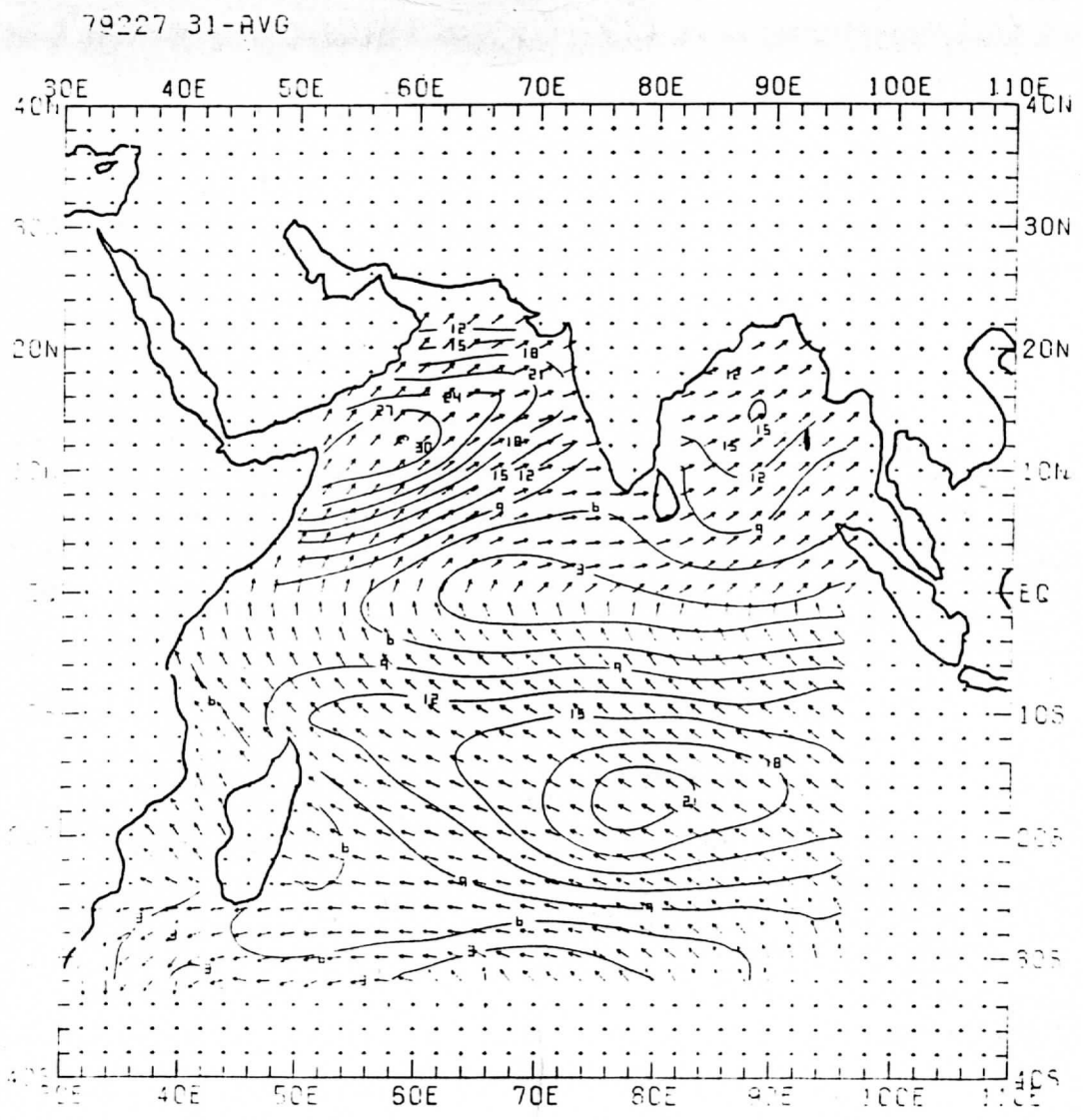
79227 31-AVG
30E
40E
50E
60E
70E
80E
90E
100E
110E
40N
30N
20N
10N
EQ
10S
20S
30S
40S

79258 30-AVG

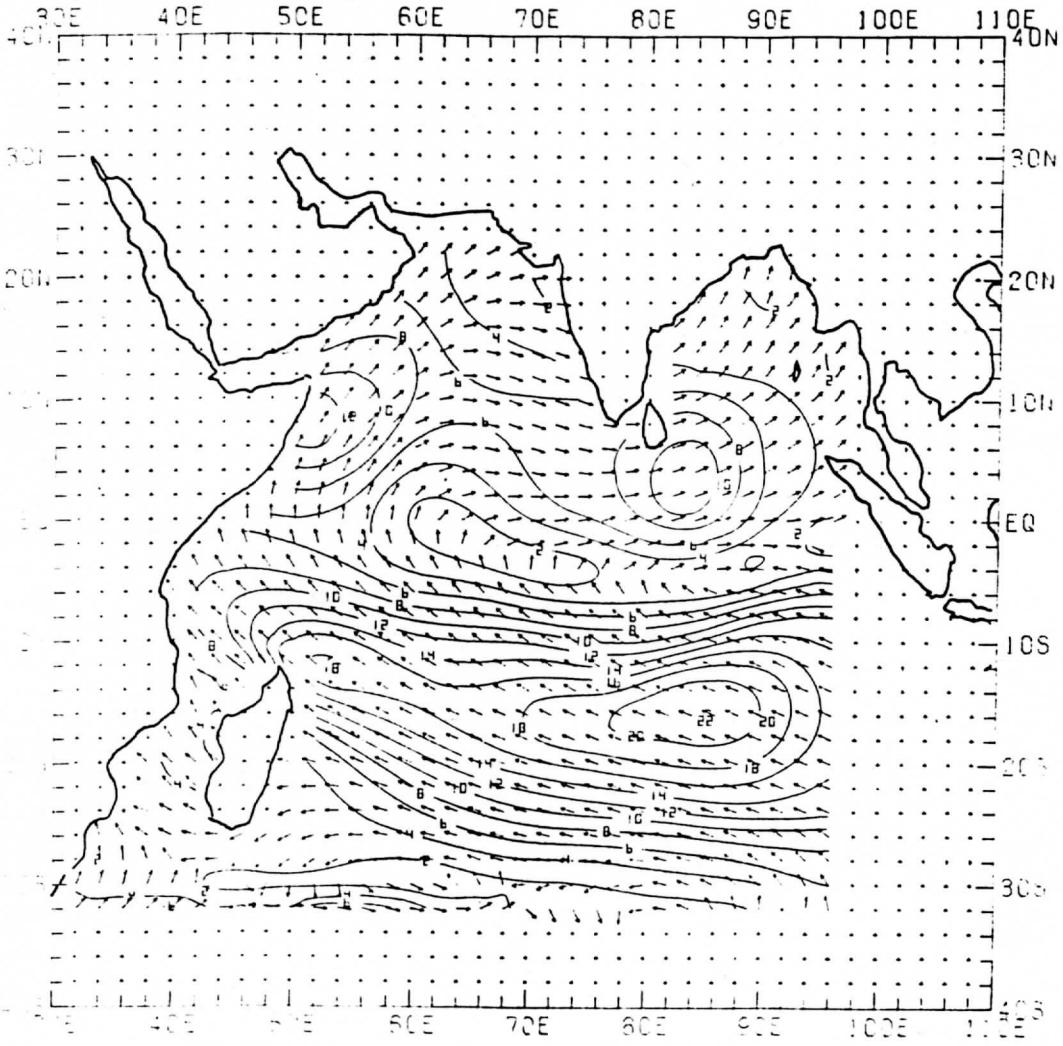
40E
50E
60E
70E
80E
90E
100E
110E
40N
30N
20N
10N
EQ
10S
60E
70E
80E
90E
100E

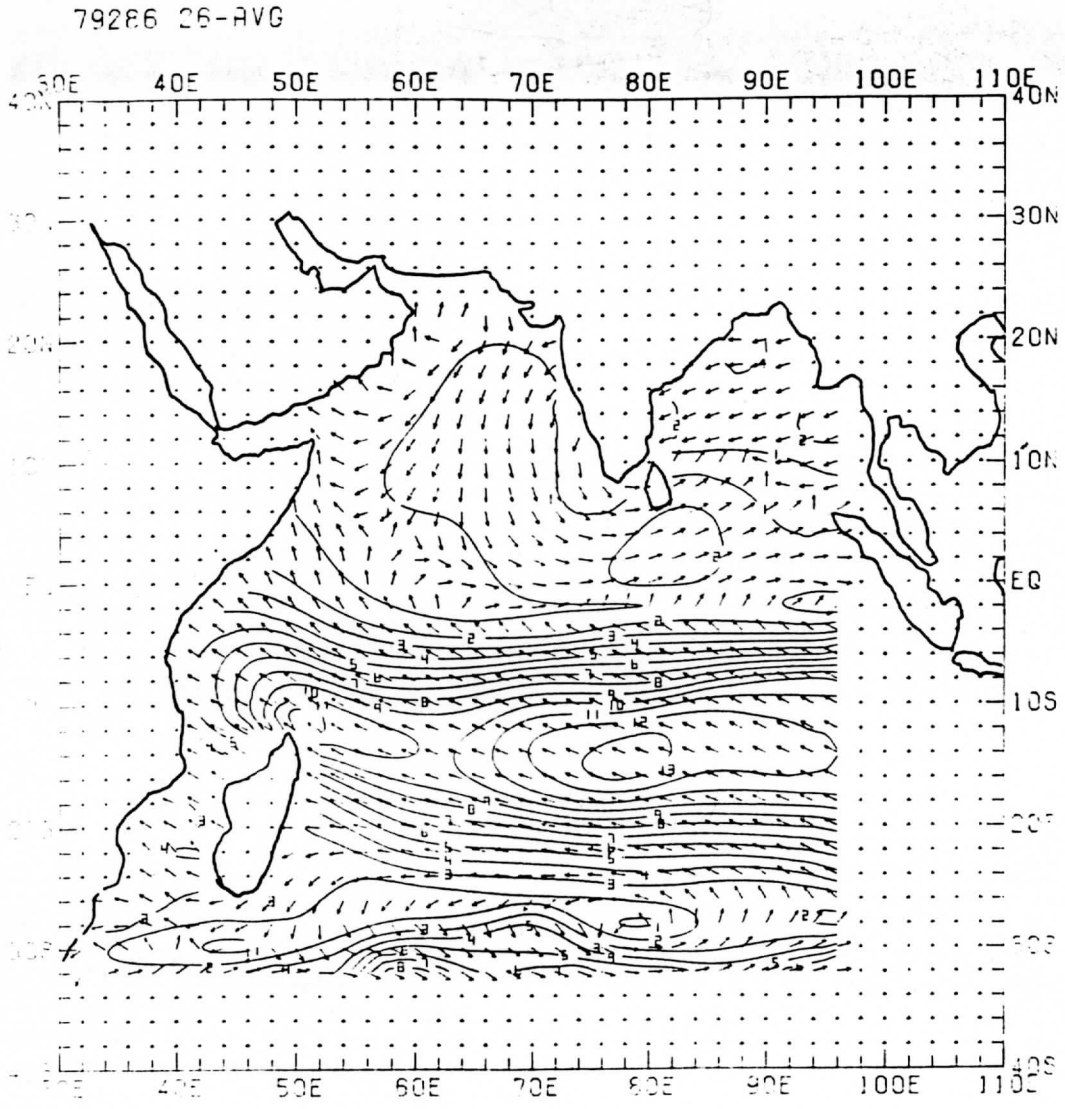
79286 26-AVG
40E
50E
60E
70E
80E
90E
100E
110E
40N
30N
20N
10N
EQ
10S
20S
40S